Structural Evaluation of Highway and Airport Pavements

A Dissertation Submitted in Fulfillment of the Requirement for the Award of the Degree of

MASTER OF ENGINEERING

in Infrastructure Engineering

Submitted By

Komaldeep

(802023009)

Under Supervision of

Dr. Tanuj Chopra

(Assistant Professor)

Dr. Kumari Monu

(Assistant Professor)

DEPARTMENT OF CIVIL ENGINEERING

THAPAR INSTITUTE OF ENGINEERING & TECHNOLOGY
(A DEEMED TO BE UNIVERSITY U/S 3 of UGC Act, 1956),
PATIALA, PUNJAB

JULY, 2022

Declaration

I hereby declare that this work entitled **"Structural Evaluation of Highway and Airport Pavements"** submitted by me to **Thapar Institute of Engineering and Technology, Patiala** in partial fulfillment of the requirement for the award of the degree of **M.E.** in field of **CIVIL ENGINEERING DEPARTMENT** is a record of authentic dissertation work carried out by me under the guidance of Dr. Tanuj Chopra (Assistant Professor, Department of Civil Engineering) & Dr. Kumari Monu (Assistant Professor, Department of Civil Engineering).

I further declare that the work reported in this dissertation has not been submitted and will not be submitted, either in part or in full, for the award of any otherdegree or diploma in this institute or any other institute or university.

Komaldeep

Date : 16-08-2022.

(KOMALDEEP)

Roll No. 802023009

This is to certify that the above declaration made by the student concerned is correct according to the best of our knowledge and belief.

Dr.Tanuj Chopra
Assistant Professor,CED
TIET, Patiala

Dr.Kumari Monu
Assistant Professor,CED
TIET, Patiala.

Acknowledgment

The work presented in this dissertation would not have been successful without the guidance from various sources throughout the work. It is my pleasure to acknowledge the help of those individuals.

First of all, I bow to the fee of the Almighty for providing me with an excellent environment to complete this work by affording me valuable person for my guidance, without whose blessing the work would not have the dawn.

I take this opportunity to express my profound gratitude, thankfulness, and deep regards to "**Dr. Tanuj Chopra** (Assistant Professor, Department of Civil Engineering) & **Dr. Kumari Monu** (Assistant Professor, Department of Civil Engineering)" for their moral guidance, monitoring, and constant encouragement throughout the course of this project. The blessing, help, and advice given by them from time to time shall carry me a long way in the journey of life on which I'm about to embark. I extend my gratitude to **Mr. Shekhar Verma** (Pavement Evaluation Expert, AIMIL Ltd.) for his kind attitude, keen interest, support, and direction.

I extend my deep appreciation and thanks to the authors of various research articles, which were helpful in the completion of this project.

Finally, I want to express profound gratitude to my beloved Father, **Mr. Baljinder Singh,** and my beloved mother, **Mrs. Davinder Kaur**. Their constant guidance, cooperation, motivation, and support have always kept me going ahead. This accomplishment would not have been possible without them. Last but not least, I want to thank all my friends who have directly and indirectly extended their constant support and co-operation during my work.

Table of Contents

LIST OF TABLES

LIST OF FIGURES

ABSTRACT

Road infrastructure is a high-value asset in the development of a modern society where its perceived quality translates into a fundamental role in security, economy, competitiveness and sustainability of the free flow of people and goods. The gradual degradation of that quality through time should be evaluated in such a manner that maintenance and rehabilitation efforts can be timely planned and carried out to maintain its specified minimum quality requirements. In pavement condition assessment, there are several parameters that gauge pavement quality. The Falling Weight Deflectometer (F/HWD) is the leading non-destructive testing equipment used to assess the bearing capacity of road and airfield pavements. This test's results are very relevant in several contexts, for example, a survey for bearing capacity in existing road or airfield pavements requiring rehabilitation intervention.

The present dissertation's objective is to assess the precision and uncertainty performance in measuring deflection and to analyze its influence in the quality of results from the testing campaign, therefore assessing the structural capacity of existing pavements (backanalysis), in view to evaluate the structural quality and support a rehabilitation project. The deflection data was first processed for repeatability and reproducibility and afterward analyzed for uncertainty quantification. Lastly, the resulting data was used for a sensitivity analysis featuring the uncertainty of the measured deflection influence on the mechanical properties (elastic moduli) estimated from the field survey (back-analysis) on flexible pavements.

The airport pavement deteriorates during service due to traffic and climate effects therefore, systematic monitoring is required to assess its structural and functional condition. This work aims to present the methodologies used nowadays for airport pavement evaluation and to contribute to their improvement in the structural analysis area

This study aims to find out and analyze the value of PCN by using the ELMOD 6 application, which consists of inspection, maintenance, and repairs on the runway if it indicates a decrease in carrying capacity. By knowing the accurate value of PCN, it will support the smooth operation of the flight. The method used in this study is a descriptive qualitative approach. Data collection by means of documentation studies, participant observation and in depth interviews.

Pavement Condition Surveys refer to activities performed to give an indication of the serviceability and physical conditions of road pavements. These activities have three main aspects: data collection, condition rating and quality management. In recent times, most state agencies are inclined towards automated and semi-automated means of collecting pavement

data. Condition rating involves quantifying the condition of pavement assets based on a chosen scale or index. The rating index selected by an agency depends on the agency's available resources and its ability to address pavement issues prevalent in the area.

CHAPTER 1
INTRODUCTION

1.1 General

Roads are an essential mode of transportation and play a significant role in a country's development. India has a network of over 6,371,847 km of roads. Most of these roads were constructed around the 80s and 90's and are now on the verge of their design life. The design life can be improved by maintaining the structure periodically. If not maintained periodically, the pavement will undergo structural and functional damage.

It is challenging to keep the road in the condition it was in when it first opened, and issues begin to show themselves as pavement cracks, holes, and undulations, among other signs. (Basir,2006)

Due to repetitive loading and application of vehicles, the deterioration of pavement will occur with time on both airport and highway pavements. Evaluating the pavement structurally and functionally becomes very important.

Structural evaluation of pavement could be defined as the measure of structural adequacy of the pavement. Pavement performance depends on the number of the standard axle, drainage condition of the pavement, temperature, soil present in the subgrade, rainfall, etc. (Abhishek 2019).

This Structural evaluation can be done by Non-Destructive testing. In the non-destructive testing (NDT) method, no damage is done to the pavement. Without disturbing their existing condition, pavement strength can be determined by NDT. NDT is also deflection based. Surface deflections are generally measured. Many standard institutions insist on using NDT equipment for the structural evaluation of pavements. NDT consists of two types currently used for structural evaluation, i.e., Falling Weight Deflectometer and Benkelman beam deflection.

1.2 Purpose of Structural Evaluation Of Pavements

Structural evaluation of in-service pavements is generally carried out to:

- Assess the structural strength
- Estimate the remaining life of pavements.
- Determine the thickness of overlay required.

1.3 Advantages of NDT

- Unlike destructive testing, non-destructive testing has the advantage that the inspected part does not have to be remanufactured.
- NDT methods can quickly gather the test data.
- Without NDT, structural data must be obtained from numerous cores, borings, and excavation pits on an existing airport pavement. This can be very disruptive to Highway operations.
- Both qualitative and quantitative data about the strength of pavement can be known at the time of testing from the deflection data collected with NDT equipment.
- The strength of the entire pavement structure is indicated by the raw deflection data directly beneath the load plate sensor obtained by NDT methods.
- The raw deflection data can also know subgrade strength from the outermost sensor.

1.4 Limitation of NDT

- NDT conducted at different times during the year may give different results due to climatic changes.
- NDT is a perfect methodology for assessing the structural condition but not evaluating the functional condition of the pavement, like smoothness and frictional characteristics.
- The Quantitative results obtained from raw NDT data are always model dependent.
- NDT provides structural capacity but no information about grain size distribution of subgrade to determine swelling & heaving potential.

1.5 Use of NDT Data

There are many ways to use the NDT data to obtain those pavement characteristics needed to identify the causes of pavement distress, conduct a pavement evaluation, or perform a strengthening design.

The methods that can be used to compute and evaluate such pavement characteristics as:

- Normalized deflections.
- Back-calculated elastic modulus of pavement layers and subgrade.
- Correlations to characterizations like California Bearing Ratio [CBR],k.
- Crack and joint load transfer efficiency.

1.6 Airport Pavement

Airside and landside are the two main sections of airports. All controlled access areas, including runways, taxiways, aprons, aircraft service areas, and air traffic control facilities, are

referred to as airside. The runways are often connected to the apron via taxiways and are used for aircraft landings and takeoffs **(Sun et al., 2022)**. An apron provides a place for aircraft parking, refueling, and the operations of loading and unloading passengers, luggage, and cargo.

Airport pavement is basically of two types Flexible airport pavement and rigid airport pavement. To provide an alternative solution for extending the service life of rigid pavements, there may be composite pavements with a flexible layer over a rigid layer constructed using Portland cement concrete (PCC) **(Mallick, El-korchi, and Group, n.d.).**

Flexible airport pavement commonly consists of four layers—

- surface layer,
- base layer,
- subbase layer, and
- subgrade layer.

Flexible airport pavement can be considered multi-layer composite pavement, and an overlay of 50-100mm thickness of dense graded bitumen is generally designed.

The airport asphalt surface maintenance operation such as resurfacing may be applied within the expectancy life of around 20 years. Based on the relationship between transportation repetitions and the strains observed by the actual performance of full-scale pavements under full-scale loading, the pavement life can be estimated to meet the requirements of airport design (Mallick, El-korchi, and Group, n.d.)

1.7 Objectives of the Study

This study incorporates two main evaluation methods, functional and structural. The structural evaluation regards the use of the F/HWD.

1.7.1 Airport pavement

- Analysis of Heavy weight deflectometer data collected from the runway and apron of the airport.
- Analyze and calculate Pavement Classification Number for the Apron for the runway strength.
- Comparison of layer moduli before and after rehabilitation works on the runway.

1.7.2 Highway pavement

- Investigate the flexible pavement defects using the Pavement Condition Index (PCI) and identify various types of distress.

- Analysis of Falling weight deflectometer data collected from a flexible pavement and determination of remaining life of the pavement.
- To design an overlay thickness of flexible pavement.

1.8 Scope of the study

- The Literature review was done for different methods of back-calculating layer moduli using Elmod-6 software and KGPBACK software.
- To collect deflection data using Heavy Weight Deflectometer on the selected pavement.
- To compare the elastic modulus values obtained before and after rehabilitation works on runway pavement.
- To find ACN/PCN values for Apron using the software.
- To Compare two software ELMOD-6 and KGPBACK, the back-calculated subgrade and granular layer modulus values of highway pavement.
- To analyze the condition of selected highway road of case study and give a PCI rating to pavements.
- To design an overlay thickness for the study stretch.

1.9 Outline of the Study

The following chapters represent the work done in the dissertation.

Chapter 1 'Introduction' includes a basic outline of the work done, the study's objective, advantages, and limitations of non-destructive testing.

Chapter 2, 'Literature review,' includes a preview of previous work on back-calculation methods and pavement testing.

Chapter 3, 'Deflection measuring equipment & back-calculation programs', is an overview of the types of deflection-measuring equipment, fundamentals of FWD testing, calibration of the equipment, and basic back-calculation concepts discussed.

Chapter 4, 'Study Area,' discusses all the selected payments and case studies taken for study.

Chapter 5 'Methodology' in this chapter, the procedure or methodology for evaluating the airport pavement, pavement condition survey is discussed in this chapter.

Chapter6 ' Data Analysis' Evaluation of selected airport and highway pavement is explained in this chapter. Analysis of the chosen layer moduli obtained from KGPBACK and ELMOD-6 were compared.

Chapter 7 ‘Conclusion’ -The conclusions derived from the analysis are discussed in this chapter.

CHAPTER 2
LITERATURE REVIEW

2.1 GENERAL

This chapter reviews various journals to outline the literature available on Falling-Weight Deflectometer analysis to determine modulus values. This chapter also provides an overview of the procedure for Back-calculation and multiple tools available for structural pavement evaluation.

2.2 Literature review on Back-Calculation Layer Moduli

"Back-analysis" is an iterative process of working reverse to determine the pavement layer moduli using measured deflections and pavement layer properties. In this process, measured surface deflection attempted to match with a calculated surface deflection generated from an identical pavement structure using assumed layer moduli. Back-calculation analysis is done to compute the strength of pavement layers. The layer strength of pavement is referred to in terms of young's modulus of elasticity or Elastic modulus. The back-calculation process requires inputs such as number of layers, layer thicknesses, Poisson's ratio of each layer & temperature, as shown in fig 2.1.

The back-calculation method can be grouped into two general categories. For both the static & Dynamic, the pavement response should be linear or non-linear.

2.2.1 Static Backcalculation Method :

EVERCALC, CHEVDEF, and MODULUS programs are based on the static back-calculation method. There are three categories: Iterative methods, Basin search methods, and Regression equations.

The Iterative method repeatedly uses a forward analysis method. Layer moduli are continuously varied in approach until the deflection basin comes equivalent to the measured deflection basin inside a particular tolerance.

The second category is the "Basin search method," which is based on searching a database on deflection basins. In this, a forward calculation scheme is used & to create a database of deflection basins different combinations of layer thickness, moduli, and type of pavement are utilized. Now, measured deflection basins are compared to the values computed from the

database using a search algorithm. From the layer moduli, a set of moduli values are interpolated to get the closest deflection basin inside the database.

(Garg and Thompson 1999) established a regression equation to find the subgrade modulus utilizing the pavement deflection at 1097 mm from the middle of the loading plate. **Horak(1987)** also proposed a regression equation for estimating the subgrade modulus using pavement deflection measured at 2000 mm radial distance from the middle of the loading plate.

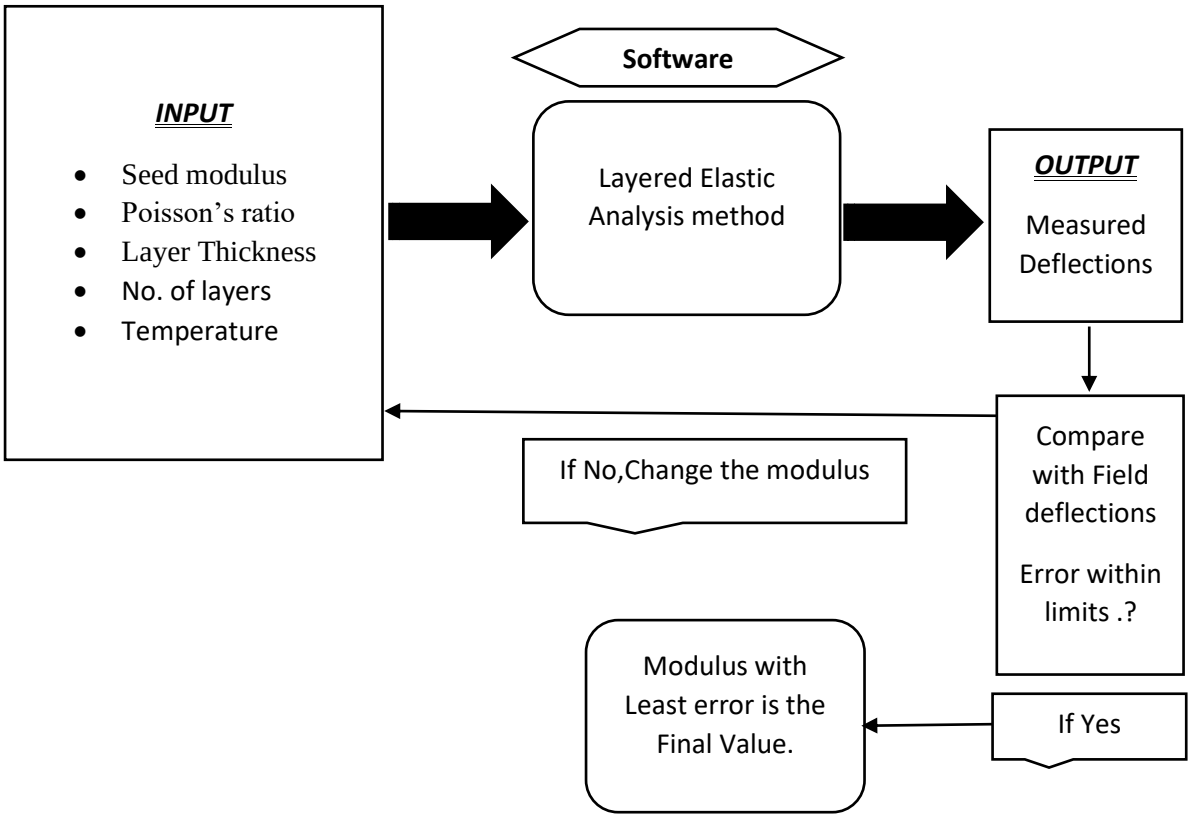

Fig 2. 1 Flow chart of Backcalculation of layer moduli

2.2.2 Dynamic Back-calculation Method:

For analyzing the dynamic response of FWD deflection, a dynamic approach is developed. This approach is based on either frequency or time-domain solutions. When pavement thickness is known, or the moduli changes within a layer, static- back-calculation may not give consistent outcomes

Some computer programs have been developed for the dynamic back-calculation of flexible pavement layer parameters. All of these programs require time histories of load and deflection sensors.

Table 2. 1. Dynamic back-calculation programs for flexible pavement

Program	Domain	Inverse method	Forward program
EVERCALCII	Time	Non-linear least square optimization with Tikhonov regularization and continuation method	FEM
DYNABACK	Frequency/time	Newton's method with least-square or singular value decomposition	SAPSI
FEDPAN	Time	Linear least squares	SAP IV

(Deol Guzzarlapudi, Kumar Adigopula, and Kumar 2017) They compared the two techniques radius of curvature method using the ELMOD 6.0 program and the analytical approach that adopts adaptive mathematical technique using Boussinesq's formulae with Odemark's consecutive three-layer system for estimating pavement layer moduli. The techniques are similar in analyzing the pavement as a minimum three-layer physical system. A flexible stretch of 20 km is selected to perform FWD at an interval of 1 km each at an impulse load of 40 kN. The results show that the moduli for the bituminous layer calculated from both techniques varies by a mean of 32.29%. At all test locations, a mean variation of 27.16% & 5.61% was there in granular and subgrade layer moduli.

(Kang et al., 1998) explained that factors such as non-uniform pressure, temperature and moisture gradients, improper loading position to the edge of the pavement, variation of material properties and nonlinearity, selection of an inappropriate forward model, and deflection-matching algorithm can cause an error in the back-calculation process.

(Zhou, Wu, and Ling 2010) Comparing the falling weight deflectometer and Benkelman beam deflectometer for the pavement evaluation. The section considered for the testing was a junction located in Jiading district, Shanghai, in China. The length of the selected junction was 3.2 km. The pavement structure was 150mm asphalt surface, 450mm base/subbase, and subgrade.

The Falling weight deflectometer test was repeated at each location, followed by the pavement coring for the in-situ layer thickness of the base and subbase. The thickness served as input to back-calculate the layer moduli. The theoretical deflections compared with the measured deflections & error are minimized until two basins show a good match. MODULUS software is used to back-calculate Subgrade elastic modulus $M_{R\ (Dyn).}$

(Patil, Shivananda, and B.R. 2018) talks about the importance and how a new layer thickness has been proposed based on the results of KGPback and IITpave software. A Section from NH-218 was taken under for the study, FWD testing was conducted at the selected locations, and the test results are analyzed as per IRC 115-2014. The Rutting and Fatigue equations are given in IRC 37-2012 and were used to calculate the allowable strains and then compared with the computed strains from IIT-Pave. The methodology adopted included the detailed condition survey followed by collecting existing crust details for calculation in KGPback software. The 24hr traffic volume data were collected for seven days as per IRC 37-2012 for the analysis of new layer thickness, the vehicle damage factor was calculated using axle load survey data, and the allowable strains were compared with the computed strains from IIT-Pave. The author concluded that for designing the crust of flexible pavement, FWD test results should be analyzed using KGP back so that the remaining life of the existing layers can be considered for realistic and economical designs.

(Sharma and Das 2008) studied how ANN can be used to solve various problems related to FWD back-calculation of asphalt pavement. The author's main focus was on the performance of ANN back-calculation with respect to the performance of other standard software, EVERCALC, and ExPaS. ANN is a tool that can give accurate results in less time if it is trained well. The remaining pavement life was estimated using ANN models that can predict a rigid layer at the bottom of the pavement and can also expect the remaining life of the pavement without back calculating the layer moduli. Then eventually, a reliability evaluation is carried out to detect back-calculation performance using ANN. The author observed that ANN models have limitations: they cannot back-calculate the layer moduli outside the ranges chosen for training the neural network. The training of the ANN is a long process and takes time. The performance of the ANN model depends on how effectively it has been trained.

(Aavik and Talvik 2008) used the deflection data to drive an equation to calculate pavement equivalent E-modulus from the load cell mounted in the center of the load cell of FWD. The rest of the six different load cells were used to create the deflection basin characterizing the pavement condition at the FWD test site. A pavement structural evaluation and repair design

system was developed based on FWD deflection, parameters like E-modulus value, and deflection basin parameters. Figure 2.2 shows the deflection basin parameters used in the study.

Deflection basin parameter	Equation	Unit	Parameter's objective
Surface Curvature Index	$SCI = d_0 - d_{300}$ $SCI = d_0 - d_r$ (used also r ∈ [450, 600])	µm, mm	Characterizing condition of bound layers
Base Damage Index	$BDI = d_{300} - d_{600}$	µm, mm	Characterzing condition of base layers
Base Curvature Index	$BCI = d_{600} - d_{900}$ (used in USA) $BCI = d_{900} - d_{1200}$ (used in Finland) $BCI = d_{1200} - d_{1500}$ (used in Estonia)	µm, mm	Characterizing condition of subase or subgrade
Area	$AREA = \frac{6(D_0 + 2D_1 + 2D_2 + D_3)}{D_0}$ $AREA = \frac{150(d_0 + 2d_{300} + 2d_{600} + d_{900})}{d_0}$	in mm	Characterizing shape of the deflection basin close to the load by the normalized area on the top of the deflection basin
Area Under Pavement Profile	$AUPP = \frac{5d_0 + 2d_{300} + 2d_{600} + d_{900}}{d_0}$		Characterizing condition of the pavement upper layers
Shape Factors	$F_1 = (d_0 - d_{600}) / d_{300}$ $F_2 = (d_{300} - d_{900}) / d_{600}$	-	Determination of condition of the layer at the equivalent depth
Deflection Ratio	$DR = d_{600} / d_0$	-	Determination of condition of the layer at the equivalent depth

d_0, d_{300}, d_{600}, d_{900}, d_{1200}, d_{1500} – measured deformations at the distance of 0, 300, 600, 900, 1200, 1500 mm from the center of the loading plate; D0, D1, D2, D3 – measured deformations at the distance of 0 ft, 1 ft (305 mm), 2 ft (610 mm), 3 ft (914mm) from the center of the loading plate.

Figure 2.2 shows the deflection basin parameters

The data bank was used to analyze and determine the influence of the deflection basin parameters (SCI, BDI, BCI). The data required is:

- Pavement type and construction time
- Traffic volume
- E-modulus (FWD measurement data)
- Pavement defect types (inventory data)

A good correlation was found between deflection basin parameters (SCI, BDI, BCI) and back-calculated pavement equivalent modulus. Strong relationships were found usually between upper layers indicators (SCI and BDI) and pavement equivalent modulus(E_{eq}). The relationship between subgrade indicator BCI and $E_{(eq)}$found in the research was not very strong.

The Falling Weight Deflectometer evaluates the pavement's structural condition (**Solanki**, Gundaliya, and Barasara 2016) carried out a study on Barnala-Mansa State Highway, a length of 20 km in Punjab state, using FWD before and after overlay as shown in Figure 2.3 & 2.4. Using the results deflection bowl parameters such as Surface Curvature Index (SCI), Middle

layer Index (MLI), and Lower layer index (LLI). The author concluded that the results of SCI, LLI, and MLI show a relation between old deteriorated and new pavement. The limiting value is found 240 microns. Above this value condition of the pavement is poor, and below 100 microns, it is considered very good. For old and new pavement, MLI values were found in the range of 140 and 100 microns, respectively. In both cases, the middle layer condition is good and correlates with the back-calculated moduli value of the intermediate layer. The average LLI value found is 20 for old and 14 for new pavement; in both cases, the lower layer condition is good and correlates with back-calculated moduli values of the lower layer.

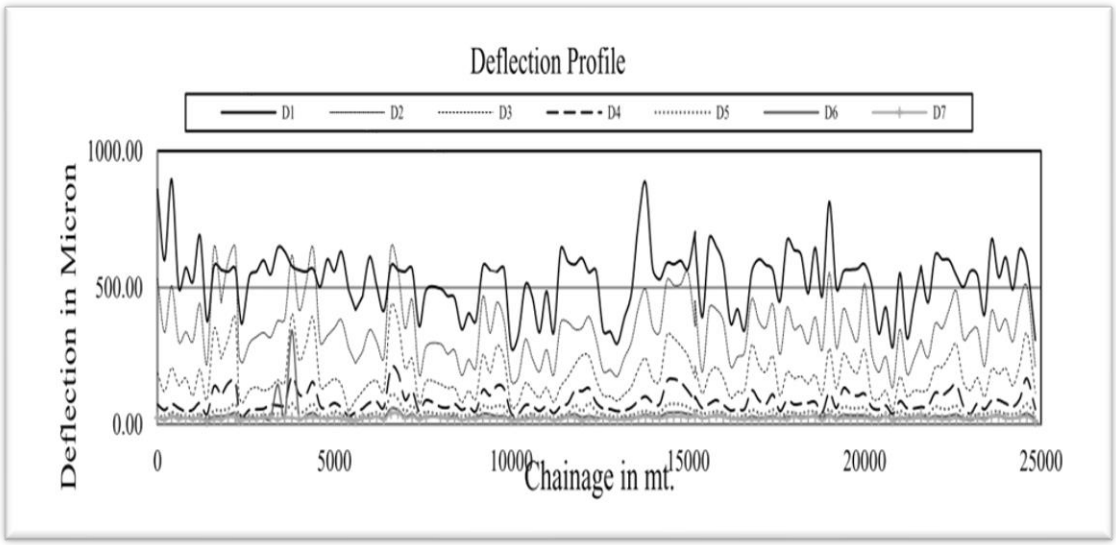

Figure 2.3 Deflection profile of old road before the overlay

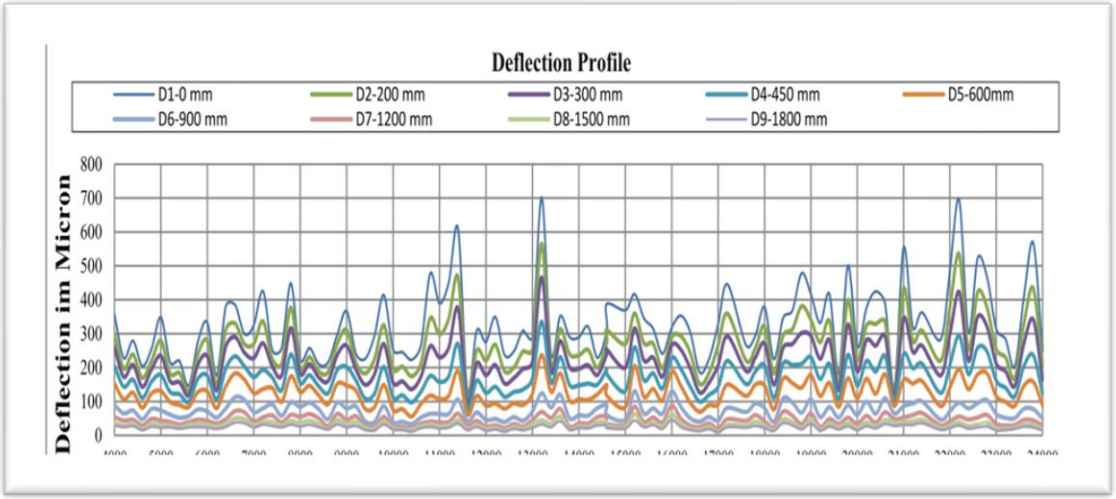

Figure 2.4 Deflection profile of new road after overlay

(Tarefder and Ahmed 2013) found the most consistent and accurate software for computing airport pavement layer modulus values in New Mexico. In this study, Laboratory tests were performed to determine the modulus of different layers, and soil samples were collected.

- Then the laboratory calculations were compared with those modulus values, which were back-calculated from the software.
- Back calculated tensile stress was compared using KENLAYER with laboratory tensile stress
- This study compared three programs: BACKFAA, MODULUS, and EVERCALC.
- Only the Indirect tensile modulus of the AC layer was determined in the laboratory and no modulus testing for subgrade and base layer moduli.
- They found that EVERCALC is more compatible software for computation of layer moduli & Evercalc gives a closer value of modulus to laboratory calculated modulus than other programs.

(Priddy, Bianchini, and Gonzalez 2015) compared the BAKFAA, ELMOD-6, and WESDEF programs and the outcomes of selected programs using the HWD data acquired during the airfield pavement evaluations. The author studied 30 pavement sections from six airfields for the back-calculation analysis. The conclusions made were the ELMOD6 program predicted higher moduli for the subgrades and did not produce similar back-calculated moduli results to those obtained using the WESDEF program.BAKFAA determined similar back-calculated moduli to those computed by the WESDEF program.

The three back-calculation software, BAKFAA, EVERCALC, and MODULUS, are evaluated for consistency and accuracy (Ahmed 2010)**.** The objective of this study was to analyze the FWD data to back-calculate modulus using different programs. The predicted values from the software are compared with the laboratory modulus values to determine the indirect tensile strength of the asphalt concrete. The study also covers variations of the time-deflection history along with the variations in layer properties, thickness, and the depth of the rigid layer. Statistical analysis using FWD deflection data was done on an airport pavement to examine the consistency. It is found that the EVERCALC software produces more consistent and accurate modulus values than the other two software. The static deflection is greater than the dynamic deflection and closer to the field FWD deflection basin. The deflection in static analysis is more sensitive to the layer modulus variation than the dynamic analysis.

Shubham Mishra (2019) has done work on comparing different programs to analyze falling weight deflectometer data. The objective of the Study:

- Analysis of FWD data using other back-calculation techniques
- Comparison of moduli values compared from KUAB, EVERCALC, KGPBACK, and Elmod programs for analyzing data. Scope of the study:
- To find a correlation between the Benkelman beam method and FWD.
- Compare the back-calculated modulus at three different loads to determine the consistency of programs
- To check the program's reliability, compare the back-calculated surface modulus determined from different programs with the laboratory resilient modulus. Methodology 1 Selection of the Road section 2 Collection of data:
- Structural Condition of Data: BBD & FWD methods have been used for revaluation.
- Traffic volume survey data: No. Of commercial vehicles can be obtained. a 5% growth factor was considered for laying of an overlay.
- Destructive testing: Core cutting was performed to obtain cores of the surface layer.

Test pits were excavated to determine the thickness values of different pavement layers. Resilient Modulus of the bituminous layer was determined in UTM (universal testing machine). Various methods for the determination of modulus values were compared.

Consistency and reliability of these methods were also evaluated. The author concluded that the BBD & FWD values after temperature and moisture correction and the peak deflection values of FWD at the middle of the loading plate were corrected for load study stretches of roads.The consistency of FWD back-calculation programs was evaluated using frequency distributions. Elmod (radius of curvature method) was found more consistent for surface modulus than Evercalc and Elmod (Deflection Basin fit method). The back-calculated surface modulus for two-roads was examined by comparing back-calculated modulus to the laboratory resilient modulus . KUAB produces modulus values close to the laboratory resilient modulus compared to the other programs

CHAPTER 3
DEFLECTION MEASURING EQUIPMENT & BACKCALCULATION PROGRAMS

3.1 GENERAL

Several techniques, including the Benkelman Beam, Deflectograph, Dynaflect, and Falling Weight Deflectometer, are used to assess the nondestructive deflection of the pavements of roads and airports (FWD). Nondestructive testing includes deflection and non-deflection measuring types of testing equipment. Depending on the load duration, the deflection-based equipment is classified as static and dynamic loading devices. Various kinds of NDT devices are discussed in this chapter, focusing mainly on dynamic loading deflection measuring devices, i.e., vibratory or impulse devices. This chapter discusses various approaches in FWD data analysis and interpretation for flexible pavements, including a review of common back-calculation programs in terms of their underlying assumptions, required inputs and resulting outputs, overall advantages and disadvantages, and user-friendliness

3.2 Dynamic Loading Equipment

There are types of Equipment:

3.2.1 Vibratory loading Equipment

These devices induce vibrations using a dynamic generator to the pavements in a steady state. A load plate is seated by a small static force-generating dynamic force that causes the pavement to deflect. Velocity transducers are used to measure the pavement deflections. Vibratory types of equipment are Heavy Vibrator, Road Rater Dynaflect.

3.2.2 Impulse Loading Equipment

These devices measure the pavement deflections by applying impulse loading to the pavement surface by dropping a free-falling weight that impacts a set of rubber pads. Velocity transducers or Linear variable differential transducers (LVDT) are used to measure the deflections. Some impulse loading devices are Light weight deflectometer, Falling weight deflectometer, and Heavyweight deflectometer.

3.3 Falling weight deflectometer

The falling weight deflectometer is a Nondestructive test device mainly used in pavement evaluation. A Falling weight deflectometer is a deflection measuring test for measuring surface deflection. The primary purpose is to determine the stiffness of each layer in the pavement structure. Deflections are measured at a number of points far from the load application, which gives the FWD system an edge over some other deflection devices. On flexible roads, FWD tests are typically conducted at intervals of 25 or 50 m. Inside the towing vehicle, a laptop is used to record the load and deflection information. The testing sequence, including a number of drops and drop heights, is set up using software supplied with the FWD device.

The following data should be recorded for each test point:

- Location (chainage, lane, transverse position in the lane)
- Time and date
- Air temperature, Pavement temperature (if measured)
- Peak Load and Peak Deflections for each drop recorded Drop number.

While a light version (LWD) applies 1–15 kN and different heavy variants (HWD) apply up to 250 kN, the load for the regular FWD typically ranges from 7 kN to 150 kN. FWD deflections are likely to change with seasonal variations. The stiffness of the Bituminous binder is inversely proportional to the change in surface temperature. Along with the increase in surface temperature, the bituminous binder stiffness reduces, and pavement deflections increase (Jin, Lee, and Kovacs 1994). Similarly, material stiffness and deflections decrease when the moisture content of the subgrade and granular material drops (Deblois, Bilodeau, and Doré 2010). A more detailed description of the FWD operation is presented in 3.4 since this is the equipment used in the present study.

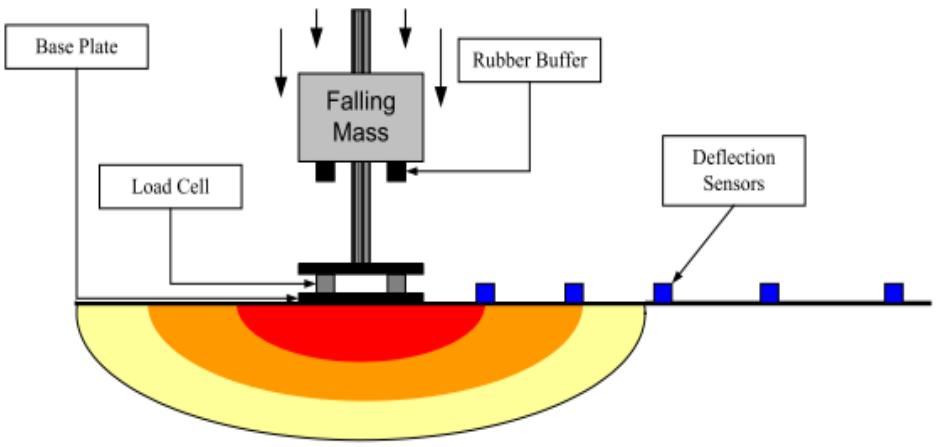

Fig 3. 1 Diagram. FWD testing schematic. (FHWA 2017)

Fig 3. 2 Trailor mounted HWD used in this study

Fig 3. 3 Another view of trailer-mounted F/HWD used in this study

It is an impulse loading device in which an impulse is generated on the surface of the pavement by dropping a falling weight on a system of springs placed over a circular steel plate then the deflected shape of the pavement is measured. For measuring the surface deflection caused by the falling weight, Geophones or Linear variable differential transducer (LVDT) are used. The geophones are placed at different radial distances starting with the center of the loading plate.

The deflection obtained from the geophones is then analyzed to evaluate the strength of the pavement. This pavement strength is expressed in terms of layer modulus.

3.4 Fundamentals of Falling Weight Deflectometer

The working principle of a typical FWD is a mass of weights is dropped from a pre-determined height onto a series of springs/buffers placed on top of a loading plate. The corresponding peak load and peak vertical surface deflections at different radial locations are measured and recorded, illustrated in Fig.3.4 DO, D1, etc., mentioned are surface deflections measured at different radial distances **(IRC:115, 2014).** Impulse load is applied using a falling mass, which is allowed to drop vertically on a system of springs placed over a circular loading plate. After the load is applied the sensors are used to measure the deflection using displacement sensors which are placed at different radial distances starting with the center of the load plate. The loading-plate and deflection transducers are elevated hydraulically when going from one test location to the next. These sensors provide the deflection bowl (as shown in Fig 3.5), which is examined and used for the back calculation of moduli values of the pavement layers. Table 3.1 explain all the specifications of FWD as per IRC:115,2014. FWD data is mainly used for:

- Pavement overlay design
- For estimating the remaining life of the pavement
- For finding the layer moduli values
- Impulse Stiffness Modulus (ISM), Dynamic Stiffness Modulus (DSM), and normalized deflection.

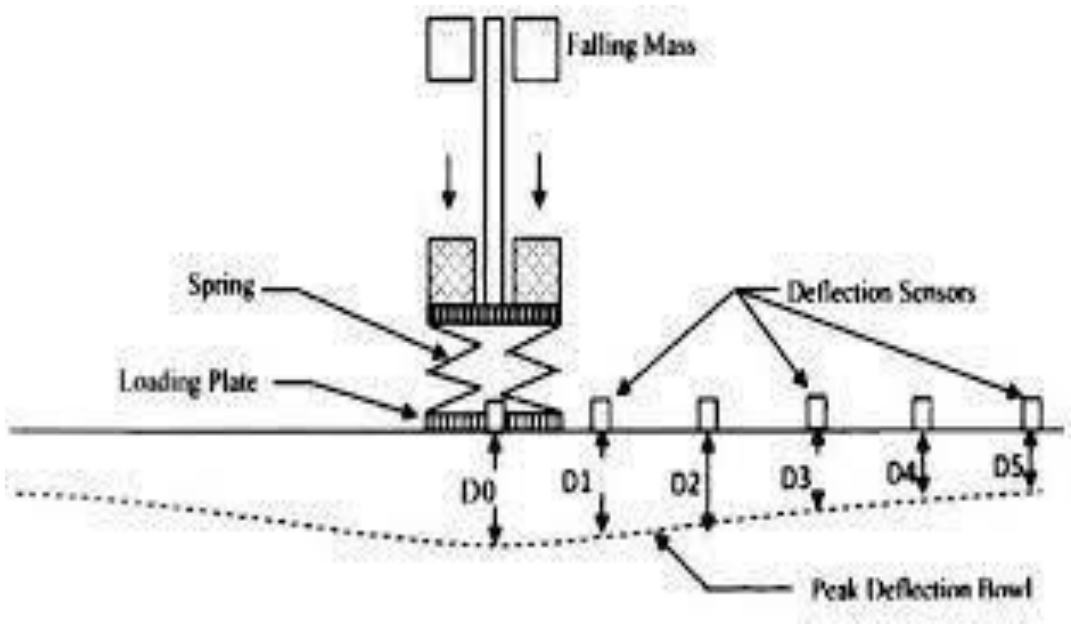

Fig 3. 4 Working Principle of Falling Weight Deflectometer (IRC:115,2014)

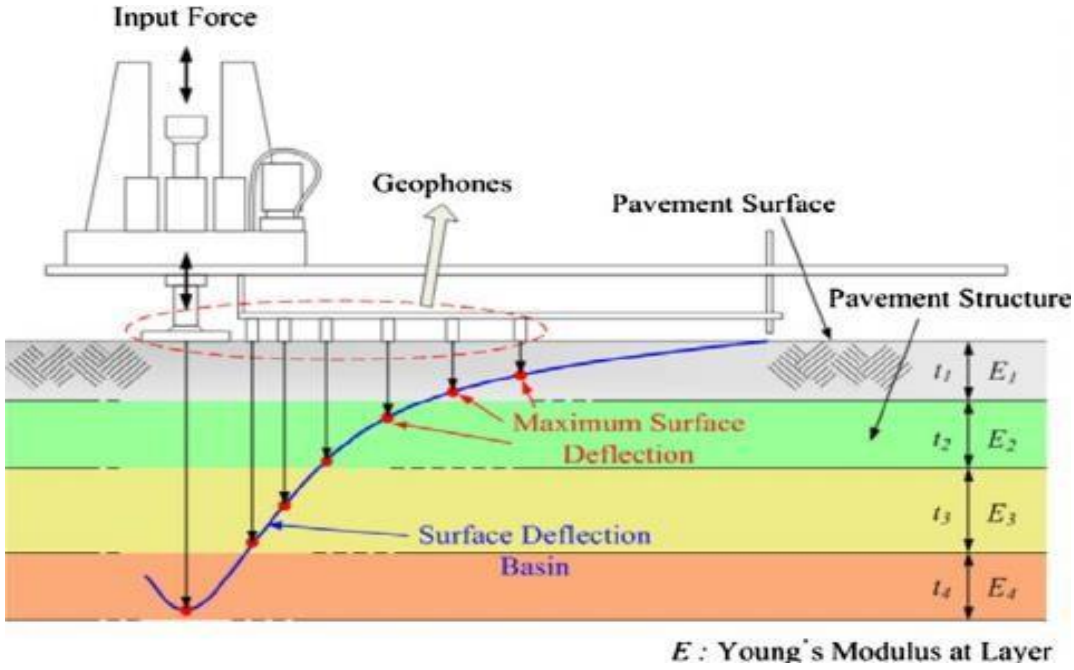

Fig 3. 5 Deflection Basin FWD

Deflection bowls are generally characterised by three parameters (Austroads,2011):

- Maximum deflection (D-0). A general indicator of pavement stiffness and response.
- Curvature (D-0 minus D-200). An indicator of the upper base course and surface layer stiffness.
- D-900: An indicator of the subgrade support condition.

Typical geophone position configurations (number and radial distances measured from center of load plate) commonly used for flexible pavement evaluation are ;-(IRC:115 , 2014)

- 7 sensors at 0, 300, 600, 900, 1200, 1500 and 1800 mm radial distances
- 7 sensors at 0, 200, 300, 450, 600, 900, 1500 mm radial distances
- 6 sensors at 0, 300, 600, 900, 1200 and 1500 mm radial distances and
- 6 sensors at 0, 200, 300, 600, 900, 1200 mm radial distances.

Fig 3. 6 Geophone location

Table3. 1 Specification of FWD As per IRC:115

S.No	FWD Components	IRC recommended Specification for FWD
1	Plate Diameter	300mm/450mm
2	Mass Density	Single Mass
3	Falling Weight Mass	50 to 350Kg
4	Height of fall	100 to 600mm
5	Target Peak Load	40KN
6	Load Pulse Time	15-50ms
7	Load Cell Accuracy	± 2%
8	Number of deflection Transducers	6 to 9
9	Deflection Sensor Types	Geophones
10	Reading of resolution of deflection transducers	Min 1um
11	Deflection transducers accuracy	± 2%

3.5 Components of Falling Weight Deflectometer

The major components are force generating vehicle, a guide system, a loading plate, a deflection sensor, a load cell, and a data processing and storage system.

1. Force Generating Vehicle (falling weight)

The force-generating is capable of being raised to one or more pre-determined heights and dropped.

2. Loading Plate

The plate uniformly distributes the load on the surface of pavement. The diameters of the loading plate are 300-450 mm for highway pavements and airport pavement. A larger load plate has the advantage of spreading the impulse load across a broader area while limiting layer

compression. However, if NDT is being performed on an unbound granular base, subbase, or subgrade, the bigger plate may be preferable. The significance of plate size is determined by the magnitude of the load, the surface temperature, and whether the surface layer is unbound or bounded **(FAA AC 150/5370- 11B, 2011).**

3. Deflection Sensor Spacing and Number

The maximum vertical movement of the pavement is measured by using the deflection sensor in the FWD device. The number and spacing of sensors depend upon the purpose of the test and the pavement layer characteristics; Displacement transducers, Velocity transducers, or accelerometers are the sensors used. The sensor spacing will be determined by the number of sensors available and the length of the sensor bar. NDT devices with additional sensors can more accurately quantify the deflection basin caused by static or dynamic loads. The position of the sensors is usually chosen from the following list **(IRC:115, 2014**); 0, 200, 300, 450, 600, 900, 1200, 1500, 1800, 2100, 2400mm

4. Load cell

The primary purpose of the load cell Figure 3.7 is to measure the applied impact load. It should be waterproof and resist mechanical shocks due to road impacts during testing, travelling, or both. A uniform loading area in good touch with the road surface is required for the test to be accurate. When using a solid circular plate on a weak structure or uneven surface, good contact is difficult to accomplish.

5. Data processing and storage system.

Air temperature, pavement surface temperature and the distance measurement data for each test point can be recorded manually or automatically. Load and deflection data is recorded.

Fig 3. 7 LOAD CELL

3.6 Load Pulse

A load pulse is created by lowering an invariant mass onto a loading plate by the use of rubber buffers. Manufacturer design differences have resulted in varied pulse forms for the same peak load. However, as per FAA and ASTM, most FWDs have a load increase duration of 5 to 30 milliseconds from the start of pulse to peak and a load pulse width of 20 to 60 milliseconds **(Fontul 2004)**. For analysis, the target load pulse is usually 40 or 50kN (Standard Wheel Load).

According to (**Fontul 2004)**, to compare the findings obtained in different places, the measured deflections must be transformed into "normalized" deflections matching the target load using a simple mathematical technique. This is known as "normalization." Thus, the findings of various test points can be compared and statistically analyzed.

3.7 Load Linearity

Engineers frequently assume that all layers in the structure respond in a linear elastic mode when analyzing deflection data. Traditional paving materials will perform linear and elastically within the load range tested for most pavement structures and testing situations (**(FAA AC 150/5370- 11B, 2011)**

3.8FWD Data Errors

According t**o (Lynne H. Irwin, and David P. Orr 2011)**, there are three primary sources of errors in FWD data: Seating errors, Random errors, and Systematic errors.

1. **Seating errors**

The rough texture of pavements contributed to seating errors, which were more significant when HMA pavements were tested. The deflection sensors may generally be made to get seated at each new test point by applying a seating drop to eliminate these errors. Data from seating drops shouldn't be utilized to examine the pavement's structure..

2. **Random errors**

These cannot be eliminated entirely however, they can be reduced by taking multiple readings and averaging the results. Random errors accompanied the deflections' analog-to-digital conversion..

3. **Systematic Errors**

Systematic errors can occur in a particular FWD equipment and its specific sensors. Systematic errors can be different for every FWD equipment. The tolerance range of these errors are on the order of ±2 percent. Systematic errors can be reduced to 0.3 percent or less for each sensor, including the load cell, through calibration.

3.9 Calibration of Falling Weight Deflectometer

Calibration of FWD device, i.e., load cell and deflection sensors, should be done every year to get accurate and reproductive results.

The step of the calibration procedure is as follows **(Lynne H. Irwin, David P. Orr 2011):**

1. The load and deflection measurement systems on an FWD are calibrated using independently calibrated reference transducers. We refer to this as reference calibration.
2. After reference calibration, relative calibration of the deflection sensors is used to refine the calibration factors (also known as gain factors).
3. The gain factors are checked for acceptability and then entered into the FWD computer's FWD operating system (i.e., the field program).
4. The gain factors are used as multipliers to the internal results from the FWD.

Annual calibration: The FWD load cell and deflection sensors should be calibrated at least once a year and as soon as feasible when a sensor is replaced.

Monthly calibration: The deflection sensors should be performed at least once monthly and promptly after a deflection sensor is replaced.

3.9.1 Calibration Type

1. Relative calibration:

With the help of relative calibration, the sensor's sensitivity and accuracy can be found. Relative calibration of the machine should be carried out approximately every month, depending on usage. Relative calibration is followed by reference calibration. This type of calibration can be done at any location, where pavement layer are strong.

2. Reference Calibration:

With the help of reference calibration sensor accuracy is ensured according to define

benchmarks. Multiple sensors are calibrated simultaneously. This type of calibration can only be done at calibration centers.

The sensors are calibrated by mounting the deflection sensors alongside a reference accelerometer in a rigid columnar stand. In the same position as reference calibration, relative calibration is carried out, and the process verifies the accuracy of the calibration. In the stand, sensors are rotated to eliminate any positional bias. Additionally, the fact that just one spin is necessary speeds up the process

3.9.2 Methods of Calibration (as per IRC:115, 2014)

1. Static calibration - The load cell(s) used in the FWD must be calibrated at a certified laboratory, and their values must be compared with the reference load cell. The FWD load cell measurements must be within 2% of the reference load cell readings.The date of the structural assessment of pavements utilising FWD should not be more than a year before the load cell calibration date.

2. Load Repeatability - Load repeatability must be checked before using the FWD. The load applied should generate a peak central deflection in the range of 250 μm to 600 μm.

3. Absolute calibration - The Stack test does the absolute calibration of geophones (as shown in Fig 3.8). This can be done by stacking all the transducers, one above the other, in a suitable rigid stand and placing the stand on the pavement surface. Deflection readings of all the transducers corresponding to a series of load drops are recorded and compared The deflections produced in this test should be in the range of 250μm to 600μm.Difference between maximum and minimum of the recorded (normalized) deflections should be within 4μ.

Fig 3. 8 Stack test for Calibration of the Geophones.

3.10 Deflection Measurement

For the augmentation of the FWD data steps which are followed are illustrated below:

1. For controlling the traffic a suitable arrangement is made.
2. For the future references paint is used to mark the test points.
3. Pavement and air temperature are recorded.
4. The FWD is placed properly over the test point so that loading plate is placed directly above the test point. Fig 3.9 shows the load pulse generating system of FWD. The Falling system is shown in Figure 3.10. It consists of the main cyclinder load cell , control box and GPS set up. The sensors or Geophones attached are shown in figure 3.11.
5. The Frame on which the sensors are attached in straigthtened and moved down on the surface of road so that probes of the sensors come in contact with ground. Then loading plate is positioned on the pavement surface as shown in figure 3.12 . Then falling weight are lifted to the desired height.
6. The data acquisition software is used with entering the suitable configurations.

Fig 3. 9 The falling weight system

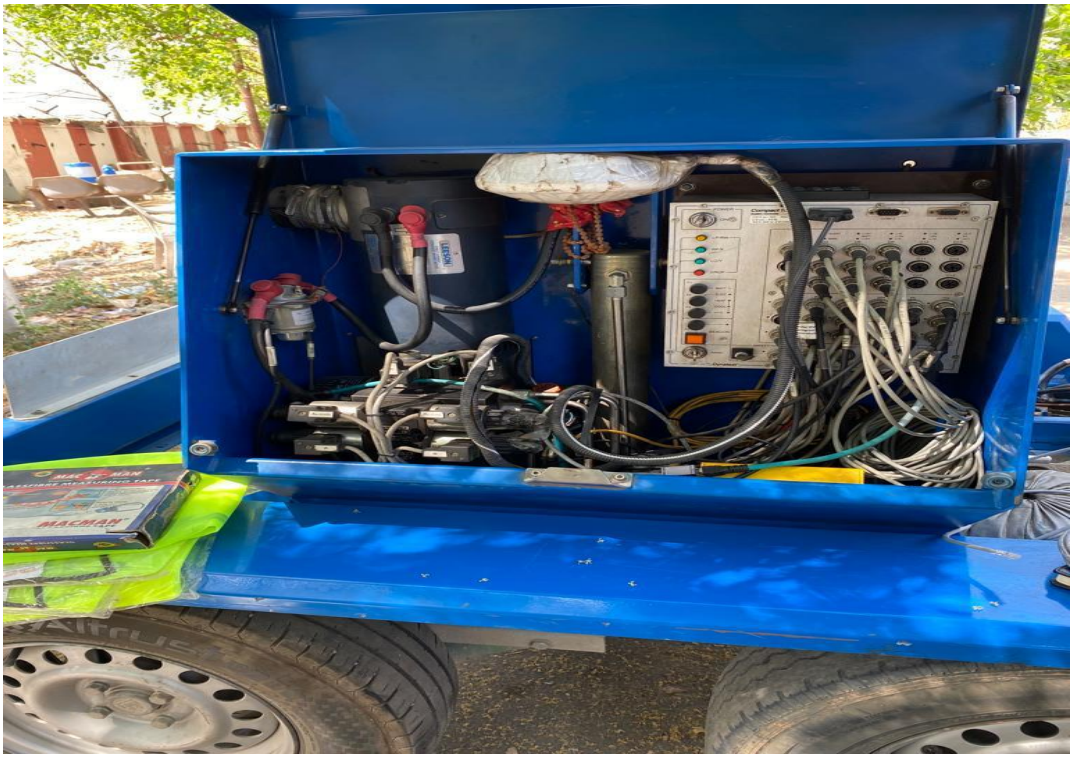

Fig 3. 10 Control Box of the FWD device

Fig 3. 11 Battery Box and GPS setup of the FWD device.

Fig 3. 12 Geophones (sensors)bar

7. The signals from the loads cell and the sensors are recorded in laptop when falling weights are dropped.

8. Firstly, one seating load is dropped on the pavement surface .Load and Deflection data is not to be recorded for the seating load.

9. The height of fall is customized in such a way so that the applied impulse load matched the desired load.

Fig 3. 13 Sensor bar in contact with the pavement surface

3.10.1 Pre-processing of measurements

In the study (Fontul 2004) discovered there are many factors such as change in temperature or peak load, that will affect the deflection during the testing. For comparing the results the measured deflection needs to be normalized first. To compare different drops generated by FWD deflections have to be "normalized" by linear extrapolation.

The aim is to eliminate the impact of these variables and reproducing the identical testing circumstances for all observed deflections The process is simple and is mathematically expressed as follows:

$$D_n = D_m \frac{Lt}{Lm}$$

Where ,

Dn – normalised deflection (µm)

Dm – measured deflection (µm);

Lt – target load (kN);

Lm – measured load (kN).

3.11 Deflection bowl evaluation

Different pavement layers have an impact on different areas of the deflection bowl..After normalizing the measured deflection bowl for target load the structural weakness can be indicated by the deflection plots.

The geometric properties of the pavement response (shape), such as curvature or amplitude, are represented by the deflection bowl parameters. The parameters (as shown in Table 3.2) , which are represented by deflections and/or relationships between them, provide information on the structural features of the pavement.

Table3. 2 Deflection bowl parameters

Name	Equation	Purpose
Distinct deflections – Centre deflection	Do	Reflects the overall pavement condition
Distinct deflections	Dr (r =1 to n)	Reflects the condition of layer at equivalent depth r
Surface Curvature Index, SCI	D0-Dr	Reflects the condition of bound layers
Base Curvature Index, BCI	Dn-1-Dn	Reflects the condition of sub-base layer
Deflection Ratio, DR	D0/Dr	Reflects the condition of layer at depth r

Where,

D0- deflection at the centre of the loaded area;
Dr- deflection at distance r from the centre of the loading plate;
Dn- deflection at the outmost deflection sensors;
Dn-1 -deflection at the next to outmost deflection sensors;
D2 -deflection at the deflection sensor closest to the edge of the loading plate.

3.12 Back-calculation

Back-Analysis is a database or iterative process for decreasing inaccuracies between measured and calculated deflections. Back calculating the pavement layer characteristics is a standard method for determining the structural performance of pavements. Layer elastic theory, layer thickness, and assumed layer moduli are used to calculate pavement deflections. Surface deflections measured are standardized to a reference load of 40 kN. The backcalculation using Nondestructive Testing (NDT) data is done to estimate the characteristics of the pavement material. Using appropriate analytic techniques, the pavement layer thicknesses and in-situ

material characteristics may be determined via back-calculation analysis from collected field data.

3.12.1 Steps included in the back-calculation process

1. Conduct FWD testing and document maximum surface deflections (the deflection basin) and determine the thickness of each layer of the pavement construction.
2. Initial moduli are used to calculate surface deflections to determine the pavement structure's stiffness. These are called seed values, usually estimated from user experience or various equations.
3. For each pavement layer, create a virtual model of the pavement structure, including thickness, estimated stiffness, and other (assumed) mechanical attributes.
4. Calculate the deflection basin caused by an FWD load using layered elastic analysis and a comparison is made between the estimated and measured deflection basins. Calculate the error based on the difference between basins.
5. Stop the operation if the error or layer stiffness has changed since the previous iteration. Alternately, alter the stiffness of the model's layers and repeat.

3.13 Corrections

There are two types of corrections applied on FWD readings:

- Correction of Temperature
- Correction of Seasonal Variation

3.13.1 Correction for Temperature

The back-calculated moduli obtained at temperatures other than the standard temperature will have to be corrected. Pavement temperature affects the back-calculated moduli of the surface layer. The standard pavement temperature is recommended as 35°C (**as per IRC 115-2014).**

$$\lambda \frac{1-0.238\ln(T1)}{1-0.238\ln(T2)} \qquad \text{.....eq (1)}$$

For Correcting the surface layer moduli value, a temperature correction factor is multiplied with the with the moduli value of surface layer for the given temperature as presented in equation below.

$$E_{T1} = \lambda\, E_{T2} \text{ .....eq(2)}$$

Where,

λ= temperature correction factor

E_{T1}= Back-calculated modulus (MPa) at temperature T1

E_{T2}= Back-calculated modulus (MPa) at temperature T2

3.13.2 Correction for Seasonal Variation

The pavement layer moduli values should pertain to the period when the subgrade is at its weakest condition. Moisture content affects the strength of subgrade and granular subbase/base layers. In India, this period occurs during the recession of the monsoon. It is, therefore, desirable to conduct deflection measurements during this period. Where the same is not feasible, a correction procedure should be adopted.

$$E\ sub\_mon = 3.351^{*}\ (E\ sub\_win\ )\ 0\text{-}7688 - 28.9 \ldots\ldots eq(3)$$

$$E\ sub\_mon = 0.8554^{*}\ (E\ sub\_sum) - 8.461 \ldots\ldots eq(4)$$

Where,

E sub_mon = subgrade modulus in monsoon (MPa)

E sub_win = subgrade modulus in winter (MPa)

E sub_sum = subgrade modulus in summer(MPa)

Seasonal correction factors for granular layers ;

$$E\ gran\text{-}mon = -\ 0.0003\ ^{*}(\ E\ gran\_sum\ )\ 2 + 0.9584^{*}\ (E\ sub\_sum) - 32.989 \ldots\ldots eq(5)$$

$$E\ gran\text{-}mon = 10.5523\ ^{*}(\ E\ gran\_win)\ 0.624 - 113.857 \ldots\ldots\ eq(6)$$

Where,

E gran-mon = granular layer modulus in monsoon (MPa)

E gran_win = granular layer modulus in winter (MPa)

E gran_sum = granular layer modulus in summer (MPa).

3.14 Back-calculation Programs:

There is a number of commercial software available for the back-calculation of layer moduli of highway and airfield pavements. Some of them are ELMOD-6, MODULUS, BAKFAA,

EVERCALC, KUAB, KGPBACK, and many more. This study includes the use of two software; the details of the software are described below:

3.14.1 KGPBACK Program

KGPBACK is software for the back-calculation and determination of pavement layer moduli recommended in IRC:115-2014. The software was developed at IIT Kharagpur and is a Genetic algorithm-based modified version of the BACKGA program. A linear elastic theory is utilized for the analysis.Three-layer system pavement model is recommended and Poissons ratio and thickness are not back-calculated. The Elastic moduli values of Surface, Base and Subgrade layers were obtained after inputting data in KGPBACK program.Table 3.3 shows the Input Parameters in KGPBACK software.

Table3. 3 Input Parameters in KGPBACK software

Parameters	Values	
Wheel Load (N)	40000	
Contact Pressure (MPa)	.56 (as per IRC:115-2014)	
Number of Deflection Measuring Sensors	9	
Radial distance (mm)	0,300,450,600,900,1200,1500,1800,2100.	
Poisson's ratio values	0.5,0.4,0.4 (as per IRC:115)	
Moduli range of layers	Granular layers (combined)	100 to 500 MPa
	BT Layer-thick layer without much cracking	750 to 3000Mpa
	BT layer in distressed condition (Fair to Poor)	100 to1500 Mpa

3.14.2 ELMOD-6

Dynatest International A/S created Elmod 6.0. Evaluation of Layer Moduli and Overlay Design (ELMOD) is a program that back calculates the mechanical material properties of uni-axial, semi-infinite pavement system i.e the elastic moduli of each structural layer in the pavement. Based on FWD deflection data, it is utilised to analyse pavement layer moduli and overlay design

There are 3 methods:

1. Radius of Curvature Method
2. Deflection basin Fit Method
3. FEM/LET/MET

Radius of curvature method: This method uses internal sensors to compute the upper pavement layer moduli and external sensors values to compute subgrade characteristics. The modulus values of the remaining layers are then calculated based on the overall pavement responseto the applied load.

Deflection basin Fit Method: It is based on the Odemark-Boussinesq approaches. In this method, the extra iteration process will use the convergence criteria based on the degree of fit among the calculated and the measured deflection basins.

The Elmod 6.0 program can directly read the Dynatest-FWD files. By selecting the analysis option, the program can automatically fit the calculated and measured deflection basins either for all points or point by point in the FWD files **(Elmod 6 Quick Start Manual, 2009).**

CHAPTER 4
STUDY AREA

4.1 GENERAL

Pavements contribute to ensuring the safe and efficient operation of transport infrastructures; they should be monitored over time to stop severe distresses due to the vertical and tangential forces transmitted by the aircraft. The Evaluation of the functional and structural performance of the pavements is done to ensure the safety and regularity of operations. The structural response of the pavement is analyzed to monitor runway evenness and predict its service life. The Airports Authority of India (AAI) must monitor the functional and structural characteristics, schedule maintenance work, and is responsible for creating, upgrading, maintaining, and managing civil aviation infrastructure in the country.

It is essential to examine the structural strength of the pavement using both destructive and non-destructive methods. A Falling weight deflectometer is a non-destructive method used for evaluating highway and airport pavements and is used to know the pavement's current conditions and suggest improvement measures.

4.2 Description Of Study Stretches.

4.2.1 Airport Pavement

A case study of a selected airport has been taken under investigation in this research. It is an international airport serving the twin cities of a state in India.

The selected airport has a total land area of 987.12 acres, making it one of the most land-constrained airports in India. The present airport includes a single runway orientated north-east to south-west.

FWD/HWD testing was performed on the main **Runway** and the new Extended **Apron** at the selected airport.

4.2.2 Brief Description Of Runway And Apron

According to International Civil Aviation Organization ICAO, a runway is a "defined rectangular area on a land aerodrome prepared for the landing and takeoff of aircraft." Runways are named between 01 and 36; the magnetic azimuth of the Runway heading in dec degrees, and the difference between the two numbers should be 18 (= 180°).

A runway numbered 09 points east (90°), runway 18 is south (180°), runway 27 points west (270°), and runway 36 points to the north (360° rather than 0°). Figure 4.3 and 4.4 show the starting and the ending point of the Runway

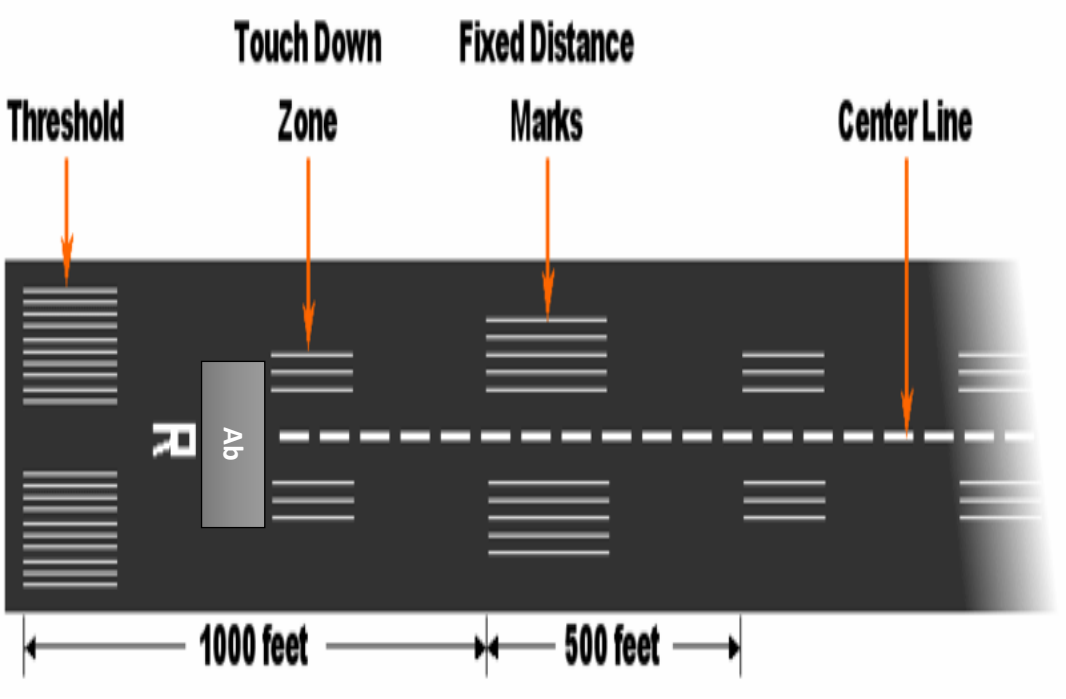

Fig 4. 1 Runway Markings (Source: https://en.wikipedia.org/wiki/Runway)

Table 4.1 Describes the total length and Width of the runway. A runway designator is a unique number given to the runway.

Table 4. 1 Description of the Runway

Runway Designator	**Ab-cd**
Total Length of Runway	**3,505 m**
Width of Runway	**45 m**

Fig 4. 2 Figure Map for the Main Runway (Ab-Cd) (Source: Google Maps)

Fig 4. 3 Starting point Main Runway end

Fig 4. 4 Ending point Main Runway end

Fig 4. 5 HWD survey on stand no. 37

To conduct pavement structural analysis of the New Extended Apron at the selected Airport, by non-destructive testing HWD testing was done. This Evaluation aims to obtain the Pavement Classification Number (PCN) of the New Extended Apron. The seven new parking stands were being operationalized at Apron-2, the international, and these bays are numbered 37 to 43 as shown in Figures 4.5 and 4.6.

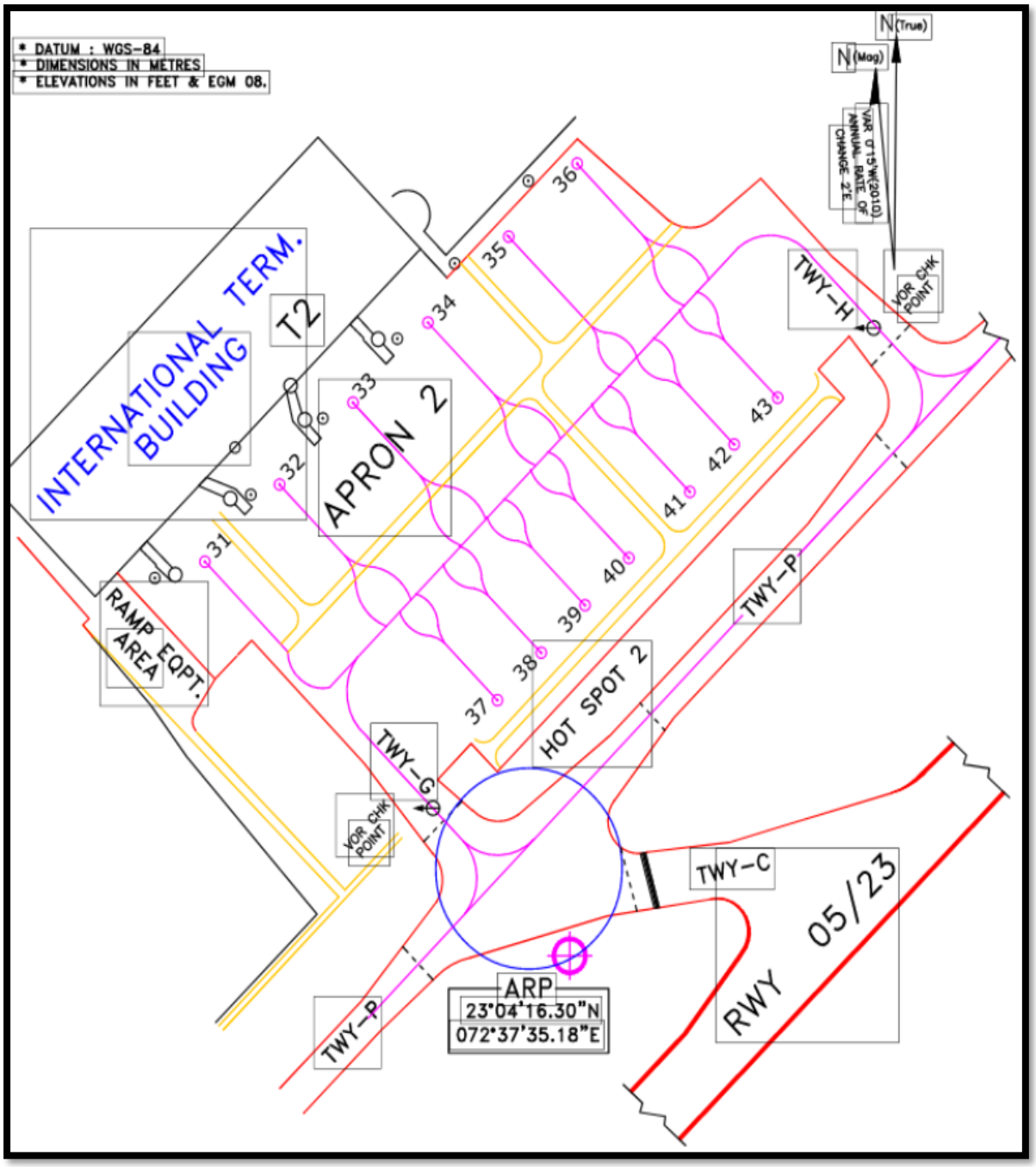

Fig 4. 6 New extended Apron-2 area

4.3 Highway Pavements

4.3.1 Case Study (Jetpur-Somnath Road, Gujrat)

NH 151, earlier known as NH 8D, connects Jetpur, a city in the Rajkot district of Gujrat, to the town of Somnath. It runs for a distance of 127 km. The road starts at Jetpur (km 0+000) at the junction of NH 8B and NH 8D, pass through Jetpur of Rajkot district & further runs across Junagadh district through Vanthali, Keshod, Veraval, and ends (km 127+000) at the approach to the Somnath temple near the western coastline. To construct four additional lanes to the Jetpur-Somnath section of the National Highway-8D in Gujarat, a section of this national highway was studied for the Pavement condition survey. This study measured each road section's cracking, potholes, rutting, and roughness. The location map of the project is given in Figure 4.7.

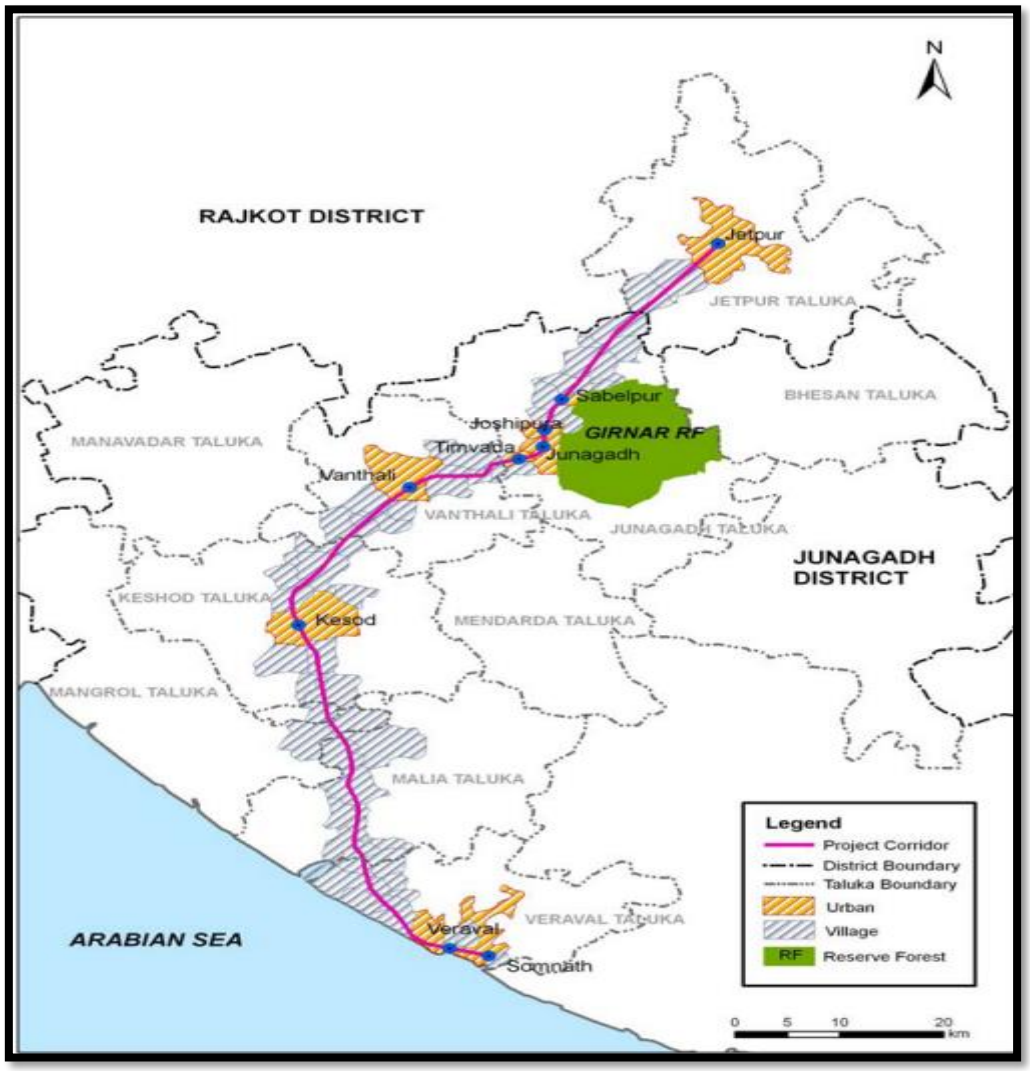

Fig 4. 7 Map for Jetpur -Somnath Road (Source: Google Maps

Table 4. 2 Details of the study stretch of road

Sl. No	Proposed Chainage (Km)		
	From	To	Length (km)
Section 1	4.00	23.00	19
Section 2	43.00	67.00	24
Section 3	79.00	127.00	48

4.3.2 Description of the Environment

1. **Climate:** Both districts' climate is characterized by a hot summer and dryness in the non-rainy seasons. The cold season from December to February is followed by the hot season from March to May. The south-west monsoon season is from June to September, followed by the post-monsoon season from October to November.

2. **Temperature:** The mean maximum temperature in the region reaches 41℃ in the warmer months from March to June. During the winter, the minimum temperature dips to 12.2℃, and the maximum temperature remains around 29℃. The lowest average monthly minimum temperature isapproximately 21℃.

3. **Rainfall:** Maximum rainfall occurs under the south-west monsoons (June-September). The annual rainfall of the project area is around 1097 mm.

4.4 Case Study of a selected Flexible pavement road.

A Highway pavement has been selected for the overlay design. A study stretch of approximately 7 km is taken. This section consists of a carriageway flexible pavement of width 7m with a shoulder of 1.5m. The existing flexible pavement with surface Layer 150mm & Granular Layer 550 mm for Pavement Overlay Design. The following pavement composition is proposed for calculations. Fwd testing was done and the was evaluated structurally.

4.4.1 Climate

The pavement location has a humid subtropical climate. With the monsoon season in the middle, summers are lengthy and hot, with very mild winters and unreliable rainfall.

Temperature range = 5℃ to 45℃.

The annual yearly precipitation = 1380 mm.

Yearly average temperature = 29℃.

CHAPTER 5

METHODOLOGY

5.1 Introduction

In this chapter, the methodology of the present research has been discussed. For Highway and Airport Pavements, deflection data was collected using F/HWD along with the temperature and test pit details. This chapter explains the methodology for Structural and functional Evaluation, the back-calculation process, and the calculation of ACN/PCN, Pavement Condition Index (PCI). A falling weight deflectometer test was done to determine the modulus of various layers.

5.2 Methodology adopted for selected Airport pavements

This study selected two pavements, the Runway and the Apron pavement of a designated airport. Structural Evaluation was done on both the runway and Apron pavements.

5.2.1 Structural Evaluation of Airport Pavement Using HWD

An airport pavement is a complex structure designed for its designated category of loading and provide support for the loads imposed depending upon the class of aircraft and to produce a firm, smooth & stable surface.

To fulfill these performance requirements, the pavement will need:

1. Pavement should have the capacity to support the imposed loads structurally.
2. Sufficient inherent stability to withstand the abrasive action of traffic, adverse environmental conditions, and other deteriorating influences;
3. To be maintained with regular and routine maintenance.

To determine if a current pavement can withstand a range of aircraft types, weights, and traffic volumes as well as to be used in the planning and construction of airport enhancements, airport pavement and structural studies are required.

5.3 Evaluation Process steps

The structural Evaluation of airport pavements is a systematic process. All evaluation projects involve a similar approach as described:

1. To review the history of weather records ,design considerations and construction data.
2. Visual condition surveys for both functional and structural pavement.It include an inspection and examination of the existing surface.
3. A condition index is specified for a pavement which indicates functional performance with

implications of structural performance. PCI is a numerical rating of the surface condition of a pavement.

4. Site inspection records search for physical tests and materials analyses. Sampling and testing provide information on the thickness, quality, and general condition of the existing pavement structure and materials.
5. A material evaluation for the design of an individual project will require more sampling and testing Nondestructive Testing (NDT) Using Falling Weight Deflectometer and Heavy Falling Weight Deflectometer.

5.4 Evaluation of selected airport pavement using HWD.

DYNATEST HWD was used in measuring the deflections and these deflections are measured by 9 different geophones at 9 different locations (0,200,300,450,600,900,1200,1500,1800).The testing was performed on the main **Runway (Ab-Cd)** and the **New Extended Apron area.** At each measurement, the designation of the measurement location, the position, time of measurement and surface temperature were recorded. The deflection data recorded at varying loads in the range of 150 kN to 300 kN was normalized to uniform load by the software simulating dynamic of mixed aircraft wheel loading.

5.4.1 Runway Pavement structure

The Airport has a total land area of 987.12 acres. The present airport includes a single runway (Ab-Cd) orientated in a north-east to south-west direction, with a length of 3,505 m and a width of 45 m. Runway (Ab-Cd) is divided into three sections along the length in this study, as shown in Table 5.1 and Figure 5.1.

Table 5. 1 Sectioning of runway

SECTION	LENGTH(m)
Section 1	0 - 2286
Section 2	2286 – 2743
Section 3	2743 - 3505

Fig 5. 1 Sectioning of Runway

The thickness values reported by AAI for three sections are given in Table 5.2(b) before the recarpeting and slope assessment works. The airport has undertaken a complete runway recarpeting after slope assessment. Cross-sections of the runway before works with layer thickness values are presented in figure 5.2. Rehabilitation of the runway is done in the year 2022,50 mm asphalt was milled, and an overlay of the required thickness is discussed further in chapter 6. Evaluation of runway before and after the slope assessment and the HWD deflection data for years 2021 and 2022 was analyzed for layer moduli.

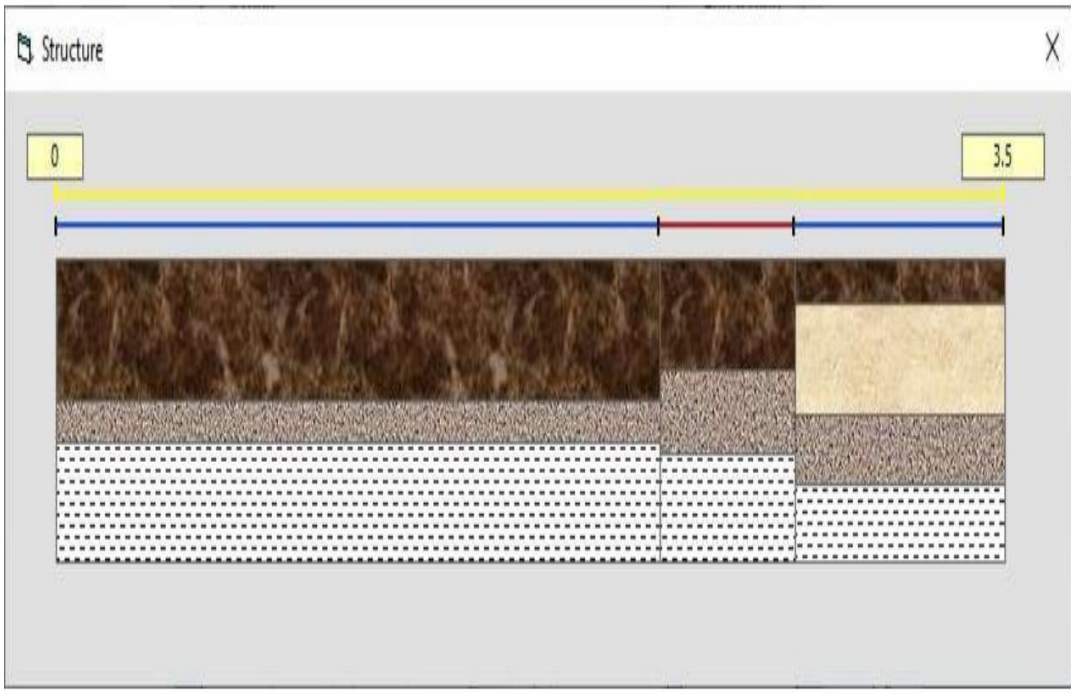

Fig 5. 2 Cross-Section of Runway Strip.

5.4.2 Steps for measuring deflection

1. Mark the test point and center the load plate over the test point on pavement Fig 5.3.

Fig 5. 3 Marking the test points.

2. The longitudinal and transverse slope of the pavement should not exceed 10 percent at the test location for accurate deflection measurement**.**
3. Lower the frame holding the displacement transducers (geophones) so that the transducers are in contact with the pavement surface.
4. Raise the mass to a pre-determined height required for producing a target load.
5. Raise the mass and drop. Record load and deflection data into the computer through a data acquisition system.
6. Raise the mass and drop. Record load and deflection data into the computer through a data acquisition system.
7. Record air & pavement temperature at an hourly interval.
8. Raise the geophone frame and load plate and move to the following test location.
9. Measure pavement temperature by drilling holes of 40mm depth into the pavement surface layer by using glycerol (Figure 5.4)
10. Deflection measurements should not be made when the pavement temperature is more than 45°c.

Fig 5. 4 Temperature Measurement

5.5 Extended Apron structure

Execution of Heavyweight deflection survey for Rigid New Extended Apron Section. The test loads were adjusted to achieve minimum deflection recorded for the farthest geophone, more than 100 µm. Three load drops were executed per test location. The deflection profile of the last drop was used for the Evaluation.

The HWD was equipped with ten geophones or deflection transducers. The transducers were arranged at distances of 0, 200, 300, 450, 600, 900, 1200, 1500, 1800, and 2100 mm from the load plate. At each measurement, the designation of the measurement location, the position on the slab, time of measurement, and surface temperature were recorded.

For every test slab, three load positions were tested on that slab, i.e. slab interior and transverse edge. The code for the interior and transverse position was 'A' and 'B, respectively. All geophones were placed on one slab, except in the case of deflection measurements across joints. The deflection measurements were undertaken on the transverse edge for the load transfer measurement across the joint. The geophones at D2 and D3 were designated for deflection recording across the joint and were placed directly at the joint in such a way that the distance from the center of the joint to these geophones was equal.

LAYER THICKNESS (As provided by AIAL) is appended below:

Table 5. 2 (a)Shows the pavement structure of Apron

Sr. No.	Layer Type	Construction Layer
1	PQC	425
2	DRLC	150
3	WMM	200
4	GSBC	600

Figures 5.5 & 5.6 is showing the HWD survey in progress on Stand 40 of the new extended Apron and flexible Runway (Ab-Cd), respectively. Crust thickness values of the runway pavement were also determined in Table 5.2(a).

This new Extended area of the airport includes several stands starting from stand 37 to stand 43. HWD was done on each of these stands.

Fig 5. 5 Heavy deflectometer testing in progress on Stand 40 Rigid.

Fig 5. 6Another view of Heavy deflectometer testing in progress on Stand 40 Rigid.

Fig 5. 7 Heavy Weight Deflectometer testing in progress on Runway (Ab-Cd)

Table 5.2 (b) Crust Details of the Runway Before Slope assessment works (Ab-Cd)

Chainage (from RWY 05)	As Reported by AAI(2013)		Layer thickness adopted in the design	
	Layers	**Thickness(mm)**	**Layers**	**Thickness(mm)**
0 -2286 m	DAC	50	Asphalt	500
	SDAC	50		
	Bituminous Concrete	400		
	PQC	150	Concrete	150
	Layers	**Thickness(mm)**	**Layers**	**Thickness(mm)**
2286 -2743 m	DAC	50	Asphalt	390
	SDAC	50		
	Bituminous Concrete	290		
	PQC	300	Concrete	300
	Layers	**Thickness(mm)**	**Layers**	**Thickness(mm)**
2743 -3505 m	DAC	50	Asphalt	150
	SDAC	80		
	DBM	100		
	PQC	400	Concrete	400
	WMM	250	WMM	250

5.6 Methodology for Back-calculation using Elmod-6 software.

There are two main methods for back-calculating pavement layer moduli and subgrade support conditions. The layered elastic theory is the foundation of method 1 and is frequently used for flexible pavement analysis discussed in Chapter 2. The second method, which is based on plate theory, was created particularly for Rigid pavements**.**

5.6.1 Back-calculation of Rigid Pavement

The PCC elastic modulus and the supporting medium's k-value are backcalculated using the deflections recorded on a PCC slab. While the k-value may be used to assess supporting layers, the PCC elastic modulus can be used to assess the PCC slab's structural health. Either a slab on an elastic solid base or a thick liquid foundation can be used to simulate the pavement structure. The AREA or Best-Fit technique can be used as the foundation for the plate theory approach.

AREA Method :

Rigid pavements are generally treated as two-layer systems because the base or subbase has little influence on the shape of the deflection basin compared with the influence of the PCC and subgrade.

The procedure consists of the following steps:

- Step 1: Drop the weight and record the applied load (P) and the resulting deflections.
- Step 2: Calculate the normalized area of the basin (AREA).
- Step 3: Determine the radius of relative stiffness
- Step 4: Backcalculate subgrade support (k or C for dense liquid or solid elastic foundation, respectively).
- Step 5: Back calculate the slab modulus of elasticity (E) if the slab thickness (h) is known, or, alternatively, define h if E is known.

5.7 Methodology for ACN/PCN Evaluation.

This section provides the methodology followed for PCN assignment and reports the bearing strength of airport pavements using the ACN-PCN system..

5.7.1 ACN/PCN METHOD

ICAO has established the ACN/PCN system to provide a load rating and evaluation system for airport operators (**ICAO 1983)**. "The bearing strength of a pavement intended for aircraft of New Extended Apron (ramp) mass greater than 5700 kg shall be made available using the aircraft classification number - pavement classification number ACN-PCN

method."**(International Civil Aviation Organization (ICAO) 2016)**.

The ACN is a unique number expressing an aircraft's relative effect on a pavement for a specified subgrade strength specifying a particular pavement thickness. It consists of a number on a scale, ranging from 0 on the lower end and with no upper limit, that is computed between two pavement types (rigid or flexible), and the subgrade support strength category.

According to ICAO standards, an aircraft with an ACN lower than or equal to the pavement load bearing capacity or PCN of the pavement structures can safely operate on the pavement without any weight restrictions.

The ICAO guidelines for PCN assessment provide for the utilization of any methodology which follows the basic pavement design and evaluation principles. The 'Technical Evaluation' method analytically assesses the pavement structural condition and further correlates the same with aircraft operations planned in the considered evaluation period for establishing the PCN value.

In this analysis the PCN value of the runway is determined by **'Technical Evaluation'** method. The PCN computations are based on the following assumptions.

- The Evaluation is computed using a design aircraft of known ACN values at maximum Operating Empty Weight and Maximum Takeoff Weight.
- The design of critical aircraft is representative of all aircraft in the fleet mix.
- The PCN-value is calculated on basis of actual damage by the traffic mix and cumulative damage factor (CDF) are also being adopted during PCN calculation.
- The PCN-value represents the critical location of pavement strength.

According to the range and bearing values of subgrade, ACN values are divided on the basis of these 4 subgrade categories shown in the table 5.3.

Table 5. 3 Ranges of standard subgrade strength (CROW-report D13-02 2013)

Subgrade Category	Pavement Type	Characteristic Subgrade Strength	Range of Subgrade Strengths
A – High	Rigid	150 $MN/m^2/m$	All k values above 120 $MN/m^2/m$
	Flexible	CBR 15%	All CBR values above 13%
B – Medium	Rigid	80 $MN/m^2/m$	60 to 120 $MN/m^2/m$
	Flexible	CBR 10%	CBR 8% to CBR 13%
C – Low	Rigid	40 $MN/m^2/m$	25 to 60 $MN/m^2/m$
	Flexible	CBR 6%	CBR 4% to CBR 8%
D – Ultra Low	Rigid	20 $MN/m^2/m$	All k values below 25 $MN/m^2/m$
	Flexible	CBR 3%	All CBR values below 4%

ACNs must be calculated using a prescribed technical method, which is clearly defined. An aircraft's ACN is calculated from its weight, wheel layout, tire pressure, and the ICAO strength category.

The ICAO PCN pavement strength reporting system involves publishing a five (5) part strength code in the form of 51 FDWT for flexible pavements or 62 RBWT for rigid concrete pavements. If desired, PCNsmay be published to an accuracy of 1/10th of a whole number.

The first number is the reported PCN value on a scale of 1 to about 130, with 1 representing a weak pavement and 130 a solid pavement. The second part of the code is either an "F" for flexible pavement systems or "R" for rigid pavement systems. The third part is a letter code A, B, C, or D indicating the subgrade/bearing strength, with A representing a high supporting strength and D a very lowstrength. The fourth part indicates the tire pressure limitation in MPa if applicable (X, Y, Z otherwise W).The fifth and final part of the PCN code indicates the evaluation method used to determine the pavement strength – "T" if derived from an engineering study or "U" if based on satisfactory aircraft usage.

Table 5. 4 PCN reporting format

PCN	Pavement Type	Subgrade category	Tire pressure	Evaluation method
	R – Rigid F – Flexible	A – Unlimited B – High C – Medium D –Very Low	Unlimited, no limit – W High, limited to 1.75 MPa – X Medium, limited to 1.25 MPa – Y Low, limited to 0.5 MPa – Z	T – Technical U – Using Aircraft

If the pavement is of composite construction, the rating should be the type that most accurately reflects the structural behavior of the pavements – either rigid or flexible. It is permissible to add a note statingthat the pavement is composite. Still, in the application, only the rating type ("R" or "F") is utilized in the assessment of the pavement capability. Pavements with gravel, compacted earth or unpaved, laterite, coral, etc. surfaces are classified as flexible for reporting, and therefore should be rated with a PCN with a pavement code "F."as shown in table 5.4.

The tire pressure limits were recently revised to accommodate the tire pressures of modern

aircraft. Theresults of two independent series of full-scale tests showed that increasing tire pressure from 1.5 MPa to to1.75 MPa did not adversely affect pavement rutting to any significant degree at HMA temperatures representative for airport operations in hot and temperate climates. The rutting, as measured in the tests, did not affect the structural capacity of the lower layers of the pavement structures. That is, the life of the pavements would not have decreased due to increasing tire pressure. The result of an ACI survey of pavement conditions at worldwide airports in all climatic regions supports the conclusions of the full-scale tests. The Pavement Study Group of the ICAOs Aerodromes Panel in 2010 reached a consensus that tire pressure categories could be formally and permanently changed to be more consistent with the tire pressures of current and future aircraft without affecting the performance of airfield studies.

Table 5. 5 New tire pressure categories and designations

Tire Pressure Category	Former ICAO designations and limits	Revised ICAO designations and limits
W	High: no pressure limit	Unlimited
X	Medium: pressure limited to 1.50 MPa	High: pressure limited to 1.75 MPa
Y	Low: pressure limited to 1.00 MPa	Medium: pressure limited to 1.25 MPa
Z	Very low: pressure limited to 0.50 MPa	Low: pressure limited to 0.50 MPa

5.8 PCN ASSIGNEMENT PROCEDURE

The PCN technique or technical evaluation method employed for this study necessitates familiarity with the pavement and its traffic. This approach involves using all the variables that go into pavement analysis, including design traffic, aircraft characteristics, pavement design specifications, and engineering expertise.

The procedure is well documented in CROW's Guideline on PCN Assignment. The PCN method presented herein is appropriate to the pavement construction type to determine the structural capability of pavement to support proposed aircraft loads and traffic levels.

The PCN numerical value is determined from the pavement's allowable load-carrying capacity or allowable load rating. Acceptable load ratings are discussed regarding aircraft gear type and mass ross weight. The allowable load to use is the maximum permissible load of the most critical aircraft that can use the pavement for the number of equivalents passes expected to be applied for or consume the remaining life.

Steps followed in PCN assignment of the flexible and rigid pavements is given below(CROW-report D13-02 2013)

Step 1- Select the PCN-pavement life course to use up the pavement's structural capacity. There are two main input parameters for calculating PCN i.e., the pavement life course and the forecasted traffic. PCN, by definition, is the ACN-load of the critical aircraft that wears out the total structural life in a certain period of time.

However, assigning a PCN to a pavement represents that the pavement can bear the forecasted aircraft without weight restrictions.

Step 2- Pavement Structure:

The characteristics of the pavement structure determine the bearing capacity of the pavement. The pavement is broken down into distinct layers and subgrades with structural parameters (Elastic Modulus, Poisson's Ratio, and thickness).

Step 3- Pavement Materials

Determine the pavement layer material types and their characteristic modulus values. A pavement deteriorates gradually. In an analytical design approach, every aircraft pass consumes a bit of the structural pavement life. The end of the structural life is reached when the Cumulative Damage Factor or CDF is 1.0.

Step 4 - Aircraft traffic

1. Determine the traffic volume in terms of the type of aircraft and number of future operations or coverages of each aircraft that the pavement had and will experience over its PCN pavement life course

2. Determine the critical aircraft of the forecasted fleet mix in terms of structural damage by simply taking the aircraft with the highest ACN or calculating the damage factors. A damage factor is the reciprocal value of the number of allowable aircraft passes. The ACNs at OEW and MTOW of that so-called critical aircraft are to be used in the PCN evaluation;

3. Determine the number of equivalent coverages of the forecasted fleet expressed in the critical aircraft. Note: The PCN is based on the actual fleet mix that uses the pavement. Lateral wander has a positive influence on pavement life. Wander effects are addressed with a normalized beta distribution. The degree of the lateral wander depends on the type of pavement, aircraft mode and width.

Step 5- PCN Assessment: pavement life and PCN calculation Based on the total expected equivalent movements of the design aircraft (with a given ACN value) and the representative calculated properties of the pavement structure, the PCN value of the structure is calculated.

1. Calculate the accumulated pavement damage in Palmgren-Miner due to the forecasted fleet (incl. wander and for the PCN-pavement life course).

2. Compute the Allowable Gross Weight (AGW) of the critical aircraft by varying the load of the undercarriage of the critical aircraft resulting in the same Miner damage as computed in the previous step;

3. Once the allowable load (or weight) is established, determining the PCN value is converting that load to a standard relative damage value (i.e., ACN). Look up the ACN using the published ACN data, and calculate the ACN of the critical aircraft at its maximum allowable weight;

4. Assign the ACN of the critical aircraft at the maximum allowable weight to be the PCN of the pavement. Should the PCN exceed the ACN of the critical aircraft, the PCN-life course can be prolonged or limited to the ACN value of the critical aircraft.

The PCN numerical value for a particular pavement is determined from the allowable load-carrying capacity of the pavement. The PCN is defined as the ACN-value of the critical aircraft operating with a Gross weight determined by the airport operator that consumes the PCN-pavement life. The PCN values are accompanied by codes indicating the Pavement Type, Subgrade Category, Aircraft Tyre Pressure Category, and the Evaluation Method.

5.9 PCN Calculation using ELMOD-6

PCN calculations can be run whenever back calculations have been carried out for the data file. Results from the PCN calculations can be viewed and compared to ACN values using the **Plot** features.

Elmod provides two different procedures for estimating PCN values. The recommended procedure is the **PCN/ACN Using Fleet Mix** method, which considers the damaging effect of each aircraft type and related traffic volume. It utilizes the material models as defined with normal mechanistic design. Using Unrestricted Traffic is still possible to use the old conventional method, referred to as PCN/ACN.

A new concept for calculating PCN values has been introduced, which is more in accordance with usual mechanistic design. This includes the damaging effect of each aircraft in the fleet

mix using each aircraft's yearly traffic and the layers' design life. Besides this, as a default, all layer damage functions are included in the analysis. For each test point, the critical aircraft and response will be found, and the PCN value is calculated as the ACN value for the weight giving a damage equal to 1(Elmod 6 Quick Start Manual 2009)

The PCN value depends on the aircraft mix and traffic volumes. If there are changes to the aircraft mix, new PCN calculations must be performed.

A strong pavement can have a low PCN value, if the calculations have only included light weighted aircraft types.

The calculation flow is as follows

1. Backcalculation of elastic moduli. When back-calculation is done, all following tasks are done automatically when starting a design and PCN calculation.

2. Calculate reference moduli and seasonal moduli according to the chosen parameter setup.

3. Calculate the subgrade category as a weighted average of the seasonal elastic moduli or k-values. The values are weighted according to the length of the seasons and the traffic volume in each season.

4. For each aircraft type and each wheel configuration, and for each season and each layer calculate the responses specified in the parameter setup.

5. Calculate the damage for each aircraft type, season, and response type using the damage criteria for the response types and design life as defined in the parameter setup.

6. Sum up the damages over the seasons for each aircraft type and response type. Export these data to the Elmod database "Damages" table to be used later for plotting.

7. Calculate total damage (D_t) for each response type as the sum of damage for each aircraft.

8. Calculate the Permissible Weight Multiplier (WM) for each defined criterion using the exponential constant B from the criterion:

$$\varepsilon \ (or \ \sigma) \ = A \cdot \left(\frac{N}{10^6}\right)^B \cdot \left(\frac{E}{E_{ref}}\right)^C$$

as: $WM = D_t^B$

9. Select the critical criterion with the lowest Permissible Weight Multiplier.

10. For each aircraft, calculate the permissible weight $W_p = W * WM$, where W is the MTOW of the aircraft (Maximum Take Off Weight). W_p will be the weight giving damage of 1.

11. For each aircraft, use W_p to calculate the PCN value. This is done by loading the ACN values from the aircraft database for the given subgrade category and pavement type for the four weights for which ACN is listed. Using linear interpolation, calculate the ACN of the aircraft for the weight W_p

12. The aircraft with the highest ACN, as found in the previous step, is identified as being the critical aircraft, and the ACN value for the weight W_p is reported as the PCN of the pavement.

5.10 Methodology adopted for selected Highway Pavements

There are two different case studies taken under in this research. The pavements had been evaluated structurally and functionally. Functional Evaluation of pavements consists of collecting road condition data related to surface distress crack area and cracking pattern, raveled area, pothole area, and surface roughness. Structural Evaluation of the pavement refers to identifying the current structural state of individual pavement layers and assessing the overall pavement strength.

5.11 Functional Evaluation of selected Pavement

Functional condition refers to the condition of pavement as its general appearance. The information about pavement characteristics affecting road users' safety and comfort is given by function evaluation. Functional conditional is concerned with ride quality and safety. The surface condition of flexible pavement can be evaluated by the ruts, patches, cracks, and unevenness. For assessing the functional properties of pavement Pavement Condition survey is done as per **(IRC 81-1997) (Clause4.2).**

5.12 Pavement Condition Survey

A pavement condition survey provides the physical condition of the pavement by visual inspection. The survey was carried out on the case study I study area (Jethpur-Somnath road) as per ASTM D-6433 to examine the functional efficiency of the existing pavement. The pavement was divided into section and each section was divided into sample units.

By visual observation, collection of distress data and measurement of various distresses along

with their magnitudes is done. Different surface distresses collected in this study for flexible pavement are cracking, rutt depth, raveling, potholes, patching, and edge break.

The survey results were summarized according to the type of damage and severity for the examined unit, then PCI values were calculated, and repair options were determined according to the type of damage **(Rusmanto, Syafi'I, and Handayani 2018)**.

5.12.1 Advantages of a Pavement Condition Survey

The type and amount of each pavement distress and overall condition rating number for each section can be known by the survey, which helps in planning the short as well as long term budget goals. Moreover, the maintenance and rehabilitation activities can be prioritized by doing a condition survey (Sharpe, Southgate, and Deen, n.d.)**.**

5.13 Conducting The Pavement Condition Survey

A trained rating team will conduct the survey. Visual obervations were made and on that basis rater will rate the distress following the definations include in the ASTM D-6433 manual.

5.14 Condition rating System

A rating dependent on the condition is given to the pavement and is based on the distress such as cracking, roughness, deflections and many more. the rating system is grouped into two part estimated condition rating and measured condition rating Fig 5.8(Okine and Adarkwa 2013)

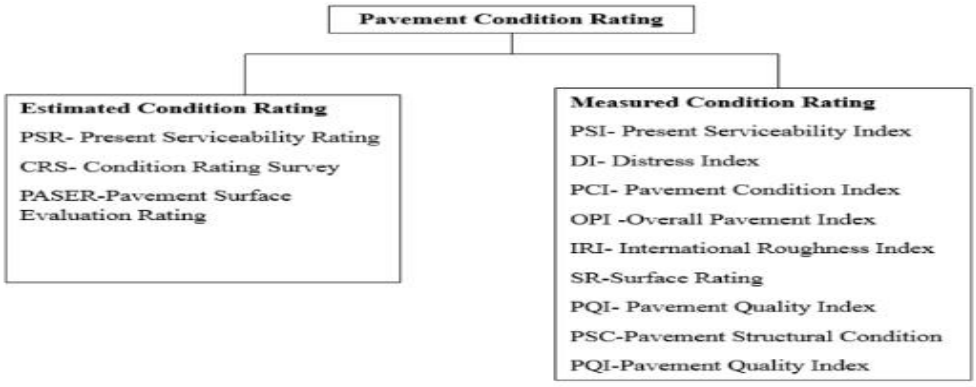

Fig 5. 8 Condition system rating(Okine and Adarkwa 2013)

Based on the ride quality of the pavement as per AASTHO the condition rating index is Pavement servicibility index (PSR). The scale used is 0 to 5 where 0 is very poor with large potholes and distress over 75% and 5 is very good distress free.

5.15 Pavement condition index.

PCI is a measured condition rating and is a numerical indicator that evaluates the overall surface

condition of a road or pavement developed by the United States Army Corps of Engineers. The PCI level is written in the 0-100 level fig 5.9. According to **(Butt, Abba, M. Y. Shahin, Samuel H. Carpenter, n.d.,1994)**The condition of the pavement road is divided into several levels

PCI Value	Pavement Condition
0-10	Failed
10-25	Very Poor
24-40	Poor
40-55	Fair
55-70	Good
70-85	Very Good
85-100	Excellent

Fig 5. 9 PCI and Pavement condition values (Butt, Abba, M. Y. Shahin, Samuel H. Carpenter, n.d,1994.)

5.15.1Various Distresses

1. Raveling: The wearing away of the pavement surface due to loss of the asphalt binder. The loss of asphalt often happens as the binder hardens with age, and the binder cannot hold the aggregates may be because of a lack of compaction during construction.

Severity Levels:

- **Low-** Small amounts of pitting may be detected. In the case of oil spillage, the oil stain can be seen, but the surface is hard and cannot be penetrated with a coin.
- **Medium** —Aggregate or binder has worn away. The texture is moderately rough and pitted. In the case of oil spillage, the surface is soft and can be penetrated with a coin.
- **High** —Aggregate or binder has been worn away considerably. The surface texture is very rough and severely pitted.(D 6433(ASTM), n.d.).

2. Aligator cracking: Cracking develops at the asphalt surface's or stabilised base's bottom, where tensile stress and strain are greatest under a wheel load. Alligator cracking, also known as fatigue cracking, is a network of interconnected fractures created by fatigue failure of the asphalt concrete surface due to repetitive traffic pressure. Only in places susceptible to frequent traffic loads, such as wheel tracks, does alligator cracking occur.

- **Low level** indicates Fine long hairline cracks
- **Medium level** indicate initial of crack pattern & **High level** the well crack pattern.

Fig 5. 10 View of cracks with medium severity at 9+300 km.

3. Potholes: These are bowl-shaped depressions on the pavement surface and are usually less than 750mm**.** High-severity alligator cracking, causing the removing of aggregates and forming a hole with sharp edges are identified as potholes. The pothole depth of 0-25 mm with 200mm wide, 25-50 mm with 500mm wide, and more than 50mm and 500mm wide is classified as low, moderate, and high severity levels, respectively. Potholes are measured by counting the number and recording them separately.

4. Edge drop: difference in elevation between the pavement edge and the shoulder. This distress is caused by shoulder erosion, shoulder settlement, or by building up the roadway without adjusting the shoulder level. Lane/shoulder drop-off is measured in linear meters (feet).

- **Low level** indicates the difference in elevation between the pavement edge and shoulder is greater than 25 mm and less than 50. **Medium level** means the difference in elevation is Greater than 50 mm (2in.) and less than 100 mm (4 in.). **High level** indicates the difference in elevation is greater than 100 mm as shown in Fig 5.11.

5. Rutting : Depression is caused by repeated traffic on the same place in the wheel paths. Pavement is lifed up from the sides of the rut. Rutting stems from a permanent deformation in any pavement layers or subgrades, usually caused by consolidated or lateral movement of the materials due to traffic load.

Low level —6 to 13 mm (1⁄4 to 1⁄2 in.)

Medium level — >13 to 25 mm (>1⁄2 to 1 in.).

High level — >25 mm

Rutting is measured in square meters (square feet) of surface area, and the mean depth of the rut determines its severity

Fig 5. 11 View of Edge Drop at 93+Fig 5.6 View of Edge Drop at 93+300km

5.16 Steps to Calculate PCI

1. Decide upon the number of defects/distress to be considered to calculate PCI.

2. Assign a particular weightage to each distress/defect. 3. Choose a particular scale to rate from for each distress.

4. Assign a rating to each particular distress depending upon the minimum and maximum value of each distress. For example, if the rating scale is 0-5, then 0 represents no defects and 5 represents maximum defects.

5.After rating each distress add all distress to obtain a sum.

6. Subtract the sum from 100 to get the PCI value.

5.17 Structural evaluation of pavement

Structural evaluation of the pavement examines the overall pavement strength. The primary objective of a structural evaluation program is to determine the effective structural capacity of the existing pavements.

Structural evaluation is done to estimate the structural capacity and predict the remaining life of pavement. The F/HWD is used for the evaluation as per IRC 115-2014.

Analysis steps :

- Raw data extraction
- Normalization & Average
- Min & Max Ranges for BT, Granular, Sub grade layers
- Crust thickness
- KGP BACK Analysis (E values)
- Temperature corrections
- Seasonal corrections
- Dividing Sections
- 15 percentile value
- Calculating strains by IIT PAV
- Calculating Fatigue & Rutting Life
- Calculating Remaining life
- Design over lay

CHAPTER 6
DATA ANALYSIS

Data gathered through the Pavement condition survey and F/HWD testing on the study stretches of Highway and Airport pavement were analyzed. For the back-calculation of Airport pavement, the ELMOD-6 program and KGPBACK software were utilized for Highway pavement. ACN/ PCN numbers were determined using the ELmod-6 software using the vehicle fleet mix. The distress values for selected highway pavements were noted, and the pavement classification index was calculated. The back-calculated pavement layer modulus values of stretches of roads under study obtained from ELMOD-6 and KGPBACK were compared.

6.1 Evaluation Of Selected Airport Pavement.

The HWD data collected from the Runway and Apron at selected airport is investigated. Airfield pavements are of two types: flexible and Rigid. A runway strip is a flexible pavement made of asphalt concrete surface that transmits the load from granular contact. The Apron has a rigid/concrete pavement made of Portland cement concrete that transfers the load like a beam.

6.1.1 Processing of Load and Deflection Data

Deflections can be calculated using load and measured deflections at 9 different sensor locations (0,300,450,600,900,1200,1500,1800,2100) using HWD. The runway strip was 3505 m long and 45 m in width. The pavement width was divided into two sections, L.H.S and R.H.S, along the centreline. The markings were made for the evaluating runway at 3m,6m, 9 m and 20 metre distance on both sides of the centerline. Fig below shows the marking done on the runway for HWD testing.

Fig above shows markings along the width of the runway.

The HWD data was collected on all of the 9 different marked located. The HWD deflection data collected for L.H.S of the runway is presented from Table 1 to Table 4 in Appendix-A.

6.1.2 Back-calculation of layer moduli using ELMOD-6 software.

The detailed operation of evaluating the Structure of a flexible airfield pavement using ELMOD-6 is explained as follows. ELMOD is a short form used for the Evaluation of Layer Moduli and Overlay Design. The software analyses the pavement response from the HWD and FWD by determining the different layers' modulus, stress, and strain.The program started by selecting the ELMOD-6 icon, and the screen in figure 6.1 was displayed.

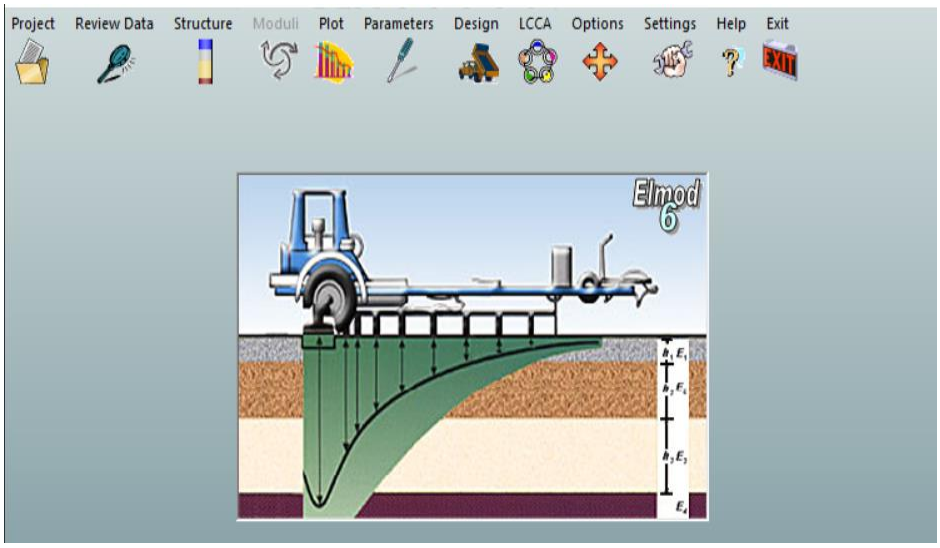

Fig 6. 1 Elmod-6 Main screen

Add the deflection data file and create new project by selecting the **Project** option as presented in figure 6.2. The user can open and analyze all standard FWD files stored by a Dynatest FWD or HWD regardless of field program version or file format. A standard dialog box enables choice of directory and subdirectory location. By default, all files having extensions as FWD, F10, F20, F25 and MDB. **(Elmod 6 Quick Start Manual 2009).**

To create a new project database select: *Project → Database → Create New*

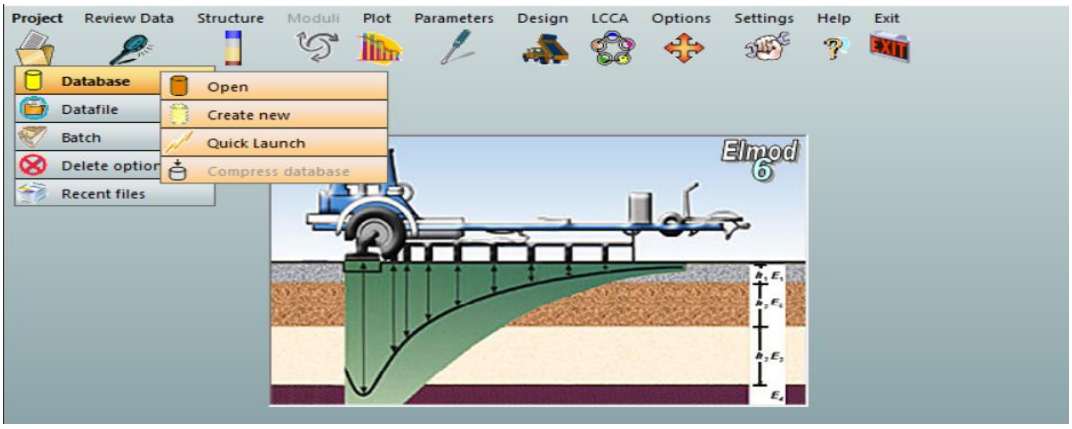

Fig 6. 2 Create the new project

I. Review Data

It permits viewing and editing of data from an opened data file. It is possible to see and change temperature curves as presented in figure 6.3.

Prior to doing any back-calculation and design calculations require knowledge about the pavement structure's composition. To do this, a number of the pavement structure's layers and thickness must be specified.

II. Structure

Select **Structure** from the main menu as presented in Figure 6.3. The road could be separated into subsections corresponding to each distinct structural pavement segment if the deflection data were collected on a road with varied layer thickness or a number of layers. To achieve this, click Add section.

Layer thickness and seed modulus are typed in fields, **Elmod 6** can handle up to 5 layers, including the subgrade shown in Fig 6.4. Layer 1 is assumed to be the surface course as thickness is entered as top to bottom. Since the subgrade is infinitely thick, no thickness information is entered for this layer. To activate the rigid layer calculations Max depth to rigid layer field is entered.

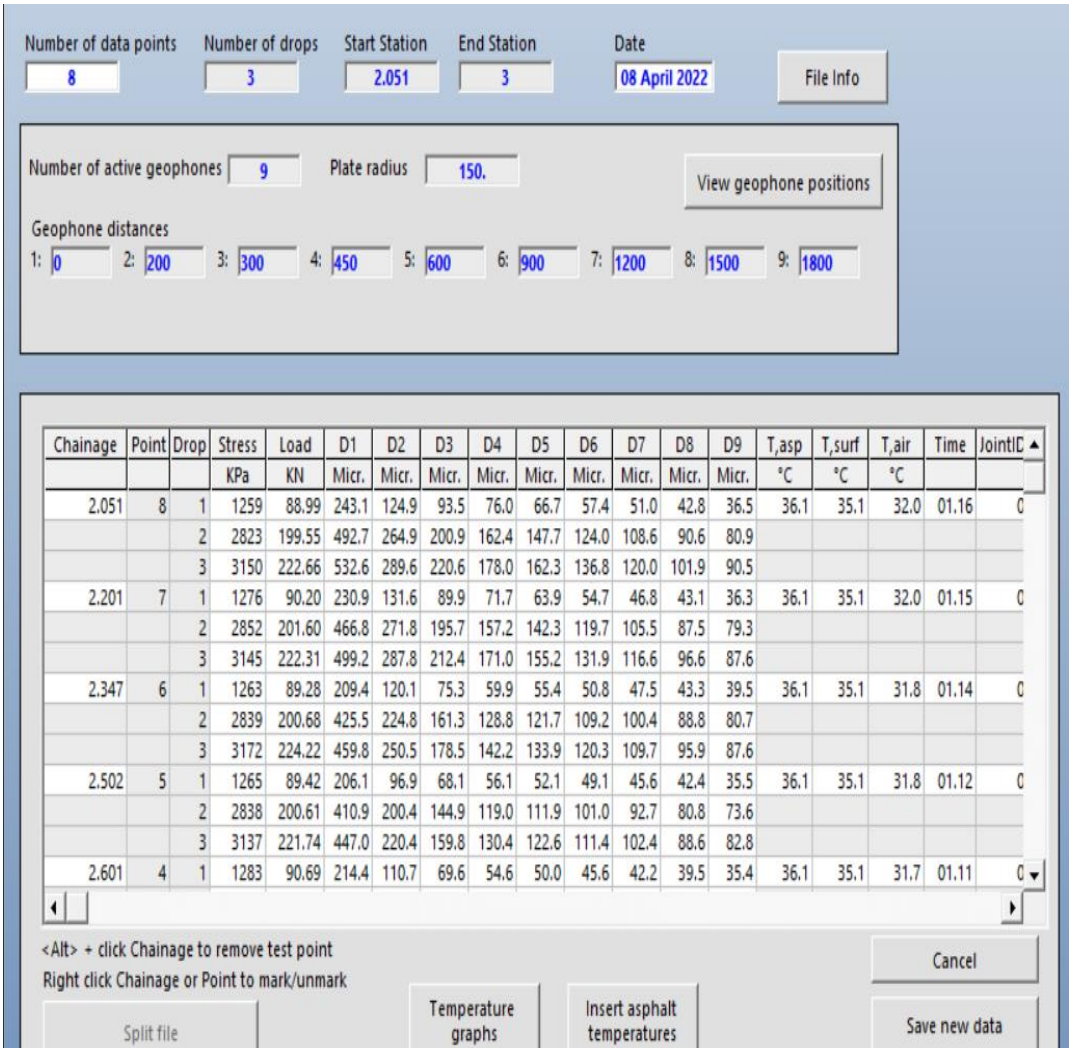

Fig 6. 3 Review Data screen

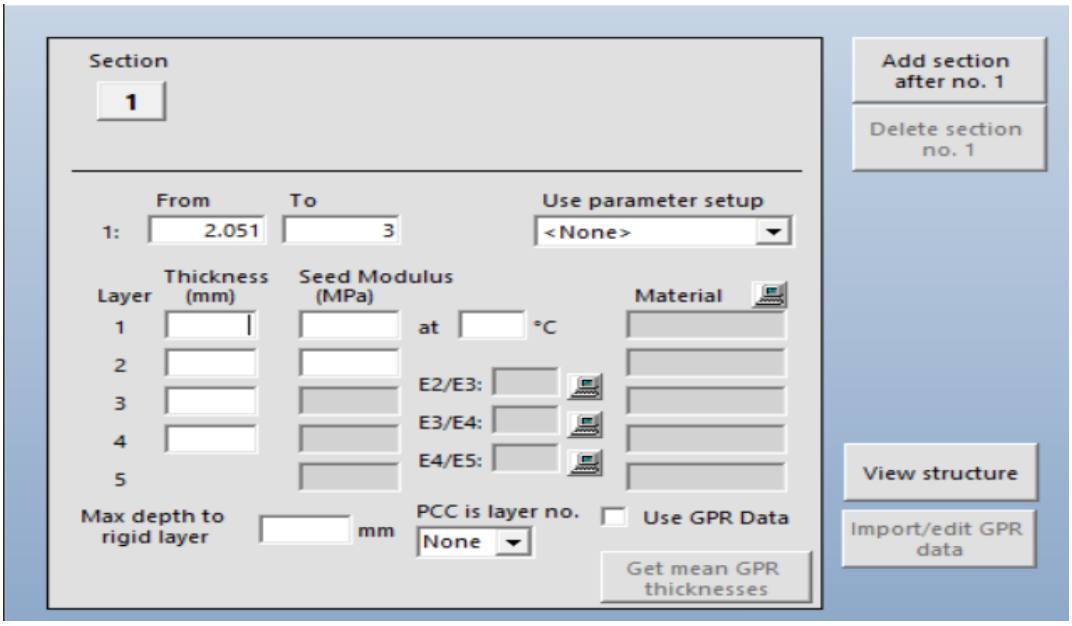

Fig 6.4 Structure input Screen

III. Moduli

After entering the pavement structure details to initiate the back-calculation of layer modulus values, click on Moduli from the main menu. The Moduli window screen will appear as presented in Figure 6.4. After selecting the drops, the section either **Radius of Curvature** or **Deflection Basin Fit** or **FEM/LET/MET** is selected for back-calculation if included.In this study Deflection Basin fit was used.

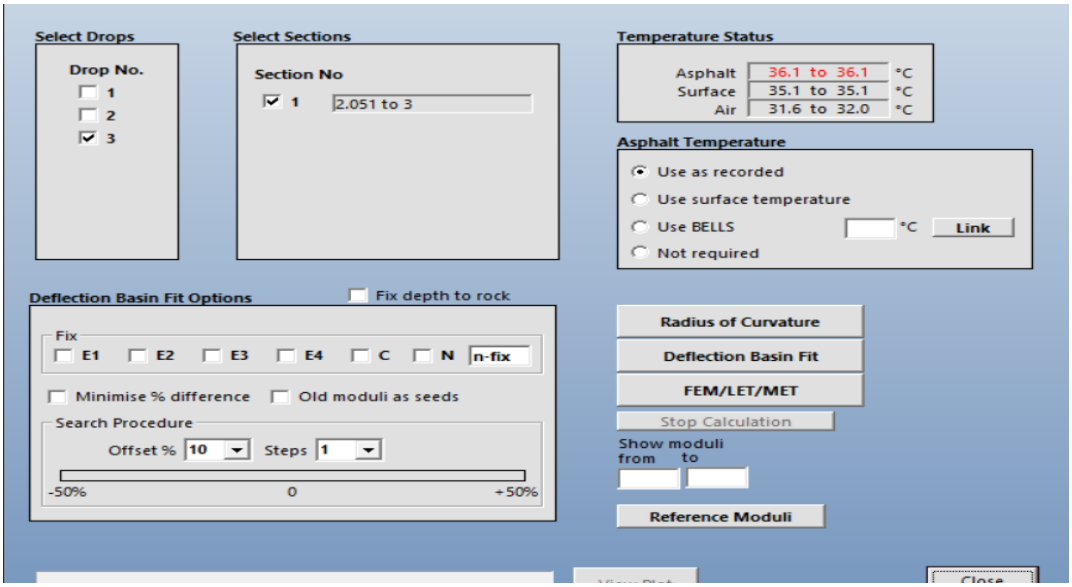

Fig 6. 4 Screen showing the Moduli window

IV. Deflection basin method

A collection of estimated pavement structural moduli is the foundation for the basin fit option technique. For this pavement construction, the theoretical deflection bowl is determined.

The difference between the estimated and measured deflections is then evaluated. The structure's moduli are then adjusted (often by 10%). If the error in either deflection bowl is smaller than the initial deflection bowl, it is assumed that this is a superior solution.

The method is repeated until there is a minimum error between the calculated and measured deflection bowls.

The Layer moduli determined after the slope assessment and recarpeting works from the basin method along 3m LHS, 6m LHS, 9 m LHS, and 20m LHS are given in Tables 5,6,7and 8(a), respectively in Appendix -A.

A similar analysis was done the previous year for the same runway before the slope assessment and recarpeting works. The layer moduli obtained along 3 m LHS is given in table 8(b) in Appendix-A.

V. Plot

After the back-calculation step, the results and the measured deflection data are presented by clicking the **Plot** option from the main menu bar.

Figures 6.5,6.6,6.7,6.8 and 6.9 show the variation of Deflection measurement at a distance of 3m LHS, 6m LHS, 9 m LHS and 20m LHS from the centreline for runway pavement, respectively.

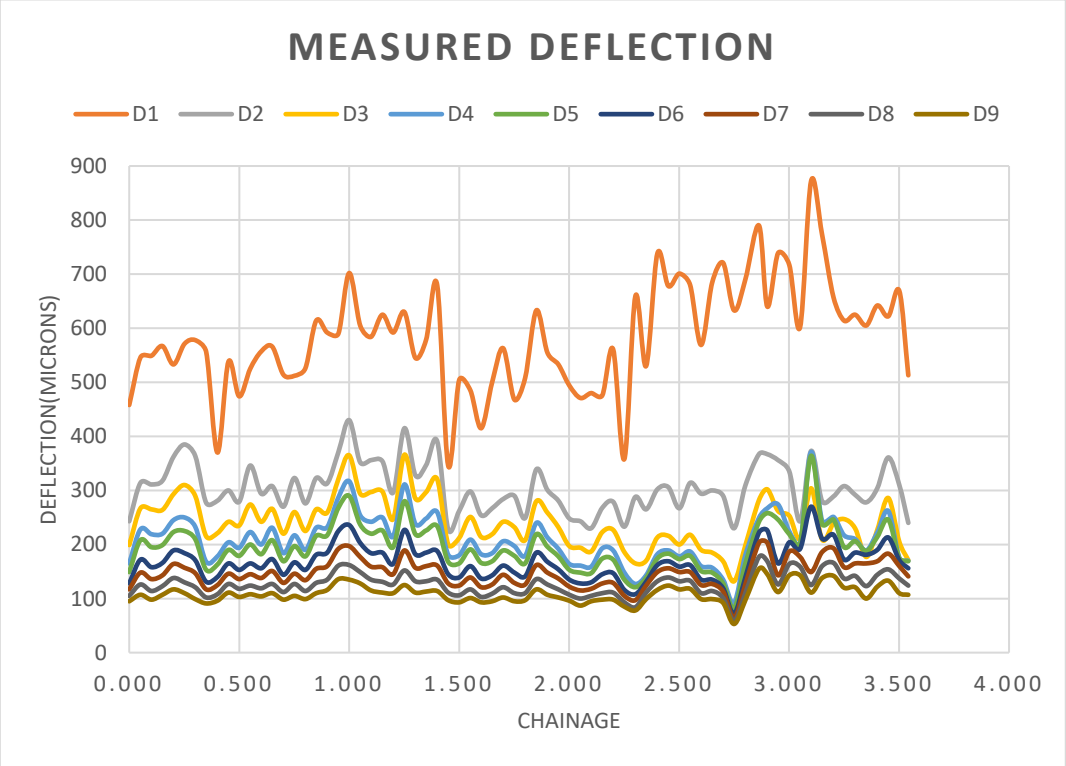

Fig 6. 5 Variation of Deflection measurement along 3m LHS from the centreline

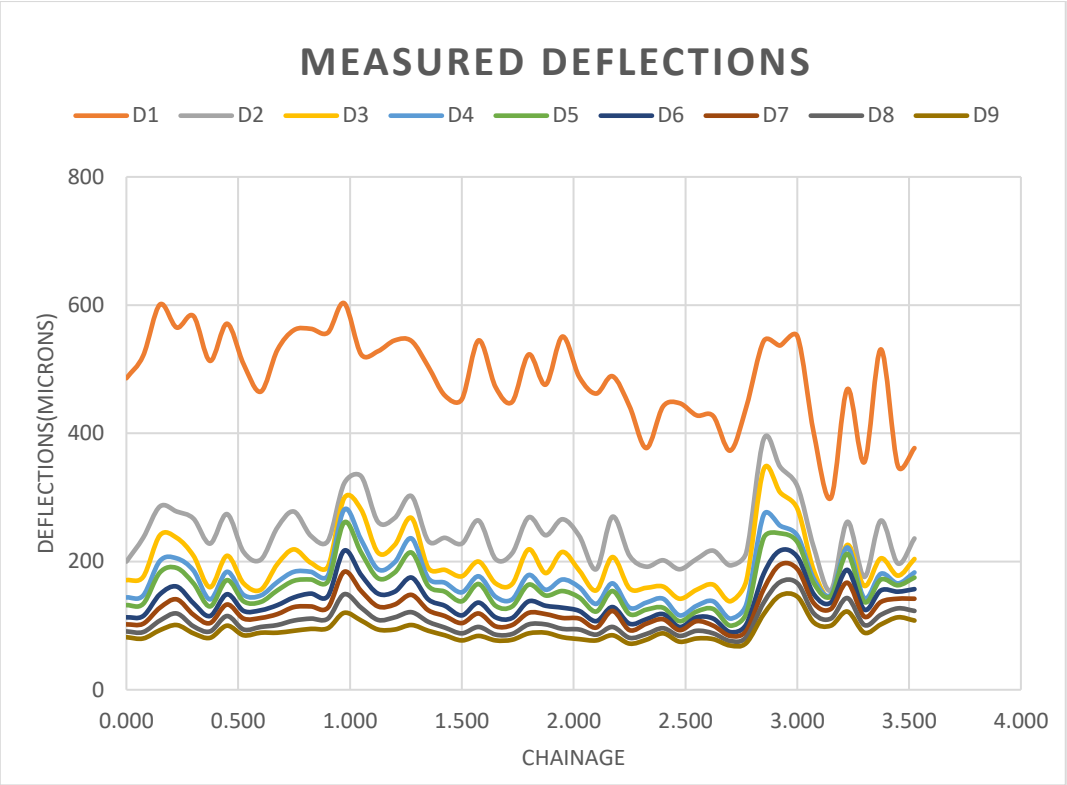

Fig 6. 6 Variation of Deflection measurement along 6 m LHS from the centreline

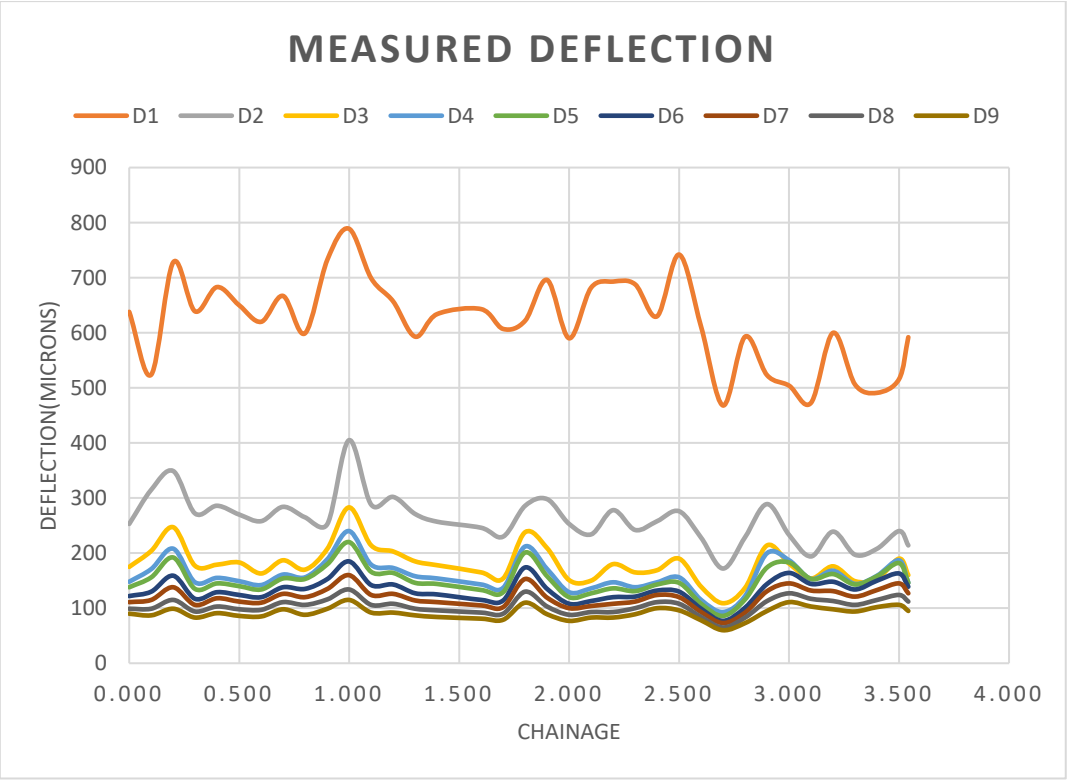

Fig 6. 7 Variation of Deflection measurement along 9 m LHS from the centreline

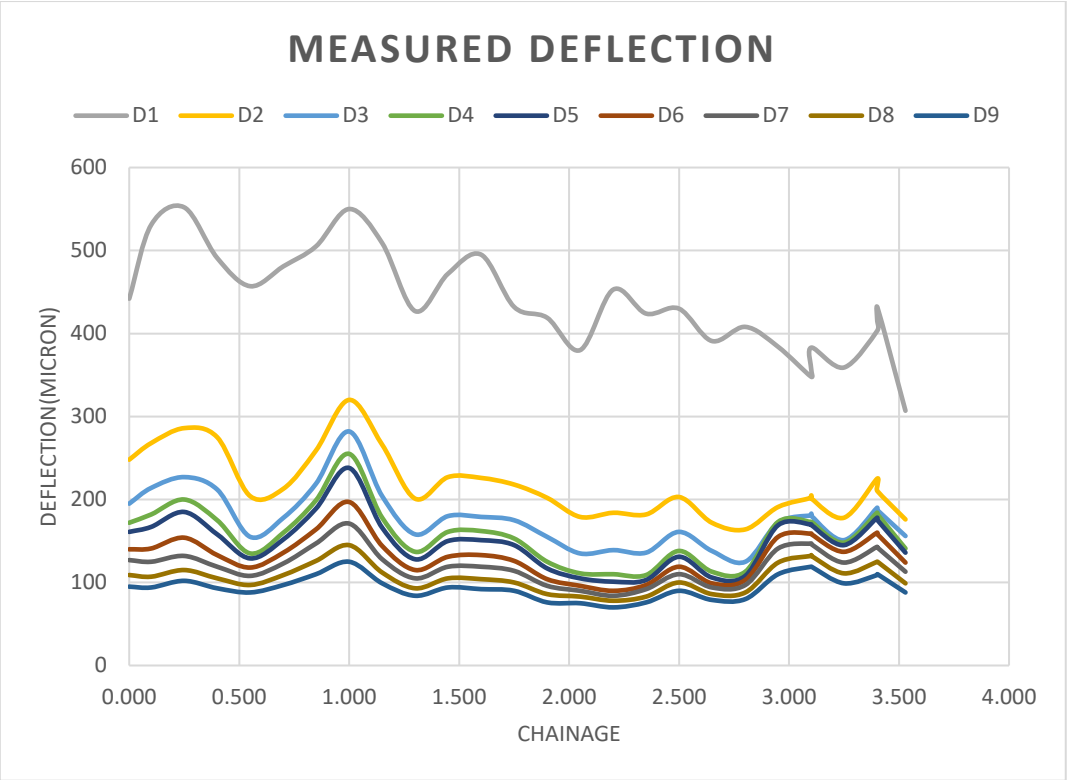

Fig 6. 8 Variation of Deflection measurement along 20m LHS from the centreline.

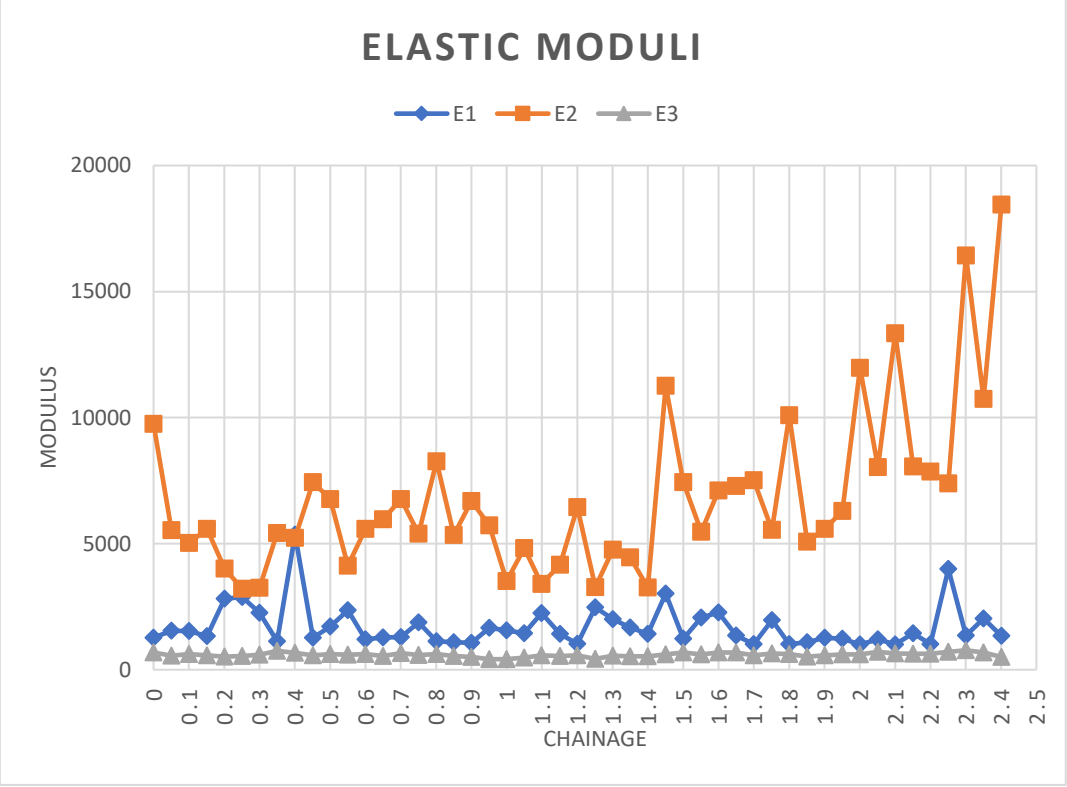

Fig 6. 9 Back-calculated Elastic modulus of 3 m LHS

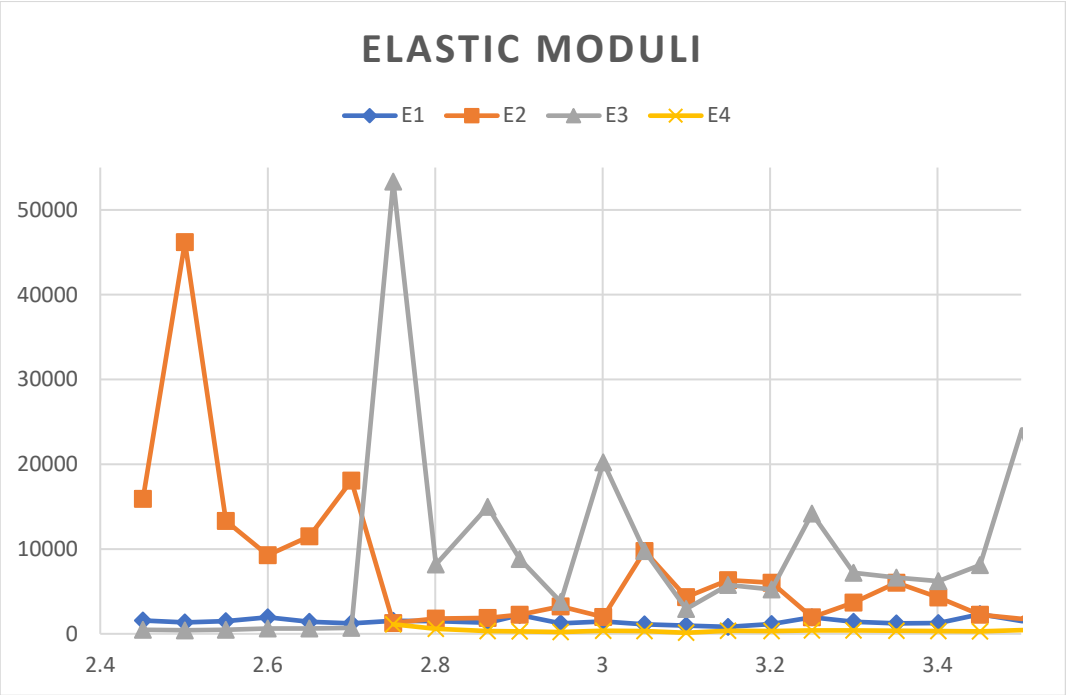

Fig 6. 10 Back-calculated Elastic modulus of 3 m LHS

6.2 Comparison of Layer Moduli Before and After work on the Runway.

The selected airport pavement undergoes significant changes and rehabilitation works. The earlier runway had a slope on one side, resulting in water accumulating on one side. The slope of section 1 of the runway constructed way back was unidirectional, and the section added later over time has a bidirectional slope which helps the water drain.

The unidirectional slope of the runway was present majorly around section 1; therefore, milling and recarpeting were done to ensure that the 3.5 km runway is level and the slope is now bidirectional, i.e., the crown of the pavement is in the center. The FAA Guidelines suggested a slope of not more than 2%. Special care will be taken at the 'touchdown zones', which experience high wear and tear.

The structural evaluation was done using the Heavy Weight Deflectometer before the slope cut-off on the runway pavement, and deflection was taken on the runway's LHS, as shown in table 8 in Appendix-A.

The layer thickness adopted in design of the pavement before the slope cut is given in Table 5.2 in chapter 5. Slope Assessment work started, and chipping and milling of the pavement in section 1 was done to match the slope of section 2 and 3. The layer thickness adopted after providing a chamber as per FAA guidelines in AC 150-5325-6F is presented in table 6.1.

The current runway is a bit higher, and for the first time, four-km storm water drainage pipes have been installed to discharge rainwater.

The deflection data collected from the HWD after working with the new overlay thickness as per Table 6.1 was analyzed for layer modulus in ELMOD-6 software. The back-calculation procedure is discussed in 6.1.2.

Table 6. 1 The layer thickness adopted after providing a chamber

Chainage(m)	Design Inputs	
	Layer Thickness	
	Layers	Thickness
0-2286	Asphalt Overlay	100
	Asphalt	400
	Subgrade	-
2286-2743	Asphalt	390
	PQC	300
	Subgrade	-
2743-3505		
	Asphalt	150
	PQC	400
	WMM	250
	Subgrade	-

The back-calculated modulus after the works is presented in table 9 in Appendix-A. After the back-calculation step, the results and the measured deflection data are shown by clicking the **Plot** option from the main menu bar.

Figure 6.9(a),6.9(b),6.9(c) shows the measured deflections values and load v/s the chainage. *The Graphical view of E-Modulus chainage wise is represented in fig 6.11,6.12,6.13.*

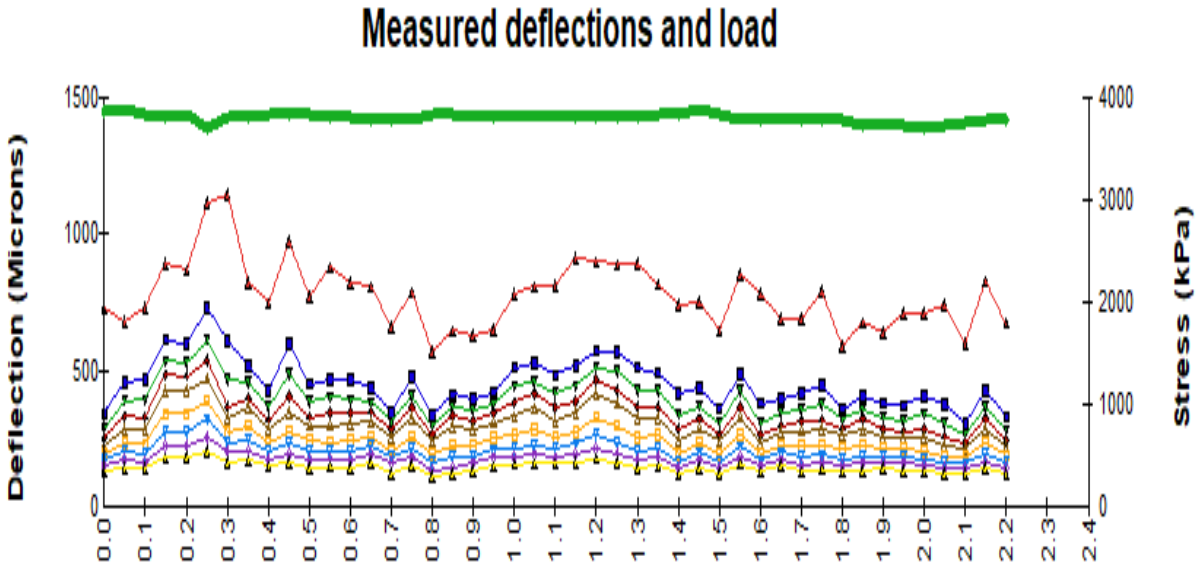

Fig 6. 11 Variation of Deflection measurement along 3m L from the centreline

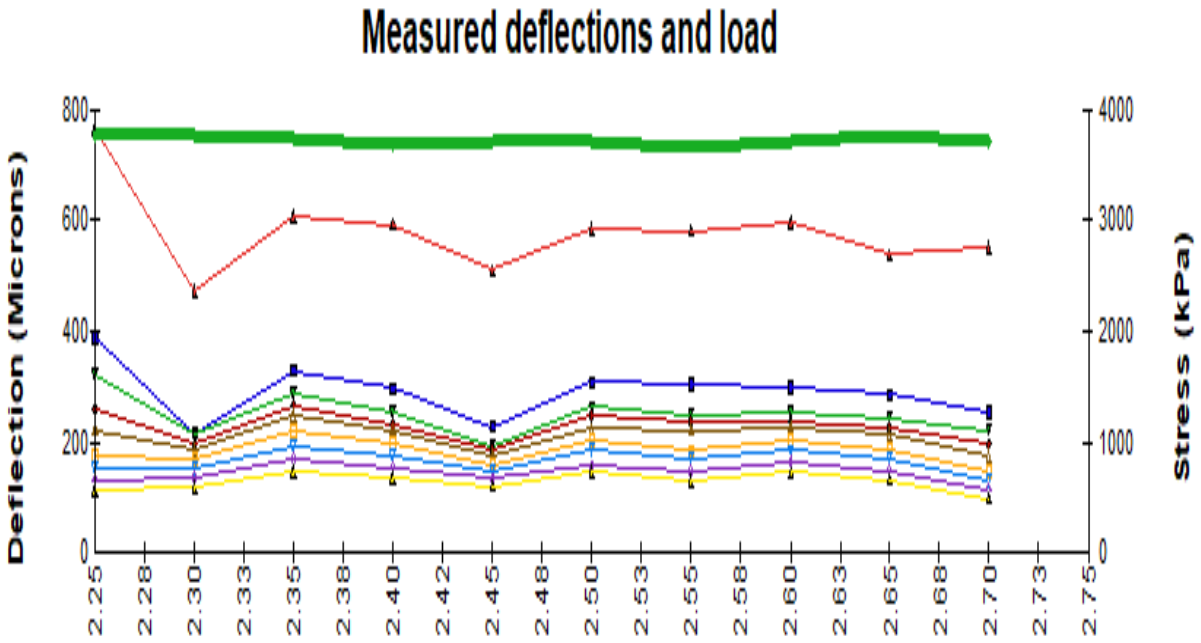

Fig 6. 12 Variation of Deflection measurement along 3m L from the centreline

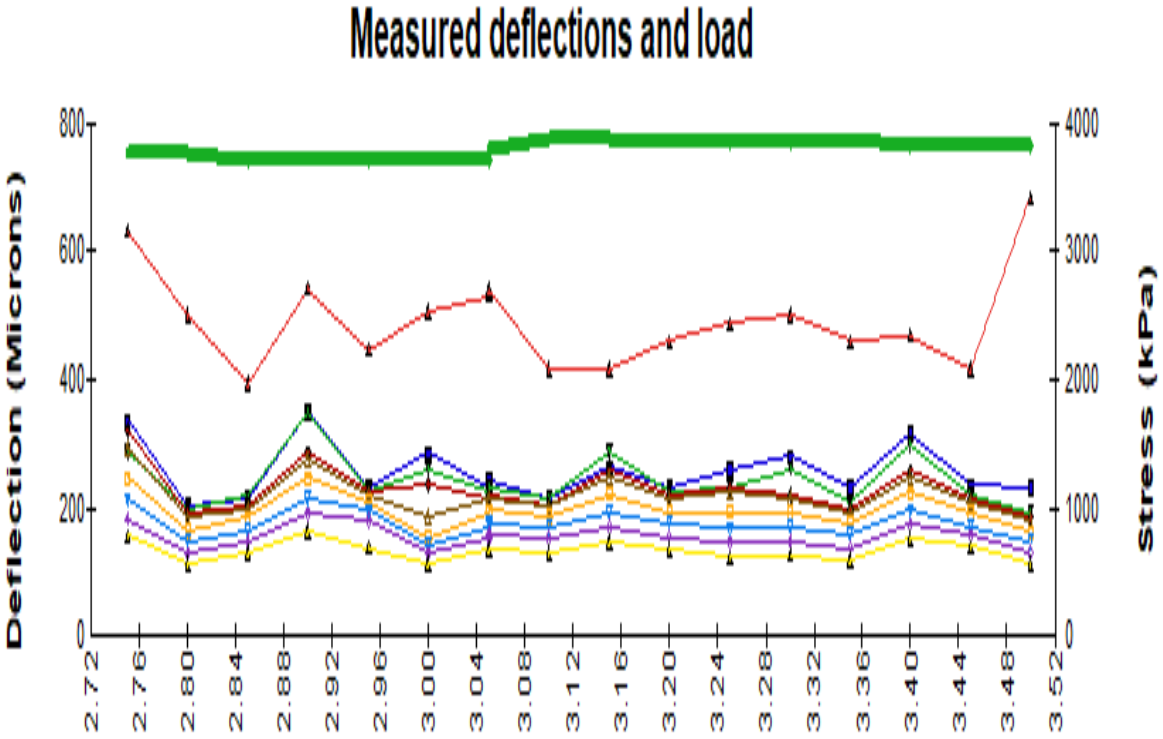

Fig 6. 13 Variation of Deflection measurement along 3m L from the centreline

Graphical view of E-Modulus chainage wise

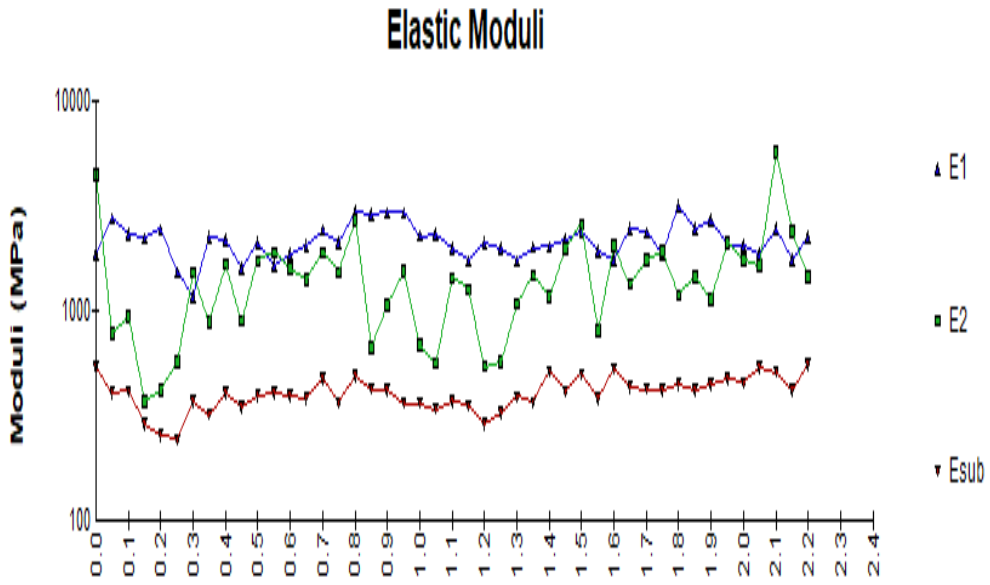

Fig 6. 14 Shows the e-modulus of 3m LHS chainagewise

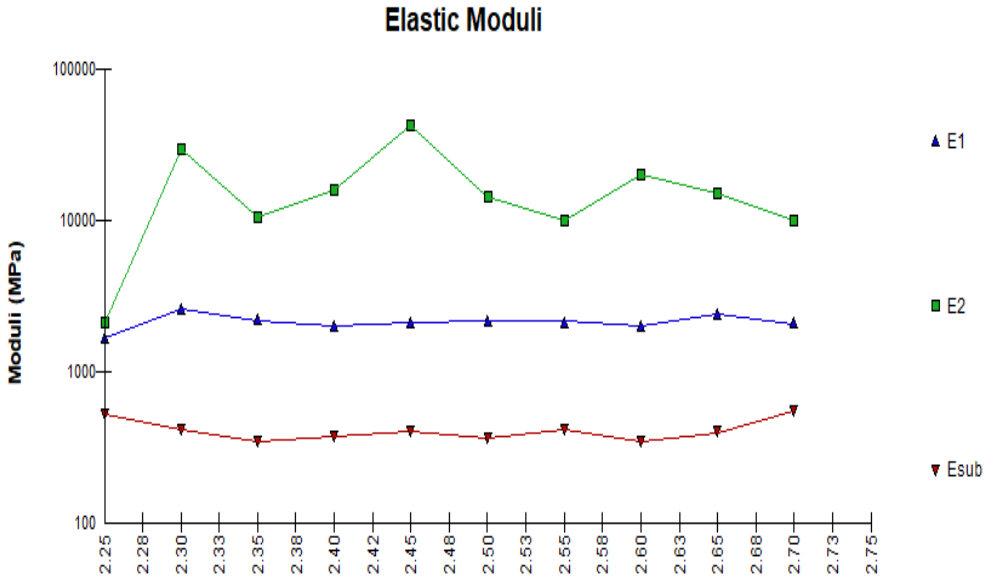

Fig 6. 15 shows the e-modulus of 3m LHS chainage wise

6.3 Evaluation of selected airport rigid pavement.

6.3.1 Processing of Load and Deflection Data

Execution of Heavy weight deflection survey for Rigid New Extended Apron Section is done. The test loads were adjusted so as to achieve minimum deflection recorded for the farthest geophone more than 100 µm. Three load drops were executed per test location. The deflection profile of the last drop was used for the Evaluation.

The HWD was equipped with 10 geophones or deflection transducers. The transducers were arranged at distances of 0, 200, 300, 450, 600, 900, 1200, 1500, 1800 and 2100 mm from the load plate. At each measurement, the designation of the measurement location, the position on the slab, time of measurement and surface temperature were recorded. For every test slab, three load positions were tested on that slab, i.e centre, slab interior and transverse edge (as shown in fig 6.16). The code for the interior and transverse position was ‘A’ and ‘B‘respectively.

All geophones were placed on one slab, except in case of deflection measurements across joints.The deflection measurements were undertaken on the transverse edge for the load transfer measurement across the joint.

The geophones at D2 and D3 were designated for deflection recording across the joint and were placed directly at the joint (as shown in Fig 6.17) in such a way that the distance from the centre of the joint to these geophones was equal.

Fig 6. 16 Load Tranfer

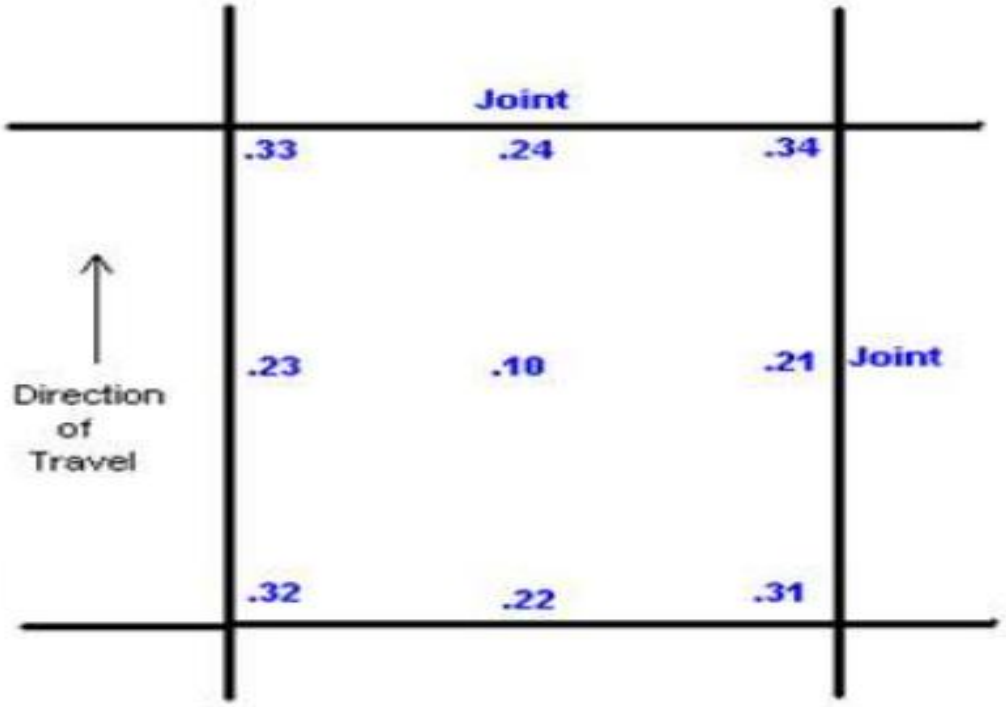

Fig 6. 17 Test location on Rigid slab

The measured deflection data for rigid New Extended Apron i.e from stand 37 to stand 43 pavement obtained from the Heavy Weight Deflectometer field observations for pavement is attached at Appendix B.

6.3.2 Pavement Structure Modelling

The deflection data was statistically analysed to determine the representative deflection bowl for analysis of each of the pavement section with homogeneous pavement profile. The deflection data recorded at varying loads in range of 150 kN to 300 kN was normalized to uniform load by the software simulating dynamic of mixed aircraft wheel loading. Construction information submitted is shown in table 6.2

Table 6. 2 Construction information

Sr. No.	Layer Type	Construction Layer
1	K value on top of DRLC	93 MN/m3
2	Sub-grade K	11.0 MN/ m3

6.3.3 Aircraft Traffic

The aircraft traffic data has been utilised for back calculations of layer elastic moduli and PCN evaluation.The Aircraft traffic data is appended in table 6.3.

Table 6. 3 Aircraft Traffic at the New Extended Apron

	Aircraft Name	Annual Departure
1.	A320/20N	20793
2.	A321	1981
3.	A330	52
4.	AT72/75/76	2346
5.	B738	2920
6.	B744	104
7.	B752/757	521
8.	B777	417
9.	B787	209
	Traffic per year	29,303
Traffic taken for calculation (20 Yrs) with traffic increase of 5%		6,30,000

6.4 Analysis Of Layer Moduli Based On Hwd Data

"Slab on grade / Westergaard's theory" regarding rigid pavements. For rigid pavements, the software analyses the elastic modulus of the PQC and effective modulus of subgrade reaction based on the input deflection bowl and the PQC thickness by back calculation.

6.5 Back-calculation of Rigid Pavement Structural Parameters

The deflection data along with pavement cross-sectional details were utilized as input for the analysis. The rigid pavement is modeled as a single slab resting on a Winkler foundation.

Finite slab size is considered. Based on deflection data, the PQC 'E' value and the achieved effective 'K' value is calculated using ELMOD-6 software.

For back calculation of these properties, the program required the following input parameters for analysis.

1. PQC thickness of 450mm, Flexural strength (4.5MPa) have been adopted.
2. Poisson's ratio value for PQC layer - Characteristic value ($\mu = 0.3$) was adopted.
3. Slab size 5 M x 5 M was considered as per the standard slab size adopted.
4. Load transfer efficiency – An average load transfer efficiency of 60% has been adopted across the rigid pavement joints, though the deflection data provides for higher load transfer efficiency. The measured load transfer ratio is actually 98% or more, which is sound for a newly constructed pavement. Since it will decrease in time, the expected minimum of 60% was adopted in this analysis, in order to demonstrate the effective PCN that can be expected towards a later stage of the design life. It is recommended to retest the pavement at regular intervals of 4 years or earlier so as to account for any

other deterioration of the pavement due to heavier trafficking or environmental effects and any loss of aggregate interlock.

5. Analysis is based on Westergaard's edge load stress, being more critical than the slab centre stress. The results of the back calculation analysis are also attached in Appendix C from table 1: stand 37 to table 7: stand 43.

6.6 Pcn Analysis Routine For Flexible & Rigid Pavements

The deflection data generated for respective test locations by the FWD equipment and the pavement structural layer thicknesses have been utilized to back-calculate the structural model of the pavement. An estimated elastic modulus for each structural layer (as modelled for analysis) of the pavement layers is back-calculated for flexible pavements. For Rigid pavements a more complex analysis is required for back-calculation of the PQC modulus value and the effective support modulus. The analysis involves computation of load transfer efficiency across joints to account for the edge load stress transfer in the analysis.

Based on the respective pavement section layer thicknesses, elastic moduli, subgrade support condition and joint load transfer efficiency (in case of rigid pavements), the stresses are computed at critical locations in the pavement structure. For flexible aircraft pavements the subgrade compressive stress is of relevance and for rigid pavements the tensile stress at bottom of slab is considered. Temperature induced tensile stress is also taken into account for rigid pavements.

Maximum ACN of the critical design aircraft is determined, based on the maximum equivalent single load that the available equivalent pavement thickness can withstand. ACN of an aircraft as defined in ICAO, Aerodrome Design Manual Part 3 – Pavements is "Two times the derived single wheel load at a standard tire pressure of 1.25 MPa, where the derived single wheel load is expressed in thousands of kilogram".

The PCN is reported as the maximum prescribed ACN for the critical aircraft in case the ACN determined by the analysis is higher. Otherwise, in case the determined ACN is lower than the maximum prescribed ACN, the ACN determined by the analysis is reported as the PCN.

6.7 Calculation Results

The PCN Values for the rigid pavements have been computed by ELMOD -6 software based on the data and analysis has been done to get the PCN values of the pavement. The calculation of PCN

Rigid pavement : The analysed PCN values by software for the rigid portion of the New Extended Apron pavement are attached in the Appendix D.

The analysed PCN values by software for the rigid portion of the New Extended Apron pavement are as per Table 6.4 and 6.5.

The PCN analysis as carried out by software based on HWD deflection data is summarised as under:-

- The PCN analysis is based on mixed aircraft for air traffic 20 years.
- The PCN analysis is based on critical aircraft B777-300E

The PCN values therefore can be adopted as **112/R/C/W/T which is ≥ the ACNs** (as shown in table 6.5) of the critical aircraft. The same may be upgraded in time when a higher ACN aircraft is expected to operate from the runway, within the actual minimum values evaluated by this analysis. However, the PCN as such reflects the present structural condition of the pavement, which may deteriorate due to factors other than projected aircraft traffic. Therefore a pavement condition survey is recommended on an annual basis and also a PCN re-evaluation at a 4 year interval over the design life.

Table 6. 4 Analysed PCN values by the software.

HWD location and Slab ID	PCN values Max	Min	ACN	CODE	Min declared PCN value
Stand 37	**115**	**122**	**110**	**R/C/W/T**	**115 R/C/W/T**
Stand 38	**113**	**129**	**110**	**R/C/W/T**	**113 R/C/W/T**
Stand 39	**120**	**135**	**110**	**R/C/W/T**	**120 R/C/W/T**
Stand 40	**114**	**130**	**110**	**R/C/W/T**	**114 R/C/W/T**
Stand 41	**114**	**132**	**110**	**R/C/W/T**	**114 R/C/W/T**
Stand 42	**114**	**128**	**110**	**R/C/W/T**	**114 R/C/W/T**
Stand 43	**114**	**128**	**110**	**R/C/W/T**	**114 R/C/W/T**

Table 6. 5 Adopted PCN value

Sr No.	Pavement Description- Rigid Area	Pcn Value
1.	Stand 37 to 43	112 R/C/W/T

6.8 Evaluation of Highway Pavement

6.8.1 Evaluation of Pavement Condition Index.

PCI is an index developed by the United States Army Corps of Engineers to indicate the general condition of the road. It is a numerical indicator that evaluates the overall surface condition of a road or pavement as per ASTM D6433. It is a statistical metric requiring manual/visual evaluation and survey of the required routes. It is a statistical indicator that calls for manual/visual Evaluation and survey of the necessary routes. PCI surveying methods for both highway and airport pavements have been standardized by ASTM International, a global standards organisation that creates and disseminates voluntary consensus standards for a wide range of services, products, and systems. Based on rating roads quantitatively, it sets qualitative criteria ranging from “failed” to “excellent.”

The Pavement Condition Index (PCI) provides a measure of the current condition of a pavement or road based on the quantity and types of “distresses” observed on its surface.PCI shows structural integrity and functional condition of the surface, but it cannot measure the pavement's structural capacity.

Pavement distress is defined as external indicators of pavement deterioration caused by loading, environmental factors, construction deficiencies, or a combination **(D 6433(ASTM)).**The "distresses" are alligator cracking, bumps, depressions, and potholes, among others. Based on how the distresses affect the 'ride quality,' they are given a severity level (low, medium, or high).

PCI yields a numeric number between 0 and 100, with 100 indicating the best possible situation and 0 indicating the worst possible condition, as shown in Figure 6.18.

The Pavement Condition Index (PCI) for a pavement section should be calculated using the information gathered during the pavement condition survey. The PCI of the specified road sections and roads, together with ratings for each attribute and weighting factor, will be determined using actual measurements. The appropriate weight (multiplier) is then applied to the rating value of each parameter after it has been given a rating number to produce the weighted rating value of each individual parameter.

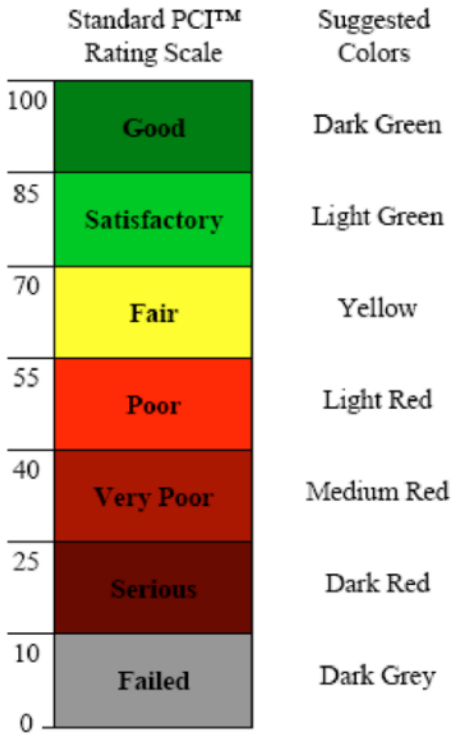

Fig 6. 18 Pavement condition index (PCI), Rating scale (Source: ASTM D;6433)

The pace of road degradation can be determined by monitoring the PCI regularly, allowing for the identification of repair and rehabilitation requirements well in advance, which may significantly reduce long-term expenses. In addition to providing performance data for validation, the PCI allows us to enhance (and perhaps revolutionize) road and pavement design and maintenance operations.

6.9 PCI calculations for Case study I (Jetpur-Somanath road)

- Distress data from the road was provided, and the amount of distress is converted to a percentage (the amount of each distress type and severity level must be converted to percent) is included in Appendix D.
- The distresses chosen to calculate the PCI were Cracking, Rut Depth, Potholes, Patching, Edge break, Ravelling, and Edge drop. These distress are already explained in the methodology of the Pavement condition survey.
- The measured distress values for the section of road along the chainage are represented in graphs from Fig 6.13 to Fig 619.
- After sorting the raw data, calculate and assign a particular weightage to each distress / defect and choose a particular PCI scale to rate as presented in Table 6.6.

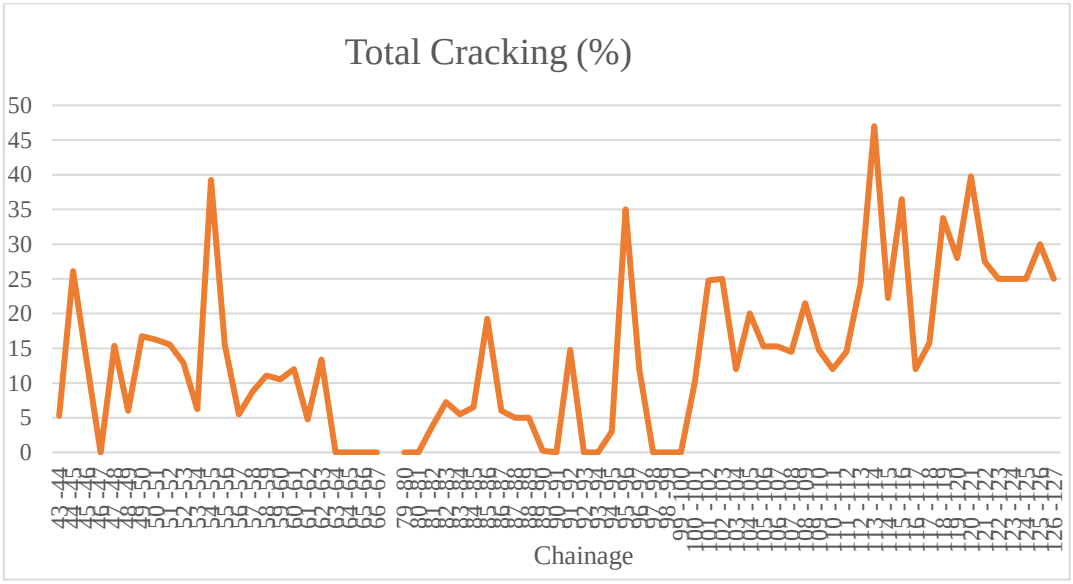

Fig 6. 19 Measured Total Cracking from Chainage (043-127)

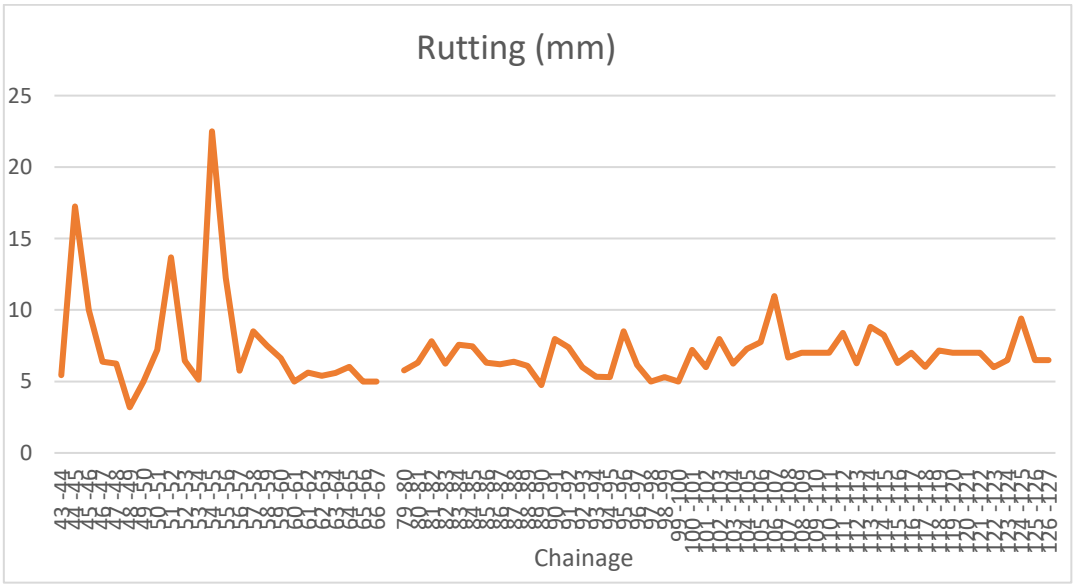

Fig 6. 20 Measured Rutting (mm) from Chainage (043-127)

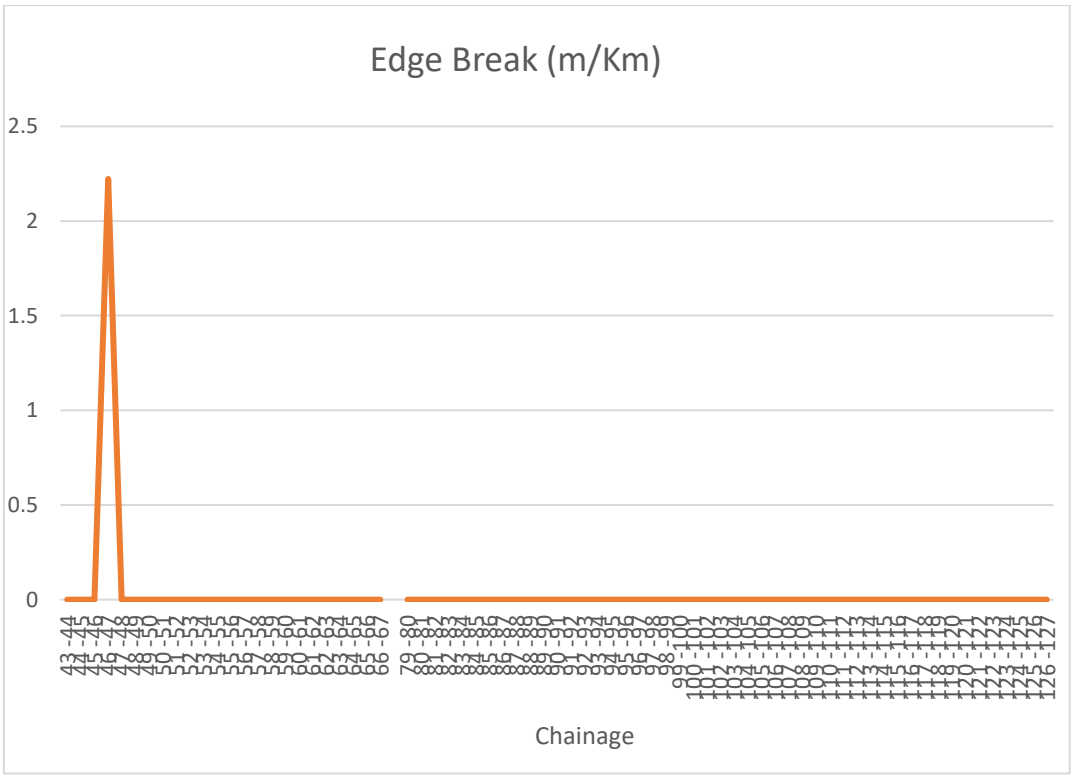

Fig 6. 21 Measured Edge Break from Chainage (043-127)m

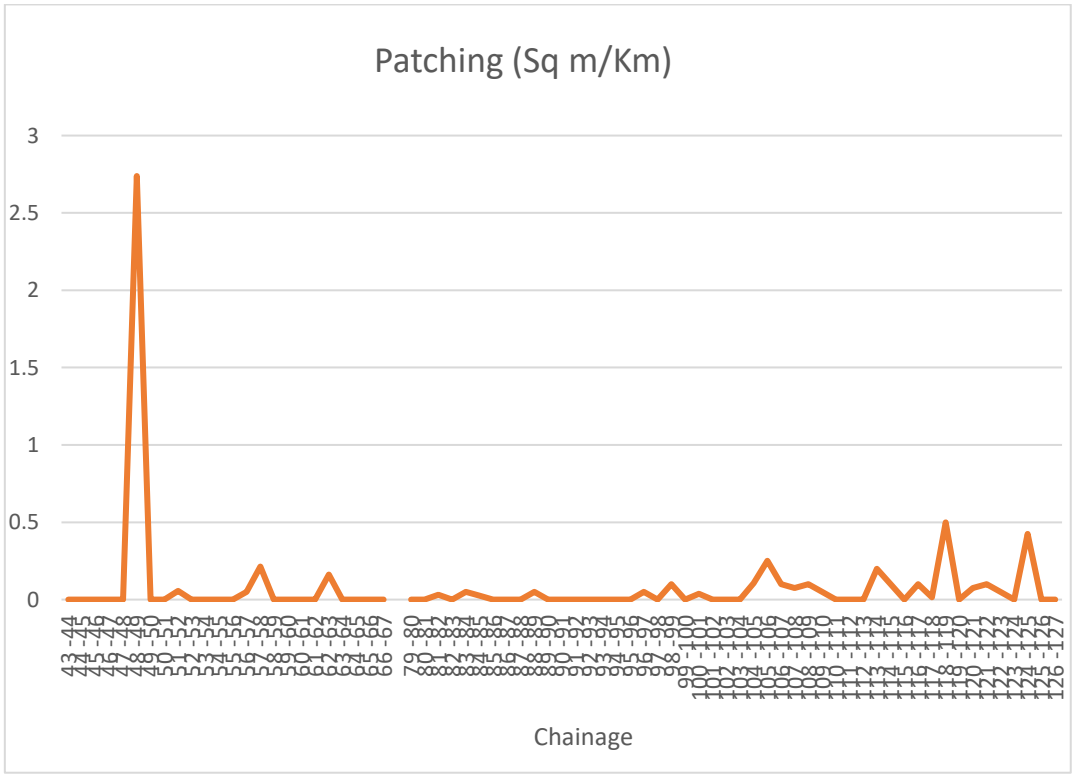

Fig 6. 22 Measured Patching work from Chainage (043-127)

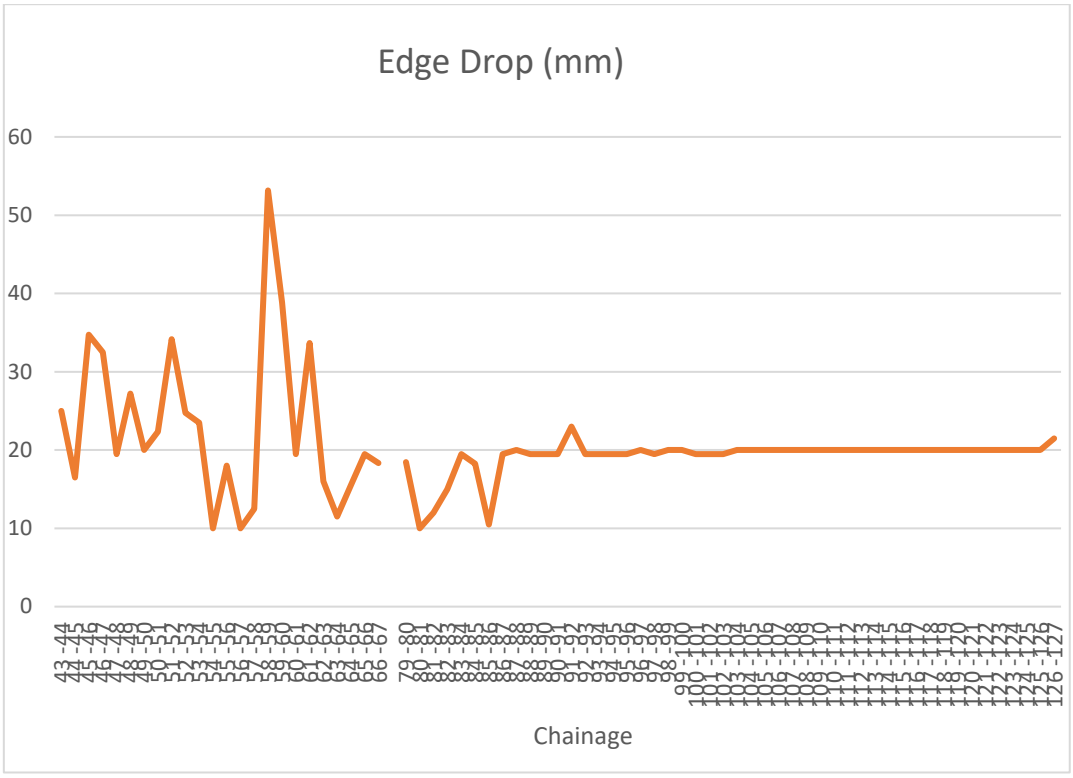

Fig 6. 23 Measured Edge Drop from Chainage (043-127)

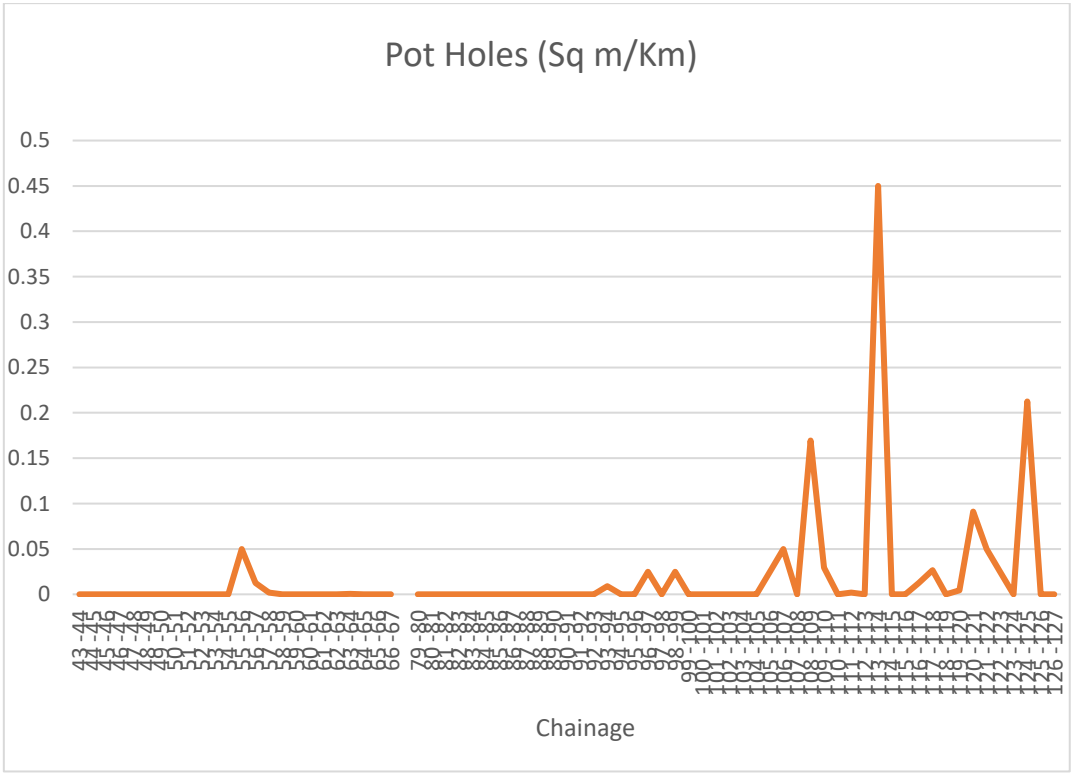

Fig 6. 24 Measured Potholes from Chainage (043-127)

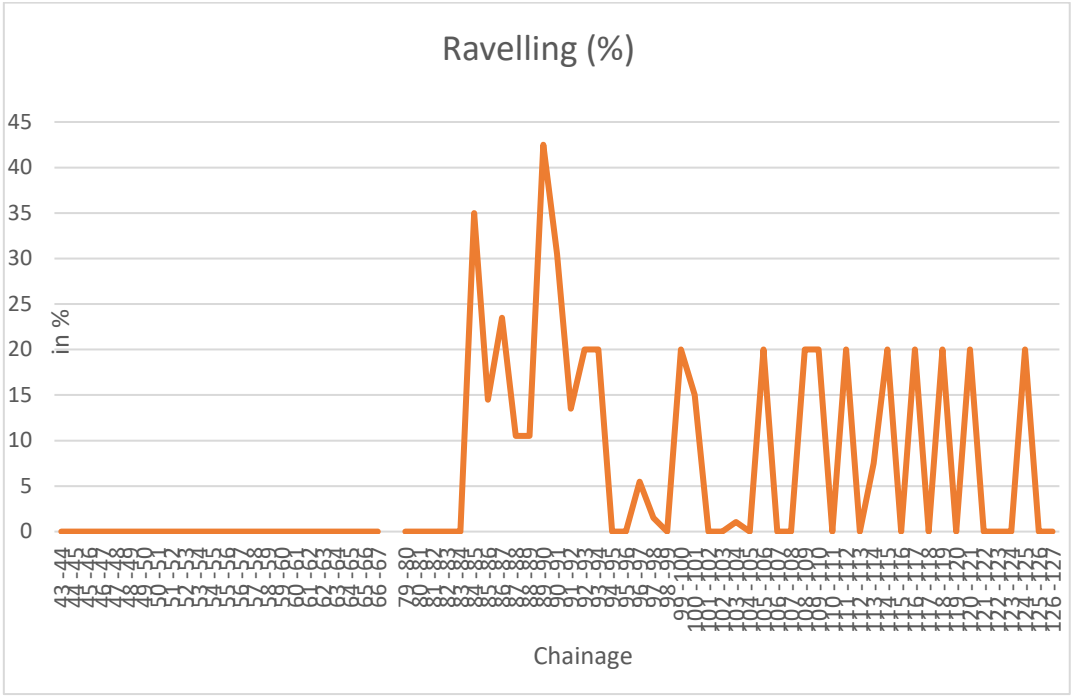

Fig 6. 25 Measured Ravelling from Chainage (043-127)

Table 6. 6 Rating considered

Distress Type on roads /junctions/Rotaries	Rating Considered
Cracking	0-40
Raveling	0-30
Potholes	0-10
Rutting	0-40
Patching	0-5
Edge drop	0-30
Edge break	0-50
Note: Maximum rating is considered based on to maximum disrtress found for respective parameters	

- Assign rating to each particular distress depending upon the minimum and maximum value of each measured distress as shown in Table 6.7

Table 6. 7 Max and min rating values

Distress	Range		Rating	
	Min	Max	Min	Max
Cracking	0	47	0	30
Raveling	0	42.50	0	20
Potholes	0	0	0	0
Rutting	3	23	0	15
Patching	0	3	0	5
Edge drop	0	53	0	25
Edge break	0	2.22	0	5

- After assigning the values according to the rating considered for each distress, add all the values obtained per rating scale to get the sum of all the distress values.
- After obtaining the sum of total distress, subtract it from 100 to get the value of PCI included in Table 2 APPENDIX -D. Figure 6.26 shows the PCI values of the road from chainage (43-127)m.
- The values obtained to tell the condition of the selected pavement are divided into groups: GOOD, FAIR, and POOR according to their PCI values as per IRC 081:1997.

  PCI < 55: The condition of the road is "POOR."

  PCI ≤ 75: The condition of the road is "FAIR."

  PCI > 75: The condition of the road is "GOOD."

  The pavement in good, fair, and poor condition is elaborated in Fig 6.27.

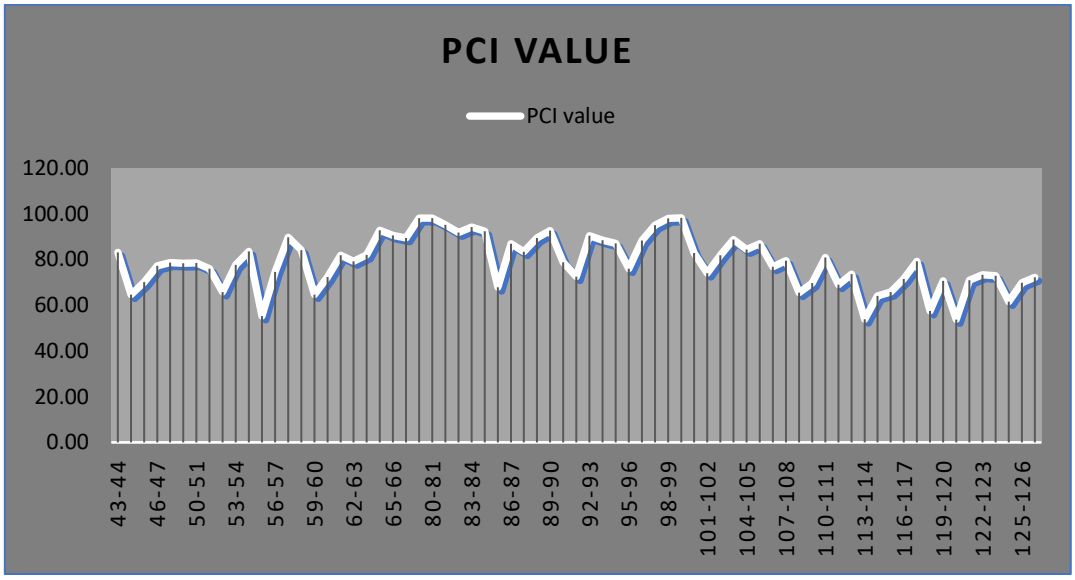

Fig 6. 26 PCI values of the selected pavement

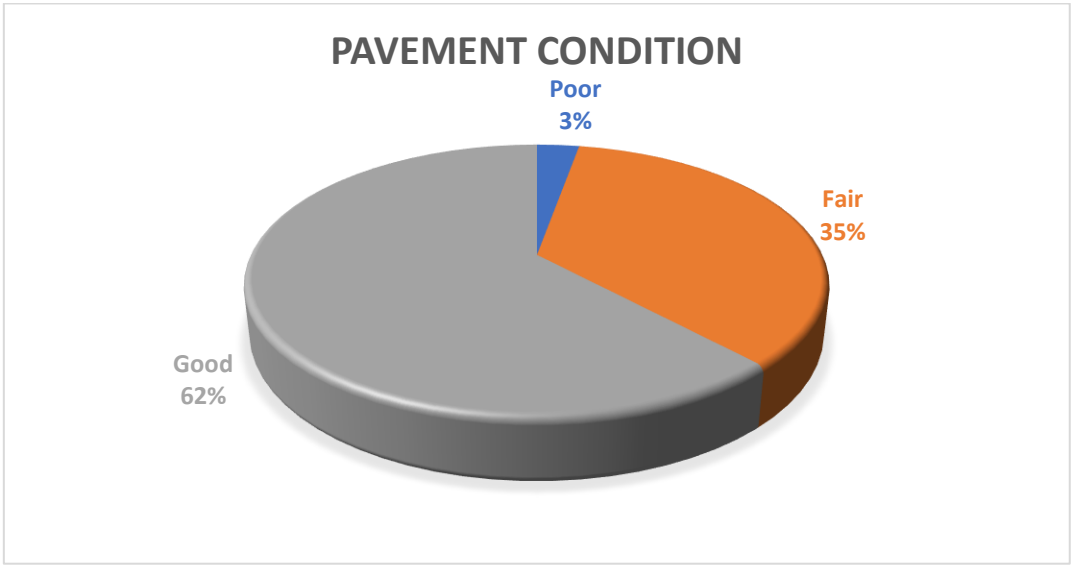

Fig 6. 27 Pavement condition

6.10 Structural Evaluation of Pavement

Structural Evaluation of the pavement refers to the diagnosis of the existing structural state of individual pavement layers as well as the Evaluation of the overall pavement strength.

Determining the actual structural capability of the current pavements is the main goal of a structural evaluation process. The flexible pavements' structural strength deteriorates with time and with traffic.

A pavement's reaction to a test load is seen when using a structural evaluation method. The structural response of a pavement may be quantified in terms of stresses, strains, and deflections.

Pavement Condition Survey shall be done before the actual deflection measurement and consists of visual observations supplemented by measurements for estimation of cracking, rutting and other distresses in the pavement.

6.11 Structural Evaluation of flexible pavement Case study II

6.11.1 Processing of Load and Deflection Data

Deflections can be calculated using load & measured deflections at 9 different sensor locations (0,300,450,600,900,1200,1500,1800,2100) using FWD presented in Table 3 Appendex -).

6.11.2 Pavement Structure

The pavement will be designed as a part of the in-service section of a Ring road. This section consists of a carriageway flexible pavement width of 7m with a shoulder of 1.5m. The Existing flexible Pavement with a surface layer of 150mm & Granular Layer 550mm composition (as shown in fig 6.28) is considered for Pavement Overlay Design.

The following pavement composition is proposed for calculations. **(IRC:37, 2018)**

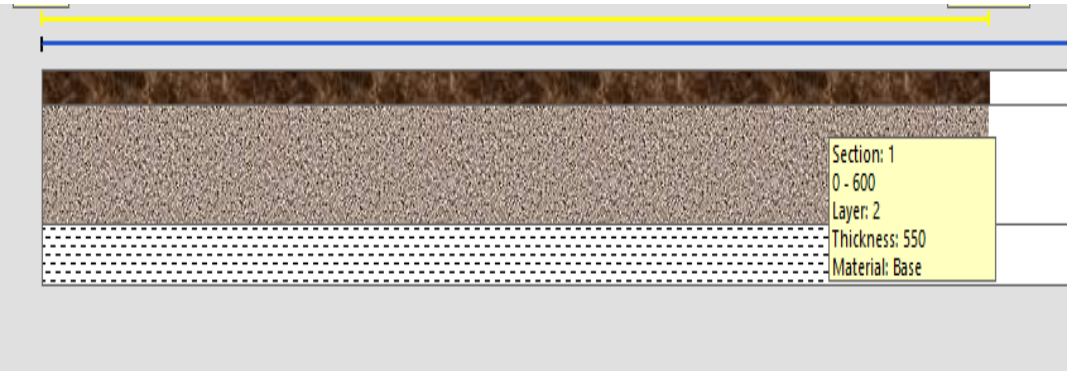

Fig 6. 28 Cross-section of the Road taken under study

6.12 Analysis of Data

6.12.1 Processing of Load and Deflection Data

Deflections can be calculated using load & measured deflections at 9 different sensor locations (0,300,450,600,900,1200,1500,1800,2100) using FWD (Ref. Table 3 Appendex D) Some of the checks that should be applied to the deflection data are:

(i) Deflections should decrease with increasing distance from the loading plate

(ii) Deflection values should not be more than the capacity of the sensors.

From the three drop, average values of load and deflections are calculated from collected test data. The loading plate is attached at D0, and while moving away from the loading plate, the deflection values are also decreasing as presented

a) Back-calculation of Layer Moduli Using KGPBACK software

The elastic modulus of the different layers of existing pavement can be back-calculated using an appropriate back-calculation technique. Measured surface deflections are normalized to a standard load of 40 kN. KGPBACK software is used for back-calculation.Input Parameters are shown in Table 6.8. By inputting the sensor locations, measured deflection values, radius of loading plate & pavement layer thickness the back-calculated modulus of different layers of the existing pavement will be found as shown in fig 6.29.

Table 6. 8 Input Parameters in KGPBACK software

Parameters	Values	
Wheel Load (N)	40000	
Contact Pressure (MPa)	.56 (as per IRC:115-2014)	
Number of Deflection Measuring Sensors	9	
Radial distance (mm)	0,300,450,600,900,1200,1500,1800,2100 .	
Poisson's ratio values	0.5,0.4,0.4 (as per IRC:115)	
Moduli range of layers	Granular layers (combined)	100 to 500 MPa
	BT Layer-thick layer without much cracking	750 to 3000Mpa
	BT layer in distressed condition (Fair to Poor)	100 to1500 Mpa

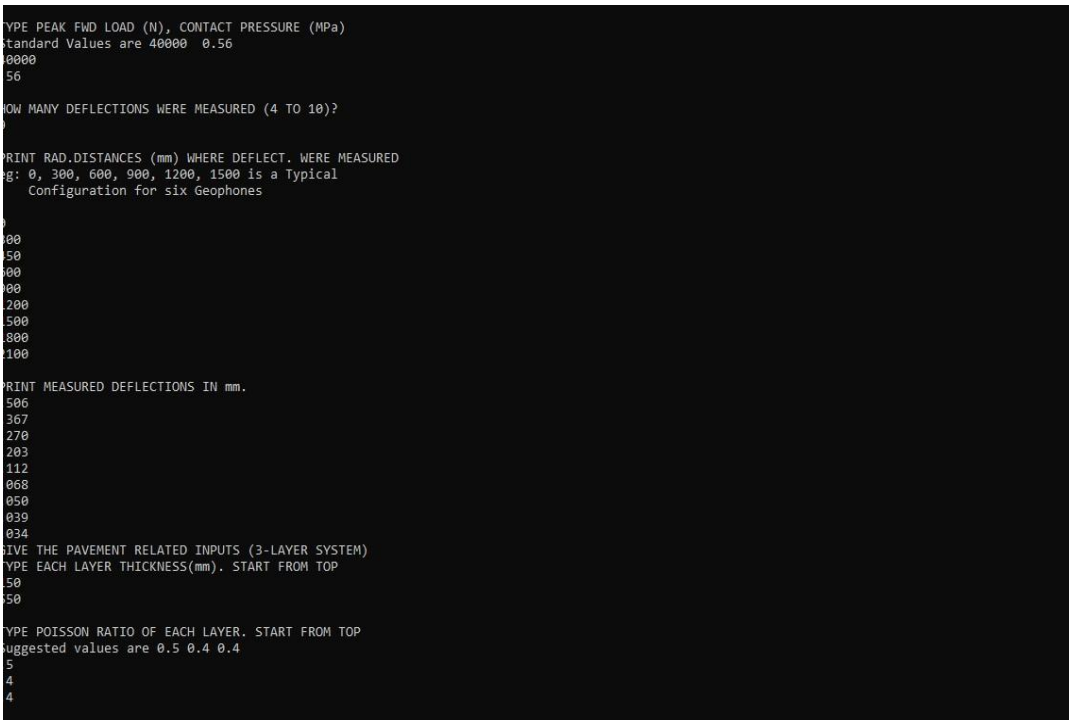

Fig 6. 29 Inputting the values in KGPBACK software

The Elastic moduli values of Surface, Base and Subgrade layers were obtained after inputting data in KGPBACK program are presented in Table 4 (Appendex-D).

b) Corrections applied on FWD readings.

Back calculation of FWD data using KGPBACK provided the elastic moduli values of individual layers. These moduli values were further corrected by applying temperature and seasonal corrections to make-up for errors due to variation in climatic conditions.

Only temperature correction were applied. After determining the corrected moduli 15th percentile value for each of the section were calculated shown in Table 4 (Appendex-D) which was used as the input parameter in IIT PAVE.

c) ITPAVE

IITPAVE software is used for the analysis of linear elastic layered pavement system. It is the mechanistic empirical pavement design software which is used for analyzing the pavement responses. The stresses, strains and defections caused at different critical locations can be computed using this software assuming as a four-layer system (overlay layer, existing surface, existing base/sub-base and existing sub-grade layers).

Table 6. 9 15th Percentile value of corrected layer modulus

15th Percentile of corrected pavement layer modulus	Corrected Surface layer moduli(MPa)	Corrected Base layer moduli (MPa)	Corrected Subgrade layer moduli (MPa)
	1458.3	**102.4**	**99.9**

Table 6. 10 Input Parameters in IIT PAVE software

Parameters	Typical Values
Number of layers (n)	3
Elastic modulus (E), in MPa	30000
Poisson's Ratio (μ)	.5, 0.4,0.4
Single Wheel Load (N),	20000
Tyre Pressure (MPa)	0.56

To obtain the peak strains at critical locations of the pavement thickness of the layers and corrected elastic moduli were used as the input values in the software, as shown in Table 6.10, while assuming a trial thickness for overlay. Fig 6.30 shows the 3-layers system in IIT PAVE, and the inputs were corrected 15th Percentile of the elastic moduli, poisson's ratio, thickness of layers, and radial distance i.e, 0 and 155. These strains are later used to find the pavement's residual fatigue and rutting strengths. The thickness of the overlay assumed must be such that the developed stresses/strains are below the allowable stress/strain values which was computed using the linear layered elastic model (Irc:37-2018 2018).

The output of IIT PAVE is shown in fig.6.31 for the results of pavement analysis presented in the screenshot of the output window. The critical mechanistic parameter, horizontal tensile strain (εt), will be the largest of the tangential and radial strains at the bottom of the bituminous layer computed at two radial distances of '0' and '155'.

Thus, horizontal tensile strain (εt) will be taken as 0.0003469 (0.3469E-03), which is the maximum out of the four strain values (tangential and radial at '0' and '155' mm radial distances), i.e., 0.0003431, 0.0003429, 0.0003429and 0.0003429.

Similarly, vertical compressive strain (εv) will be taken from the results corresponding to the lower line of the two sets of results available for the interface between granular layer and subgrade.

Thus, the vertical compressive strain (εv) value of 0.0002438 (0.2438E-03) which is the larger of the two strain values i.e., 0.0002438 and 0.0002279 as shown in Table 6.11.

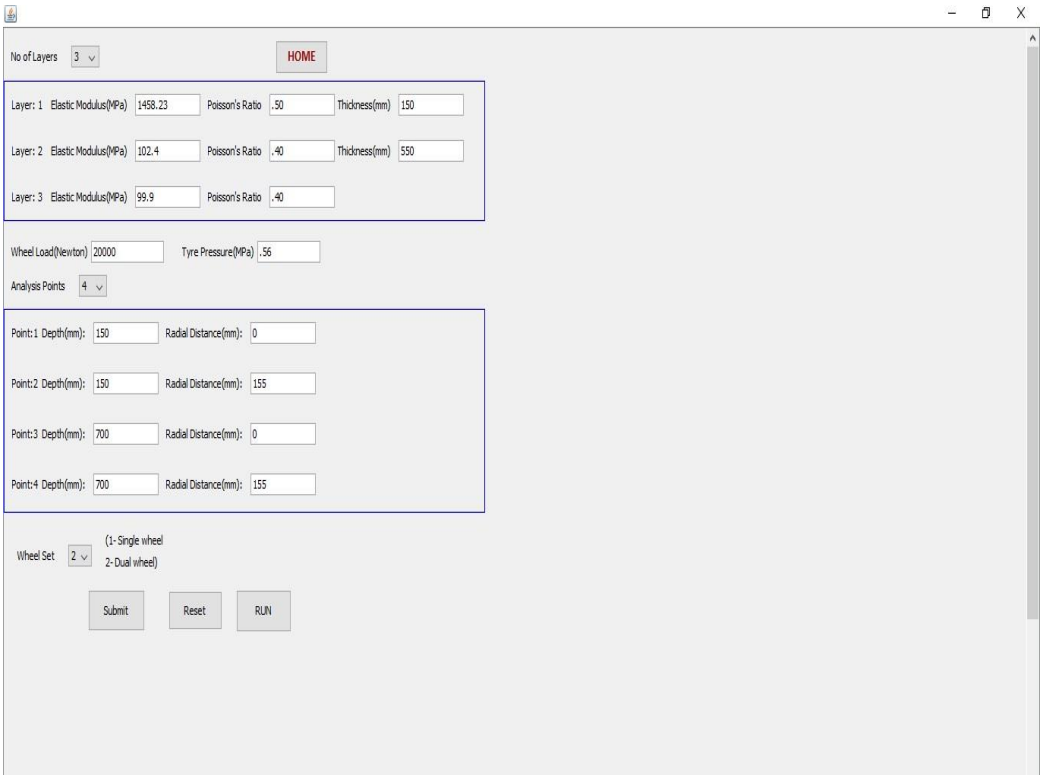

Fig 6. 30 Three- layer system in IIT Pave before overlay.

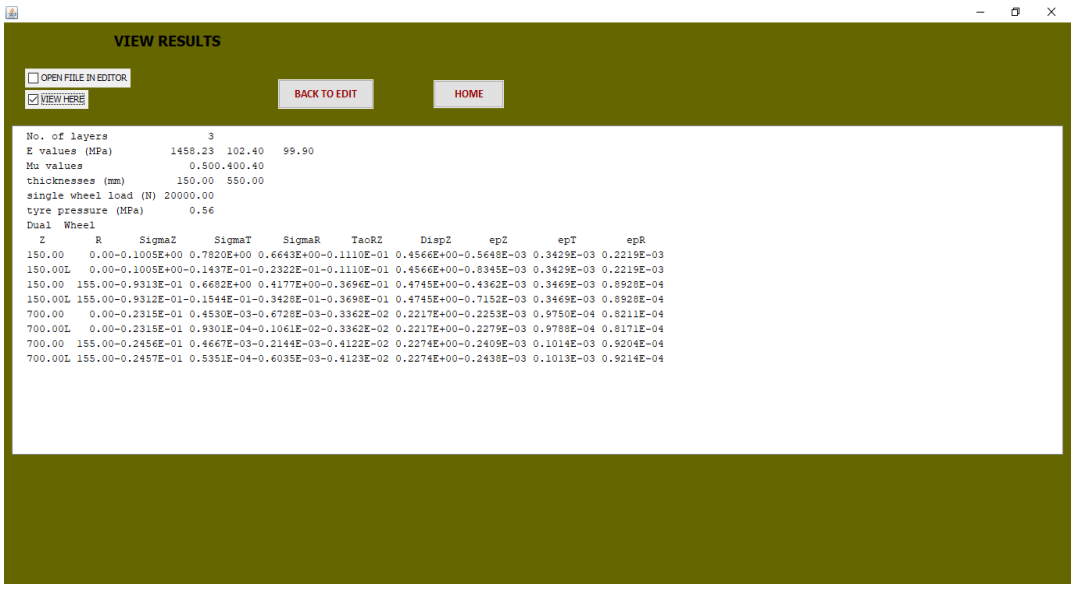

Fig 6. 31 Output of IIT PAVE

Table 6. 11 Three-layer system in IIT PAVE software

Pavement section (m)	Thickness(mm)		15th percentile corrected E values for temperature and seasonal (MPa)			Horizontal tensile strain at the bottom of bituminous layer calculated using IITPAVE	Vertical compressive strain at the top of subgrade layer calculated using IITPAVE
	Bituminous layer	Granular Base/subbase layer	E1	E2	E3		
0-6270	150	550	1458.3	102.4	99.9	0.3469E-03	0.2438E-03

6.13 Trial/Proposed Overlay thickness

A four-layer system (overlay layer, existing surface, existing base/sub-base, and existing sub-grade layers) was considered in the IITPAVE software, which was used to compute the stress/strain values as shown in figure 6.32. The inputs were corrected 15th Percentile elastic moduli of surface & base layer, Poisson's ratio, the thickness of layers, and radial distance, i.e., 0 and 155.

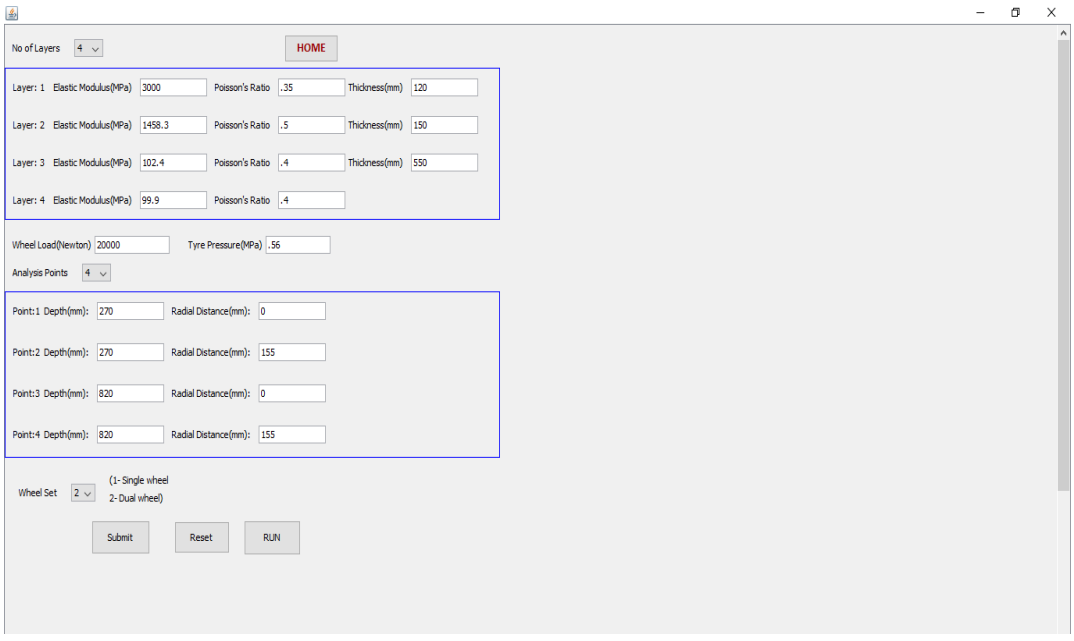

Fig 6. 32 : Four-layer system in IIT PAVE with Trial thickness120mm.

The Elastic moduli and poison's ratio of the overlay layer **(as per IRC:37-2018)** is taken to be 3000 Mpa and 0.35, respectively, as shown in Fig 6.33.The material type for the overlay layer was selected as a Bituminous layer with VG-40 or modified bitumen on the basis of annual pavement temperature as per Table 9.2 of IRC:37-2018.

Trials of overlay thickness were made with different thicknesses in IIT PAVE, and it was found that an optimum overlay of 120 mm, as shown in fig 6.26. The output of IIT PAVE is shown in table 6.12 for the results of pavement analysis.

Material Type	Elastic/Resilient modulus (MPa)	Poisson's ratio
Bituminous layer with VG40 or Modified Bitumen	3000 or tested value (whichever is less)	0.35
Bituminous layer with VG30	2000 or tested value (whichever is less)	0.35
Cement treated base	5000	0.25
Cold recycled base	800	0.35
Granular interlayer	450	0.35
Cement treated sub-base	600	0.25
Unbound granular layers	Use Eq. 7.1	0.35
Unbound granular base over CTSB sub-base	300 for natural gravel 350 for crushed aggregates	0.35 0.35
Subgrade	Use Eq. 6.1 or 6.2	0.35

Fig 6. 33 Recommended material properties for structural layers (as per IRC:37-2018)

Table 6. 12 Predicted overlay summary for the selected pavement sections

Pavement section (m)	Thickness(mm)			15th percentile corrected E values for temperature and seasonal (MPa)				Horizontal tensile strain at the bottom of bituminous layer calculated using IITPAVE	Vertical compressive strain at the top of subgrade layer calculated using IITPAVE
	Overlay thickness (mm)	Bituminous layer (mm)	Granular Base/ Subbase layer (mm)	E1	E2	E3	E4		
0-6270	120	150	550	3000	1458.3	102	99	0.1517E-03	0.1313E-03

6.14 Structural Analysis

To determine the design life of the pavement structures to withstand the predicted traffic load FWD deflection data is used . For Evaluation of pavements mechanistic-empirical methods are used. The critical location in the pavement structure are:

1. The horizontal strains at the bottom of a bituminous surface
2. The vertical strain (deformation) at the top of unbound base sub-base layers and the

sub grade**(Irc:37-2018)**

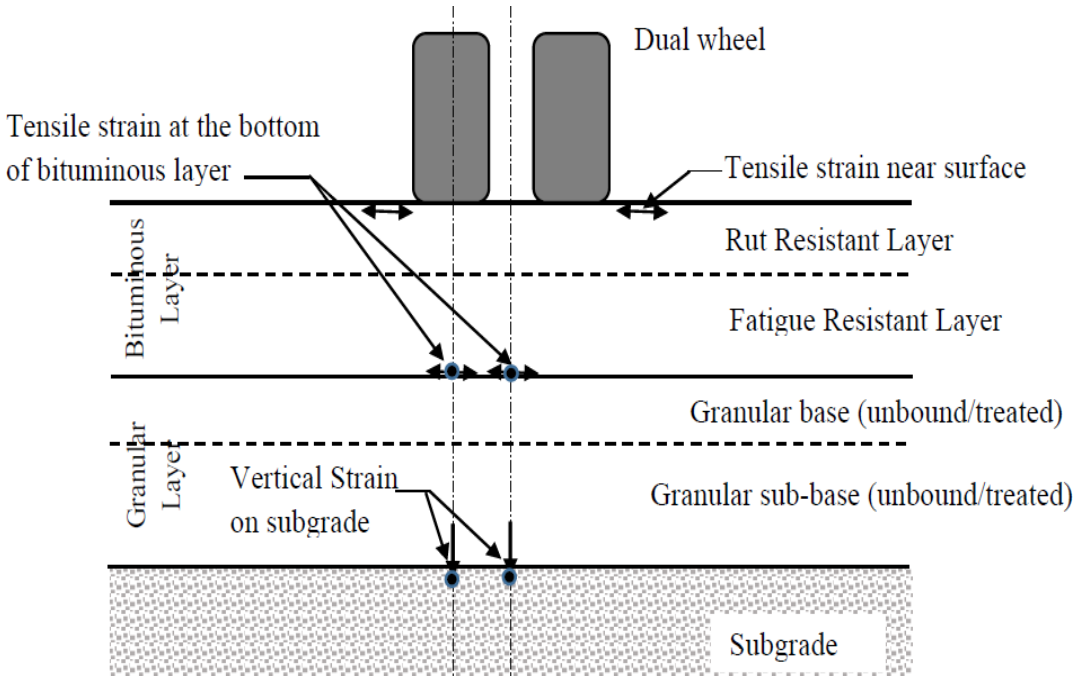

Fig 6. 34 Critical Location in Pavement Structure

All of the top layers have finite thicknesses and are supposed to have an infinite horizontal length, except for the subgrade, which is thought to be semi-infinite. To determine the stresses, strains, and deflections caused by the load placed on pavement, Values for the thickness, Poisson's ratio, and elastic modulus are inputs. Pavement analysis has been done using IITPAVE software.

For the purpose of preventing subgrade rutting, vertical compressive strain on top of the subgrade is taken into account. The horizontal tensile strain at the bottom of the bottom bituminous layer is thought to be the causative mechanistic parameter that must be restricted to control bottom-up cracking in the bituminous layer.

6.15 Remaining Service Life

The back-calculated layer moduli values are utilized to calculate the required strain parameters for the prediction of remaining life of pavement. Those strain results were used to calculate the fatigue and rutting life of the bitumen layer. The stress parameters are calculated from IIT-PAVE software and rutting and fatigue life can found in Clause 6.2.2 of IRC 37-2018.The process which is followed for remaining life determination is shown in fig 6.36.

The remaining service life before overlay for fatigue life 90% & rutting life 90% is 4.06 msa & 338.32msa respectively. After overlay the remaining service for fatigue life 90% & rutting life 90% is101.37 & 5595.54 msa respectively. It was found out that an optimum overlay of 120 mm if provided to section would result in an increase in fatigue and rutting life as shown in fig 6.35.

Fig 6. 35 : Summary of remaining life after and before overlay thickness.

Before Overlay	Overlay thickness =120mm
For Rutting Life (90%) =338.32 msa For Fatigue Life (90%) =4.066	For Rutting Life 90% =5595.54msa For Fatigue Life 90% = 101.37 msa

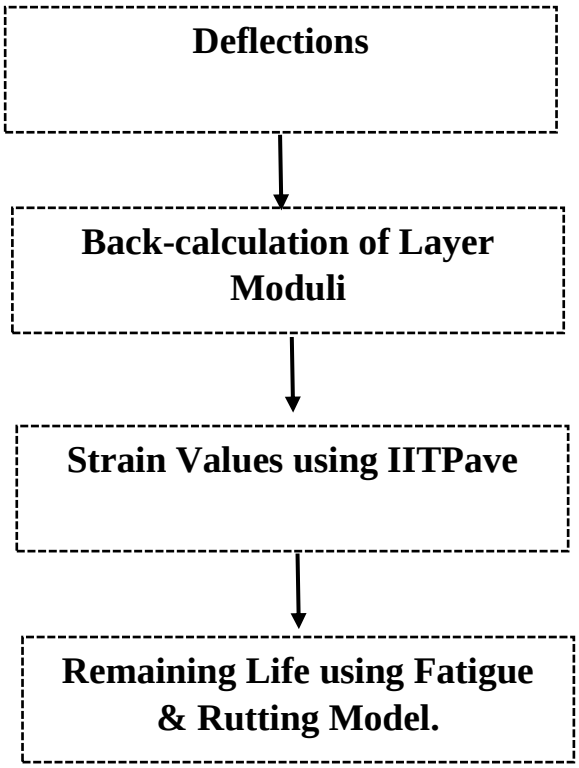

Fig 6. 36 Remaining life of pavement

6.16 Comparison of Back-calculation of layer moduli

There are several back-calculations programs available. In this study, two software KGPBACK and ELmod-6 were compared to evaluate the highway pavement. A section of pavement from case study II is taken under investigation for comparison.

Same Fwd deflection data was used for analysis in both the software. The FWD data for section taken into investigation is represented in Table 5 Appendex-D.

Layer moduli calculation using Elmod-6 Software and KGPBACK software are discussed in brief in clause 6.1.2 and 6.12.

6.17 Analysis of Layer Moduli

Layer moduli determined from both the software for Surface, Granular and Sub-grade layer were compared for the study section.Modulus values given from both the software are given in Table-6 Appendex -D.

6.17.1 Subgrade Modulus

Subgrade Modulus was back-calculated using both KGPBACK & ELMOD (Deflection Basin Fit) programs and using CBR values from IRC 37: 2018 .The modulus values obtained from the software are given in the table 6.13.

Table 6. 13 Comaprison of Average Subgrade layer modulus

KGPBACK VALUE	ELMOD VALUE	IRC 37:018
100	65	69.5

6.17.2 Granular Modulus

Granular Modulus was back-calculated using both KGPBACK & ELMOD (Deflection Basin Fit) programs and using CBR values from IRC 37: 2018 .The modulus values obtained from the software are given in the table 6.14.

Table 6. 14 Comaprison of Average Subgrade layer modulus

KGPBACK VALUE	ELMOD VALUE	IRC 37:018
164	136	162.9

6.17.3 Surface Modulus

Surface Modulus was back-calculated using both KGPBACK & ELMOD (Deflection Basin Fit) programs.The modulus values obtained from the software are given in the table 6.15.

Table 6. 15 Comaprison of Average Subgrade layer modulus

KGPBACK VALUE	ELMOD VALUE
1444	3015

CHAPTER 7

CONCLUSIONS

The major conclusions derived from this study are as follows:

7.1 Airport Pavements

I. For Runway (Ab-Cd) the average back-calculated values obtained from the Elmod-6 software at different distances from the centreline are

- **At 3m LHS**

For section 1 , layer thickness H1(overlay thickness)100mm and H2 (Asphalt)400 mm.

E1 (Mpa)	E2	E3
2056	6247	587

For section 2 , layer thickness H1(Asphalt)390mm and H2 (PQC)300 mm.

E1 (Mpa)	E2	E3
1777.2	16726.6	601

For section 3, layer thickness H1(Asphalt)150mm and H2 (PQC)400 mm and H3 (WMM)250mm.

E1 (Mpa)	E2	E3	E4
1451	3748	12269	399.6

- **At 6m LHS**

For section 1 , layer thickness H1(overlay thickness)100mm and H2 (Asphalt)400 mm.

E1 (Mpa)	E2	E3
2018	13230	587

For section 2 , layer thickness H1(Asphalt)390mm and H2 (PQC)300 mm.

E1 (Mpa)	E2	E3
2217	123373	652

For section 3 , layer thickness H1(Asphalt)150mm and H2 (PQC)400 mm and H3 (WMM)250mm.

E1 (Mpa)	E2	E3	E4
2634	4705	9374	356

- **At 9m LHS**

For section 1 , layer thickness H1(overlay thickness)100mm and H2 (Asphalt)400 mm.

E1 (Mpa)	E2	E3
1422	15551	653

For section 2 , layer thickness H1(Asphalt)390mm and H2 (PQC)300 mm.

E1 (Mpa)	E2	E3
1224	18545	629

For section 3 , layer thickness H1(Asphalt)150mm and H2 (PQC)400 mm and H3 (WMM)250mm.

E1 (Mpa)	E2	E3	E4
1329	4612	3322	496

- **At 20m LHS**

For section 1 , layer thickness H1(overlay thickness)100mm and H2 (Asphalt)400 mm.

E1 (Mpa)	E2	E3
2264	20369	578

For section 2 , layer thickness H1(Asphalt)390mm and H2 (PQC)300 mm.

E1 (Mpa)	E2	E3
1988	20567	635

For section 3 , layer thickness H1(Asphalt)150mm and H2 (PQC)400 mm and H3 (WMM)250mm.

E1 (Mpa)	E2	E3	E4
2163	7645	11043	346

II. For New extended Apron i.e from stand 37 to stand 43 ,the PCN analysis was carried out based on the critical aircraft B777-300ER, ACN was rigid pavement as per subgrade categories (FAA guidelines) is 109.

From stand 37 to 43 ACN values were obtained. It is concluded that PCN values adopted is 112/R/C/W/T which is ≥ the ACNs of the critical aircraft i.e 109.

III. In case of runway pavement, slope assessment work was done to make the chamber bidirectional from unidirectional. Slope cut-off work was done at the requied chainage, milling and overlay of thickness 50/100mm as per FAARIELD design inputs provided.

The layer thickness before the work was done at section 1, H1(asphalt)500mm, H2(PQC) 150mm.

The overlay provided was 100 mm and asphalt thickness is 400mm i.e thickness of new bidirectional slope section.

It is concluded that the 400mm thickness of asphalt(BC) is laid over a period of time . The modulus obtained for is very higher.Higher modulus values indicates less fatigue life but over a period of time the 400mm asphalt has become so stiff but there is no cracking in the asphalt layer.Therefore higher modulus of 400 mm asphalt is justified.

7.2 Highway Pavement

7.2.1 Case study (Jetpur-Somnath road)

Surveys on the condition of the pavement are crucial for managing the pavement. The selected road from the case study's evaluation revealed that all of the sections were in good condition, with the majority of the deterioration coming from longitudinal and transverse fractures and ravelling. The road is divided into sections that are 62% GOOD, 35% FAIR, and 3% POOR. Timely maintenance may increase the lifespan of a pavement.

Using the Pavement Condition Index (PCI) approach, this case study was conducted to visually examine the condition of flexible pavement.

The PCI value can provide information on the overall condition, specific distress information, rate of deterioration, indication of structural condition, and functional pavement condition number.

The gathering of data is another essential component of condition surveys. Ratings of pavement condition are numerical descriptions or representations of individual pavement segments or complete networks.

7.2.2 Case study II

- For overlay designs of flexible pavements, Falling weight deflectometer testing should be done (as per IRC 115-2014) results should be analysed using KGP back so that remaining life of the existing layers can be considered for the realistic and economical designs.
- The remaining life of the existing layers came less than the design traffic then Overlay needs to be provided.
- Comparison of the layer moduli values obtained from KGPBACK software and ELMOD-6 software resulted that the average value of subgrade modulus determined using Elmod-6 (Deflection basin fit) was nearly similar to modulus obtained from IRC37:2018.
- The layer moduli values obtained from KGPBACK software and ELMOD-6 software resulted that the average value of Granular modulus determined using KGPBACK nearly gave similar values to IRC37:2018.

REFERENCES

Aavik, Andrus, and Ott Talvik. 2008. “Use of Falling Weight Deflectometer (Fwd) Measurement Data Environmental.” *The 7th International Conference of Environmental Engineering*, no. May: 8.

Abhishek, R. 2019. “Structural Evaluation of Flexible Pavement” 8 (05): 489–94.

Ahmed, MU. 2010. “Evaluation of FWD Software and Deflection Basin for Airport Pavements,” 181. http://repository.unm.edu/handle/1928/11076.

Butt, Abba, M. Y. Shahin, Samuel H. Carpenter, James V.Carnahan. n.d. “Application of Markov Process.”

CROW-report D13-02. 2013. “Guideline on PCN Assignment in the Netherlands 2013 2 Nd Edition of the Guideline on Airport Pavement Strength Rating and Directive for Reporting.”

D 6433(ASTM). n.d. “Standard Practice for Roads and Paking Lots Pavement Condition Survey.”

Deblois, Kate, Jean Pascal Bilodeau, and Guy Doré. 2010. “Use of Falling Weight Deflectometer Time History Data for the Analysis of Seasonal Variation in Pavement Response.” *Canadian Journal of Civil Engineering* 37 (9): 1224–31. https://doi.org/10.1139/L10-069.

Deol Guzzarlapudi, Sunny, Vinod Kumar Adigopula, and Rakesh Kumar. 2017. “Comparative Study of Flexible Pavement Layers Moduli Backcalculation Using Approximate and Static Approach.” *Materials Today: Proceedings* 4 (9): 9812–16. https://doi.org/10.1016/j.matpr.2017.06.272.

Elmod 6 Quick Start Manual. 2009. “Quick Start Manual –2009” 27 (27): 0–1.

FAA AC 150/5370- 11B. n.d. “AC : 150/5370- 11b.”

FHWA. 2017. “Enhanced Analysis of Falling Weight Deflectometer Data for Use With Mechanistic-Empirical Flexible Pavement Design and Analysis and Recommendations for Improvements to Falling Weight Deflectometers, FHWA-HRT-15-063.” *Federal Highway Administration Publications*, no. March: 324. https://rosap.ntl.bts.gov/view/dot/38336.

Fontul, Simona. 2004. “Strutural Evaluation of Flexible Pavements Using Non-Destrutive

Tests," no. November: 292.

Garg, Navneet, and Marshall R. Thompson. 1999. "Structural Response of LVR Flexible Pavements at Mn/Road Project." *Journal of Transportation Engineering* 125 (3): 238–44. https://doi.org/10.1061/(ASCE)0733-947X(1999)125:3(238).

ICAO, International Civil Aviation Organization -. 1983. "ICAO 9157 Aerodrome Design Manual - Part 3 - Pavements."

International Civil Aviation Organization (ICAO). 2016. *Aerodromes Design & Operations - Annex 14. Convention on International Civil Aviation*. Vol. I. http://cockpitdata.com/Software/ICAO Annex 14 Volume 1 7th Edition 2016.

IRC:, 115. 2014. "IRC : 115 -2014 GUIDELINES FOR STRUCTURAL EVALUATION AND STRENGTHENING OF FLEXIBLE ROAD PAVEMENTS USING FALLING WEIGHT DEFLECTOMETER (FWD) TECHNIQUE."

Irc:37-2018. 2018. "Guidelines for the Design of Flexible Pavements (Fourth Revision). IRC 37-2018. New Delhi, India."

Jin, Myung S., K. Wayne Lee, and William D. Kovacs. 1994. "Seasonal Variation of Resilient Modulus of Subgrade Soils." *Journal of Transportation Engineering* 120 (4): 603–16. https://doi.org/10.1061/(ASCE)0733-947X(1994)120:4(603).

Lynne H. Irwin, David P. Orr, and Daniel Atkins. 2011. "FWD Calibration Center and Operational Improvements : Redevelopment of the Calibration Protocol and Equipment" 5 (october).

Mallick, Rajib B, Tahar El-korchi, and Francis Group. n.d. *PAVEMENT ENGINEERING Principles and Practice*.

Okine, Attonh, and Offei Adarkwa. 2013. "Pavement Condition Surveys – Overview of Current Practices." *Delaware Center for Transportation, University of Delaware* 19716 (302): 1–71.

Patil, Chetan C, P Shivananda, and Vinod B.R. 2018. "Flexible Pavement Evaluation By Falling Weight Deflectometer Test Using IIT-Pave And KGP Back Software." *International Journal of Applied Engineering Research* 13 (7): 180–83.

Priddy, Lucy P, Alessandra Bianchini, and Carlos R Gonzalez. 2015. "Evaluation of Procedures for Backcalculation of Airfield Pavement Moduli Geotechnical and Structures Laboratory," no. August.

Rusmanto, Untung, Syafi'I, and Dewi Handayani. 2018. "Structural and Functional Prediction of Pavement Condition (A Case Study on South Arterial Road, Yogyakarta)." *AIP Conference Proceedings* 1977 (June 2018). https://doi.org/10.1063/1.5042984.

Sharma, Sunil, and Animesh Das. 2008. "Backcalculation of Pavement Layer Moduli from Falling Weight Deflectometer Data Using an Artificial Neural Network," no. Lenngren 1991. https://doi.org/10.1139/L07-083.

Sharpe, Gary W, Herbert F Southgate, and Robert C Deen. n.d. "USER ' S GUIDE FOR by I . PAVEMENT CONDITION SURVEY," no. June 1987.

Solanki, Ujjval, P Gundaliya, and M Barasara. 2016. "Structural Evaluation of Flexible Pavement Using Falling Weight Deflectometer." *Multi-Disciplinary Sustainable Engineering: Current and Future Trends*, no. May: 141–46. https://doi.org/10.1201/b20013-23.

Sun, Junyu, Gary Chai, Erwin Oh, and Phil Bell. 2022. "A Review of PCN Determination of Airport Pavements Using FWD/HWD Test." *International Journal of Pavement Research and Technology*. https://doi.org/10.1007/s42947-022-00170-1.

Tarefder, R. A., and M. U. Ahmed. 2013. "Consistency and Accuracy of Selected FWD Backcalculation Software for Computing Layer Modulus of Airport Pavements." *International Journal of Geotechnical Engineering* 7 (1): 21–35. https://doi.org/10.1179/1938636212Z.0000000009.

Zhou, Liang, Qingfeng Wu, and Jianming Ling. 2010. "Comparison of FWD and Benkelman Beam in Evaluation of Pavement Structure Capacity," 405–11. https://doi.org/10.1061/41104(377)51.

APPENDIX

APPENDIX-A

Table 1 Measured deflection at 3 ml on Runway (Ab-Cd)

Geophones			0	200	300	450	600	900	1200	1500	1800
Chainage	Drop	Stress kPa	D1	D2	D3	D4	D5	D6	D7	D8	D9
0.000	1	1300	180	92	76	62	56	49	45	40	36
0.000	2	2869	359	191	158	130	117	101	93	83	75
0.000	3	3704	458	243	199	165	149	128	117	105	95
0.051	1	1288	209	113	94	81	73	59	51	42	36
0.051	2	2834	419	240	204	174	157	130	112	93	81
0.051	3	3744	546	314	267	228	208	172	148	126	107
0.101	1	1277	213	112	95	77	68	54	46	39	33
0.101	2	2840	428	239	203	167	149	119	101	85	72
0.101	3	3788	549	311	265	219	195	158	136	114	98
0.151	1	1252	219	114	93	75	69	55	49	39	34
0.151	2	2803	447	247	205	169	152	125	108	91	78
0.151	3	3720	567	318	264	220	199	166	143	123	107
0.201	1	1260	234	124	98	83	73	62	52	45	37
0.201	2	2810	479	273	223	187	170	143	124	104	89
0.201	3	3727	533	362	293	245	223	189	164	138	117
0.251	1	1257	263	132	106	84	76	55	53	43	39
0.251	2	2798	532	288	234	191	172	139	117	97	83
0.251	3	3729	571	385	310	250	225	184	157	130	110
0.300	1	1246	239	121	96	78	69	56	47	39	33
0.300	2	2812	494	272	220	178	160	129	109	91	77
0.300	3	3725	578	364	290	233	210	171	147	121	99
0.350	1	1255	208	94	74	59	54	47	40	35	32
0.350	2	2814	416	204	162	130	118	99	90	79	70
0.350	3	3743	556	277	215	168	153	131	117	102	91
0.401	1	1258	203	99	78	64	58	49	44	38	34
0.401	2	2827	408	213	170	138	125	107	95	82	73
0.401	3	3650	370	281	221	178	163	140	125	108	96
0.451	1	1262	204	104	83	71	66	57	51	43	37
0.451	2	2823	414	227	185	156	145	125	111	96	83
0.451	3	3758	538	300	242	204	190	165	146	127	111
0.500	1	1259	173	96	81	64	61	51	46	39	34
0.500	2	2841	359	210	179	148	136	117	104	89	78
0.500	3	3708	474	279	235	194	179	153	136	118	103
0.550	1	1239	220	121	95	79	69	56	48	41	35
0.550	2	2821	461	264	212	174	155	126	110	94	81
0.550	3	3735	525	346	274	223	200	165	145	124	108
0.600	1	1257	208	100	80	68	62	53	45	38	33
0.600	2	2823	421	221	182	154	140	119	105	91	80
0.600	3	3665	557	294	242	200	182	156	138	119	104
0.650	1	1268	216	109	93	78	70	58	50	42	37
0.650	2	2805	433	238	206	176	158	131	113	95	82
0.650	3	3678	566	308	266	231	208	173	151	127	110
0.701	1	1257	202	92	75	64	57	49	44	37	33
0.701	2	2814	402	201	166	141	128	109	97	85	74
0.701	3	3722	514	270	220	184	169	144	129	112	98
0.751	1	1258	211	110	90	75	68	57	50	44	36
0.751	2	2803	425	242	197	165	150	126	110	94	80
0.751	3	3754	512	323	260	217	197	167	146	127	105
0.801	1	1263	201	95	77	66	61	52	45	39	30
0.801	2	2807	411	206	171	145	135	116	101	85	73
0.801	3	3764	526	276	225	190	178	153	134	114	99
0.850	1	1257	231	115	94	83	77	63	54	44	39
0.850	2	2807	461	244	202	178	165	137	116	96	81
0.850	3	3655	614	323	265	231	216	181	155	129	110
0.900	1	1265	220	113	94	82	80	64	58	48	42
0.900	2	2812	436	238	199	180	167	141	122	102	88
0.900	3	3656	592	313	259	232	217	185	160	135	116
0.951	1	1248	237	131	113	102	95	77	66	48	45
0.951	2	2809	484	283	246	222	206	172	146	122	103
0.951	3	3745	590	371	321	287	268	225	192	161	136
1.000	1	1252	274	155	133	114	103	81	66	53	43
1.000	2	2804	551	329	282	246	224	180	149	121	100
1.000	3	3723	702	430	365	317	290	236	197	162	135

Geophones			0	200	300	450	600	900	1200	1500	1800
Chainage	Drop	Stress kPa	D1	D2	D3	D4	D5	D6	D7	D8	D9
1.050	1	1259	228	122	100	88	81	67	60	49	42
1.050	2	2788	463	265	223	194	179	152	131	111	95
1.050	3	3685	605	352	294	254	237	203	177	149	128
1.099	1	1264	219	124	101	84	74	61	53	45	38
1.099	2	2799	450	268	223	183	165	137	117	99	84
1.099	3	3740	584	356	297	242	220	184	159	135	115
1.151	1	1249	236	122	102	86	77	61	53	42	37
1.151	2	2798	469	265	226	190	171	138	117	97	83
1.151	3	3785	625	354	298	250	226	185	158	131	111
1.200	1	1257	226	109	85	75	66	55	48	41	36
1.200	2	2802	454	229	189	164	148	124	108	93	82
1.200	3	3668	592	296	247	215	195	164	145	126	110
1.251	1	1251	251	144	125	108	95	77	59	51	38
1.251	2	2803	511	314	278	237	214	170	141	112	94
1.251	3	3673	630	415	366	311	280	227	189	152	125
1.301	1	1273	203	115	100	84	77	63	55	43	38
1.301	2	2803	410	246	216	181	165	137	118	98	83
1.301	3	3795	545	328	285	238	219	182	157	132	111
1.350	1	1248	229	118	99	84	76	62	51	42	36
1.350	2	2822	471	259	223	188	170	139	118	98	83
1.350	3	3712	579	347	297	248	226	185	160	132	113
1.400	1	1248	262	131	109	88	78	61	53	42	37
1.400	2	2808	533	290	241	197	176	140	119	99	84
1.400	3	3740	680	391	321	260	234	188	161	135	114
1.450	1	1259	175	75	68	64	58	50	46	39	32
1.450	2	2817	357	165	151	139	130	110	98	84	73
1.450	3	3725	346	228	200	181	168	145	128	111	97
1.500	1	1249	193	91	74	62	58	48	42	36	31
1.500	2	2812	385	194	161	137	125	105	92	79	70
1.500	3	3755	504	262	212	180	165	139	124	106	93
1.551	1	1245	187	102	84	71	65	53	46	40	35
1.551	2	2806	388	222	189	160	146	121	104	87	75
1.551	3	3724	485	298	251	209	191	160	139	117	101
1.600	1	1228	182	84	71	62	54	45	39	34	29
1.600	2	2803	377	188	162	139	125	103	90	77	68
1.600	3	3741	415	254	214	182	166	137	121	103	93
1.650	1	1251	208	92	76	63	58	48	41	35	30
1.650	2	2800	413	198	165	139	128	108	95	82	71
1.650	3	3813	500	267	219	184	169	143	126	109	95
1.700	1	1245	210	98	83	72	66	55	49	41	37
1.700	2	2805	429	213	187	159	146	123	108	92	80
1.700	3	3673	563	284	242	206	189	161	144	121	102
1.751	1	1253	204	103	83	71	64	52	45	39	33
1.751	2	2808	420	221	181	154	140	115	99	84	72
1.751	3	3689	468	290	232	197	179	148	129	110	95
1.800	1	1233	195	90	73	63	58	49	45	39	34
1.800	2	2802	389	196	163	139	128	110	96	83	73
1.800	3	3650	508	249	208	179	165	141	126	110	97
1.851	1	1256	238	116	96	81	73	60	53	44	38
1.851	2	2785	485	256	213	183	165	138	119	101	86
1.851	3	3687	633	339	280	240	219	185	162	136	117
1.901	1	1252	212	104	87	72	65	54	47	40	34
1.901	2	2807	427	228	197	162	148	126	110	94	79
1.901	3	3624	555	301	259	213	196	168	148	126	107
1.951	1	1245	202	96	77	65	59	50	42	35	29
1.951	2	2801	409	212	177	146	135	116	102	88	76
1.951	3	3604	533	281	232	192	178	154	137	117	102
2.001	1	1232	190	84	67	57	52	45	41	36	32
2.001	2	2797	385	185	150	127	117	103	92	82	73
2.001	3	3638	494	248	197	164	153	135	122	107	96

2.051	1	1245	197	82	68	56	52	44	39	34	32
2.051	2	2809	390	181	149	124	113	98	88	78	69
2.051	3	3596	471	243	194	161	148	128	115	100	87
2.100	1	1254	194	80	66	56	51	45	41	36	33
2.100	2	2815	394	173	142	121	111	98	89	79	71
2.100	3	3662	480	230	187	159	147	130	118	105	95
2.151	1	1246	204	90	74	63	58	47	42	37	31
2.151	2	2820	404	195	167	145	130	107	93	81	72
2.151	3	3748	476	268	223	193	174	145	128	110	98
2.200	1	1243	208	95	77	61	55	47	41	36	33
2.200	2	2799	425	211	171	141	128	109	96	82	72
2.200	3	3803	561	279	227	189	172	147	129	111	98
2.251	1	1256	183	81	63	51	46	40	35	32	28
2.251	2	2827	364	173	140	112	102	88	80	71	63
2.251	3	3792	358	233	186	148	135	116	105	93	85
2.301	1	1234	276	99	58	45	42	38	35	29	26
2.301	2	2786	532	206	127	98	93	84	76	65	59
2.301	3	3733	659	288	165	127	121	108	97	84	78
2.350	1	1254	238	89	59	50	47	45	42	37	34
2.350	2	2821	456	189	128	109	105	99	93	84	76
2.350	3	3738	530	265	170	143	138	131	124	111	99
2.401	1	1221	282	100	64	58	56	51	46	42	38
2.401	2	2793	557	220	156	137	131	120	110	97	86
2.401	3	3780	738	302	213	182	174	162	149	132	116
2.451	1	1249	282	103	72	64	62	57	54	49	43
2.451	2	2785	540	224	161	142	138	128	118	105	93
2.451	3	3792	678	306	216	189	183	169	156	139	124
2.501	1	1221	283	98	67	61	59	54	50	45	39
2.501	2	2794	543	207	153	136	132	121	113	100	88
2.501	3	3704	701	267	200	178	173	159	149	132	117
2.550	1	1238	284	107	75	64	61	56	52	45	41
2.550	2	2788	545	225	163	141	135	122	111	99	89
2.550	3	3709	680	314	218	187	179	162	149	133	118
2.600	1	1230	273	98	62	53	49	46	41	35	31
2.600	2	2797	531	211	142	121	113	103	94	83	74
2.600	3	3721	569	294	190	160	151	135	125	110	99
2.650	1	1245	288	105	64	55	51	47	45	37	36
2.650	2	2796	539	217	139	120	113	103	96	85	77
2.650	3	3676	684	300	185	157	148	135	127	114	99
2.700	1	1234	294	99	53	46	44	41	38	35	32
2.700	2	2797	544	211	124	101	97	90	85	76	71
2.700	3	3705	721	290	169	135	128	119	113	101	92
2.750	1	1242	256	86	43	31	27	24	22	19	17
2.750	2	2797	475	179	98	69	62	53	49	44	40
2.750	3	3741	633	230	132	92	82	72	65	59	53
2.801	1	1224	295	94	63	60	55	47	43	36	33
2.801	2	2770	581	212	145	135	124	105	94	83	75
2.801	3	3750	690	309	198	180	164	139	126	110	97
2.863	1	1234	293	106	80	72	72	64	62	54	49
2.863	2	2788	587	246	196	175	171	158	144	127	111
2.863	3	3760	790	367	282	249	242	222	203	177	155
2.901	1	1236	256	102	89	83	79	70	63	54	47
2.901	2	2791	531	247	214	195	186	165	148	124	105
2.901	3	3782	640	367	302	267	258	226	203	169	145
2.950	1	1218	295	109	77	83	80	57	47	43	38
2.950	2	2782	575	247	188	201	186	125	107	95	86
2.950	3	3710	739	356	262	274	246	165	143	126	112
3.001	1	1230	287	99	74	69	68	65	58	52	46
3.001	2	2781	550	228	179	163	159	149	136	120	106
3.001	3	3784	717	335	253	224	219	204	187	164	143
3.050	1	1228	236	77	68	69	66	65	59	54	48
3.050	2	2756	451	174	154	150	150	142	132	118	108
3.050	3	3696	602	243	211	202	201	192	177	159	143

Table 2: Measured Deflection at 6 mL on Runway (Ab-Cd)

Geophones			0	200	300	450	600	900	1200	1500	1800
Chainage	Stress	Load	D1	D2	D3	D4	D5	D6	D7	D8	D9
0.000	1	1256	226	77	70	61	56	48	43	38	35
0.000	2	2813	440	171	154	131	120	103	93	82	74
0.000	3	3090	486	200	171	144	132	113	102	91	82
0.075	1	1241	252	91	72	60	56	48	46	42	35
0.075	2	2812	484	198	157	134	122	104	93	82	72
0.075	3	3147	521	237	176	147	134	115	103	90	80
0.150	1	1241	274	120	93	81	73	59	50	43	38
0.150	2	2793	532	256	217	185	167	136	117	98	85
0.150	3	3103	601	286	241	201	183	149	128	108	93
0.225	1	1227	267	114	94	80	75	62	55	46	40
0.225	2	2776	518	248	213	186	172	145	126	107	91
0.225	3	3118	565	278	237	205	190	161	141	119	101
0.300	1	1232	266	104	86	77	67	55	47	41	36
0.300	2	2782	516	224	189	171	152	122	105	89	79
0.300	3	3104	583	267	209	186	166	135	117	99	88
0.374	1	1237	256	86	66	58	54	48	43	37	35
0.374	2	2797	482	189	144	129	119	105	94	83	73
0.374	3	3113	513	228	160	141	130	115	104	91	81
0.450	1	1248	267	105	85	75	70	61	55	48	42
0.450	2	2789	517	235	189	167	155	133	117	102	90
0.450	3	3114	571	274	209	184	171	149	133	115	100
0.524	1	1244	232	79	69	61	57	50	46	39	36
0.524	2	2813	446	178	152	135	127	112	101	88	77
0.524	3	3117	508	215	166	148	138	123	111	94	85
0.601	1	1243	234	78	63	58	57	50	45	40	36
0.601	2	2818	439	171	141	130	123	111	100	88	80
0.601	3	3113	465	203	156	147	137	124	112	98	89
0.675	1	1234	247	102	80	69	63	53	48	42	35
0.675	2	2796	467	216	177	153	141	120	106	92	80
0.675	3	3073	530	253	196	168	155	132	118	101	89
0.749	1	1246	233	107	88	74	68	59	53	46	41
0.749	2	2804	468	236	200	168	156	132	116	97	85
0.749	3	3146	561	278	219	184	170	144	129	108	92
0.825	1	1242	249	102	79	75	71	61	53	44	38
0.825	2	2788	471	222	182	168	159	137	119	101	86
0.825	3	3036	563	240	198	184	172	150	130	111	95
0.901	1	1236	239	95	78	74	71	60	52	45	40
0.901	2	2809	477	209	175	165	155	135	119	102	88
0.901	3	3056	557	232	192	178	169	146	128	111	96
0.974	1	1241	262	127	124	116	109	89	76	60	49
0.974	2	2800	519	277	270	255	239	198	166	134	110
0.974	3	3113	603	322	299	281	261	217	184	149	120
1.050	1	1224	263	134	114	95	86	73	63	51	44
1.050	2	2783	538	290	254	214	195	161	139	115	98
1.050	3	3129	523	333	281	234	214	179	154	128	108

Geophones			0	200	300	450	600	900	1200	1500	1800
Chainage	Stress	Load	D1	D2	D3	D4	D5	D6	D7	D8	D9
1.125	1	1229	252	103	87	77	71	59	53	44	40
1.125	2	2772	498	226	193	172	159	134	115	98	83
1.125	3	3124	528	262	214	188	174	150	130	109	94
1.200	1	1237	246	107	93	82	76	62	55	46	39
1.200	2	2799	481	231	206	183	167	140	120	100	86
1.200	3	3073	545	268	226	199	183	153	133	113	94
1.275	1	1243	275	117	111	98	89	70	60	49	40
1.275	2	2783	529	260	244	217	196	159	133	109	91
1.275	3	3098	544	302	268	236	214	175	148	121	101
1.350	1	1245	226	92	79	72	68	60	53	44	39
1.350	2	2818	435	200	173	159	148	127	111	93	80
1.350	3	3094	504	232	190	174	162	141	124	106	92
1.424	1	1237	215	93	77	69	63	53	47	39	35
1.424	2	2806	419	202	170	152	141	118	104	89	78
1.424	3	3047	459	237	187	167	153	131	115	97	85
1.500	1	1222	217	92	76	63	58	48	43	36	31
1.500	2	2801	441	200	165	139	127	106	93	81	71
1.500	3	3105	453	228	177	152	138	116	104	88	77
1.575	1	1247	267	106	85	74	70	55	50	41	35
1.575	2	2790	504	227	182	161	150	123	104	88	74
1.575	3	3105	545	264	200	177	165	136	119	98	84
1.651	1	1234	231	74	66	59	54	45	41	35	33
1.651	2	2807	444	175	153	133	121	103	91	79	70
1.651	3	3136	472	204	166	145	131	113	99	86	77
1.725	1	1240	214	82	67	58	53	44	41	25	32
1.725	2	2819	417	180	151	129	118	101	91	79	69
1.725	3	3087	449	213	165	141	130	112	101	87	78
1.799	1	1248	229	112	90	74	67	56	49	42	36
1.799	2	2799	450	243	201	165	151	126	110	93	80
1.799	3	3096	523	269	219	179	164	138	120	102	88
1.875	1	1262	241	92	73	63	59	52	47	41	36
1.875	2	2830	479	205	163	142	133	118	106	92	80
1.875	3	3117	476	241	182	156	147	131	118	102	89
1.950	1	1231	266	104	86	71	64	52	46	39	34
1.950	2	2793	501	226	192	156	140	116	100	85	74
1.950	3	3110	551	266	215	172	154	128	112	95	82
2.025	1	1240	225	92	77	66	59	50	44	38	32
2.025	2	2814	442	204	170	144	130	110	98	84	74
2.025	3	3152	488	240	186	160	144	123	111	94	79
2.101	1	1246	203	79	66	56	52	45	40	35	32
2.101	2	2795	396	171	142	122	111	97	87	77	69
2.101	3	3037	462	188	155	134	122	107	97	86	77
2.174	1	1236	238	108	85	70	63	52	46	40	35
2.174	2	2794	471	238	191	157	142	118	104	90	78
2.174	3	3083	489	270	207	166	154	129	123	98	85
2.250	1	1229	204	84	68	54	49	43	39	34	32
2.250	2	2790	400	182	145	119	109	95	85	74	66
2.250	3	3081	442	209	158	128	118	103	93	81	72

Geophones			0	200	300	450	600	900	1200	1500	1800
Chainage	Stress	Load	D1	D2	D3	D4	D5	D6	D7	D8	D9
2.325	1	1226	198	76	68	58	54	47	43	38	34
2.325	2	2799	393	164	147	126	115	101	92	81	73
2.325	3	3054	377	192	159	136	125	110	103	87	78
2.400	1	1235	203	84	67	53	54	49	46	40	36
2.400	2	2806	391	179	147	125	119	109	99	90	81
2.400	3	3039	442	202	161	142	128	118	110	96	88
2.474	1	1242	213	81	62	51	47	43	41	36	36
2.474	2	2796	401	166	130	106	97	89	83	76	70
2.474	3	3094	447	188	142	116	107	98	93	84	75
2.550	1	1247	214	83	67	56	53	48	45	39	37
2.550	2	2806	412	179	143	119	114	102	95	85	77
2.550	3	3076	428	204	156	131	122	113	107	92	80
2.624	1	1233	213	87	68	58	53	46	41	36	33
2.624	2	2789	409	190	150	128	117	102	91	81	73
2.624	3	3086	427	217	164	138	126	111	100	88	79
2.700	1	1238	217	80	60	48	44	39	37	32	29
2.700	2	2812	418	168	127	101	92	83	77	70	64
2.700	3	3060	373	194	138	111	100	90	84	76	69
2.772	1	1237	212	86	72	56	51	42	39	34	32
2.772	2	2802	412	188	156	122	109	92	85	74	68
2.772	3	3065	441	214	170	133	119	102	92	82	73
2.850	1	1232	264	144	129	108	92	71	61	52	46
2.850	2	2793	567	347	317	255	220	164	141	123	110
2.850	3	3057	544	391	344	273	237	181	157	136	118
2.923	1	1250	239	135	123	100	96	85	76	64	57
2.923	2	2792	498	309	281	233	222	196	176	152	132
2.923	3	3078	537	348	308	256	244	217	195	168	147
3.001	1	1242	242	125	117	93	90	81	73	63	57
3.001	2	2799	498	289	265	223	214	191	173	151	131
3.001	3	3053	551	317	282	240	230	207	188	166	145
3.074	1	1251	178	90	76	71	68	61	57	49	44
3.074	2	2822	359	197	170	158	152	136	123	109	95
3.074	3	3100	400	222	186	173	166	149	135	119	105
3.150	1	1259	155	58	62	63	63	58	54	48	43
3.150	2	2837	298	130	131	135	133	124	113	101	90
3.150	3	3119	299	155	145	148	146	136	126	111	100
3.224	1	1239	227	99	85	88	85	75	65	56	49
3.224	2	2796	457	226	200	203	194	171	150	130	111
3.224	3	3101	469	262	226	222	212	187	167	143	122
3.300	1	1257	175	70	70	61	58	53	49	43	37
3.300	2	2825	342	149	149	131	125	114	104	92	80
3.300	3	3095	355	176	162	143	137	125	114	101	89
3.374	1	1245	245	107	81	71	67	61	54	46	40
3.374	2	2794	467	230	182	163	155	138	123	105	90
3.374	3	3105	531	264	205	181	172	155	137	117	102
3.450	1	1249	169	78	72	69	68	64	62	57	48
3.450	2	2814	342	172	161	151	149	139	129	115	103
3.450	3	3115	349	197	178	166	163	153	142	127	113
3.524	1	1248	146	76	65	59	57	51	46	40	35
3.524	2	2838	305	171	151	136	130	116	104	91	79
3.524	3	3835	377	236	204	183	175	157	142	123	108

Table 3 : Measured deflection at 9 ml on Runway(Ab-Cd)

Geophones			0	200	300	450	600	900	1200	1500	1800
Chainage	Stress	Load	D1	D2	D3	D4	D5	D6	D7	D8	D9
0.000	1	1253	292	110	73	63	57	53	50	43	39
0.000	2	2803	560	234	158	136	126	112	102	90	82
0.000	3	3036	638	253	175	148	138	122	111	99	90
0.100	1	1242	332	119	79	72	65	54	48	41	36
0.100	2	2796	635	266	180	157	143	119	104	89	79
0.100	3	3107	524	315	204	171	156	130	115	99	87
0.200	1	1233	343	136	96	81	76	64	54	46	40
0.200	2	2792	665	303	219	188	175	144	124	104	89
0.200	3	3112	728	349	247	208	192	159	138	115	99
0.299	1	1232	303	103	70	59	55	48	44	39	35
0.299	2	2800	581	229	157	134	124	107	97	85	76
0.299	3	3098	639	272	177	147	135	117	106	94	83
0.399	1	1233	323	108	72	65	60	54	50	44	42
0.399	2	2792	617	240	159	142	134	119	108	94	85
0.399	3	3073	683	286	179	155	145	129	118	103	91
0.500	1	1225	329	108	74	63	58	52	47	40	35
0.500	2	2774	625	238	163	136	128	112	101	88	77
0.500	3	3049	650	270	183	149	140	124	112	98	86
0.600	1	1231	307	103	67	60	56	50	47	41	36
0.600	2	2786	578	222	146	130	122	109	100	88	78
0.600	3	3072	620	258	163	142	134	120	110	97	85
0.699	1	1238	318	109	76	68	66	59	54	47	42
0.699	2	2795	613	237	165	147	140	126	114	100	89
0.699	3	3134	667	284	187	161	154	138	126	111	98
0.799	1	1220	295	93	67	64	62	54	48	40	35
0.799	2	2772	593	210	150	143	139	122	108	93	80
0.799	3	3131	599	265	170	156	153	135	120	106	88
0.901	1	1215	315	103	88	80	76	64	56	47	41
0.901	2	2779	629	230	193	178	168	142	124	105	90
0.901	3	2983	733	253	208	189	180	153	135	116	99
0.999	1	1220	353	159	113	101	91	76	65	55	47
0.999	2	2775	697	346	253	221	203	169	146	122	104
0.999	3	3083	789	405	283	240	220	185	160	134	115
1.100	1	1240	344	112	89	76	70	59	52	45	40
1.100	2	2784	679	243	193	165	153	130	114	97	84
1.100	3	3095	699	288	214	179	166	142	124	106	92
1.200	1	1229	346	113	78	70	67	59	52	44	38
1.200	2	2784	655	254	179	158	150	131	116	99	84
1.200	3	3130	657	302	203	173	164	143	126	108	92
1.300	1	1233	299	99	74	65	60	52	47	41	36
1.300	2	2801	575	224	166	145	134	116	104	90	79
1.300	3	3073	593	271	185	158	146	127	114	99	87
1.400	1	1228	300	90	70	64	60	52	47	40	36
1.400	2	2789	573	209	157	141	132	115	102	88	77
1.400	3	3116	634	257	178	154	144	125	111	96	84
1.500	1	1235	308	85	60	54	51	46	41	36	33

Geophones			0	200	300	450	600	900	1200	1500	1800
Chainage	Stress	Load	D1	D2	D3	D4	D5	D6	D7	D8	D9
1.600	1	1237	311	92	67	60	55	48	44	38	34
1.600	2	2774	595	200	146	130	120	104	94	82	71
1.600	3	3108	643	246	165	143	133	115	105	92	81
1.700	1	1240	282	79	61	57	54	48	44	38	34
1.700	2	2796	551	181	135	124	117	103	93	81	72
1.700	3	3137	607	230	154	137	129	114	102	90	79
1.800	1	1232	265	98	93	84	78	69	62	51	44
1.800	2	2799	531	232	215	193	182	157	138	116	100
1.800	3	3131	622	286	238	212	201	174	153	130	110
1.900	1	1218	313	113	82	69	63	56	49	41	35
1.900	2	2779	611	255	187	157	144	123	109	93	80
1.900	3	3026	696	298	209	171	158	135	119	103	89
2.000	1	1233	325	84	55	52	48	44	41	36	32
2.000	2	2788	604	199	129	114	108	97	89	80	71
2.000	3	3118	590	253	151	129	120	108	100	88	77
2.100	1	1233	304	81	57	55	51	47	43	37	36
2.100	2	2794	603	183	129	121	114	102	93	83	74
2.100	3	3124	682	234	150	136	127	113	104	93	83
2.200	1	1241	325	105	71	60	54	48	44	38	33
2.200	2	2802	639	236	160	134	124	108	97	84	74
2.200	3	3110	693	278	180	147	136	120	108	93	83
2.300	1	1242	311	88	67	57	55	50	46	42	37
2.300	2	2793	590	193	145	124	118	109	101	89	80
2.300	3	3117	688	242	165	138	131	121	112	100	89
2.400	1	1222	296	97	67	61	59	54	51	47	45
2.400	2	2793	577	211	147	133	129	120	112	101	91
2.400	3	3121	630	258	169	147	143	132	124	111	100
2.500	1	1216	333	111	78	62	62	55	50	42	40
2.500	2	2753	653	237	169	142	134	119	108	98	87
2.500	3	3021	742	276	190	156	146	130	120	108	96
2.600	1	1232	290	91	58	49	45	44	41	33	33
2.600	2	2792	546	193	123	104	98	90	84	75	69
2.600	3	3070	611	228	139	115	108	99	93	84	78
2.700	1	1234	228	57	42	39	35	32	31	29	27
2.700	2	2806	426	134	94	85	78	71	66	59	55
2.700	3	3142	468	172	109	93	86	77	73	65	60
2.800	1	1238	270	84	53	50	47	43	40	36	31
2.800	2	2776	524	186	119	111	104	91	83	73	67
2.800	3	3110	593	229	137	122	116	101	92	83	73
2.900	1	1246	274	105	81	82	73	61	56	49	42
2.900	2	2804	539	244	191	183	158	130	119	105	93
2.900	3	3101	523	289	214	200	174	144	131	113	95
3.000	1	1237	224	80	69	74	71	66	64	54	44
3.000	2	2794	456	189	159	167	164	147	133	115	100
3.000	3	3108	504	233	181	187	183	164	145	127	111
3.100	1	1250	229	68	62	62	61	58	53	50	42
3.100	2	2826	441	159	135	136	137	129	117	102	91
3.100	3	3136	473	194	154	153	153	144	132	117	103
3.200	1	1238	278	88	68	65	64	59	53	44	39
3.200	2	2799	545	198	154	150	145	131	118	101	88
3.200	3	3151	600	239	176	168	162	148	131	113	98
3.300	1	1244	249	66	59	58	57	53	50	44	39
3.300	2	2797	469	151	131	126	127	119	108	95	84
3.300	3	3141	506	197	149	144	143	134	121	106	94
3.400	1	1249	233	72	57	62	62	59	53	43	40
3.400	2	2816	444	167	134	142	141	135	117	102	90
3.400	3	3132	491	208	153	159	158	150	133	115	102
3.500	1	1244	244	77	69	70	69	62	56	48	41
3.500	2	2819	466	188	166	164	162	144	128	110	95
3.500	3	3147	516	240	190	187	182	163	145	124	106
3.542	1	1254	270	80	61	59	59	56	52	47	38
3.542	2	2817	530	184	140	131	130	124	113	99	84
3.542	3	3126	592	214	160	146	146	139	127	112	95

Table 4 : Measured Deflection at 20 ml on Runway (Ab-Cd)

Geophones			0	200	300	450	600	900	1200	1500	1800
Chainage	Stress	Load	D1	D2	D3	D4	D5	D6	D7	D8	D9
0.000	1	1258	237	96	80	73	68	59	53	47	41
0.000	2	2804	466	212	178	158	147	127	114	100	89
0.000	3	3105	442	248	195	172	161	140	127	109	95
0.100	1	1259	248	106	88	76	69	58	54	45	37
0.100	2	2811	491	235	192	166	151	127	113	97	85
0.100	3	3147	531	268	214	182	167	141	125	107	94
0.250	1	1262	253	118	97	87	79	65	56	50	44
0.250	2	2828	503	252	206	183	169	141	120	105	93
0.250	3	3116	552	286	227	200	185	154	132	115	102
0.400	1	1253	245	114	90	74	68	57	52	46	41
0.400	2	2818	491	244	193	161	145	122	108	96	84
0.400	3	3059	491	275	212	175	158	133	119	105	93
0.550	1	1261	209	86	68	59	57	51	50	45	38
0.550	2	2821	407	180	141	123	118	108	100	89	82
0.550	3	3113	457	204	155	135	129	118	108	97	88
0.701	1	1267	225	89	76	70	65	60	54	47	42
0.701	2	2822	446	188	162	146	139	123	111	98	88
0.701	3	3126	481	213	178	160	152	136	123	109	97
0.849	1	1269	241	107	94	86	82	71	63	55	48
0.849	2	2811	484	232	201	183	174	147	131	114	102
0.849	3	3092	505	259	219	199	189	164	147	126	110
1.000	1	1259	246	132	120	107	100	83	73	62	52
1.000	2	2817	498	286	257	233	217	180	155	131	113
1.000	3	3127	550	320	282	255	238	197	171	145	125
1.150	1	1261	245	108	87	76	71	62	57	48	42
1.150	2	2808	487	231	184	163	151	131	116	101	90
1.150	3	3115	509	266	204	178	166	144	128	112	99
1.300	1	1268	187	85	68	60	56	51	47	43	36
1.300	2	2843	367	181	143	126	118	105	96	85	77
1.300	3	3101	427	201	158	137	128	115	105	93	84
1.449	1	1268	222	96	78	70	64	57	52	45	41
1.449	2	2849	429	202	165	147	137	119	108	96	85
1.449	3	3133	472	227	180	161	150	131	119	105	94
1.600	1	1253	227	91	76	70	65	57	53	45	39
1.600	2	2807	444	197	162	147	137	121	108	95	83
1.600	3	3086	495	226	179	162	151	133	119	104	92
1.750	1	1249	199	94	76	69	65	57	52	45	41
1.750	2	2805	408	203	167	148	140	122	110	97	86
1.750	3	2916	432	218	175	153	145	126	114	100	90
1.900	1	1237	197	88	67	56	52	48	45	38	36
1.900	2	2784	400	186	146	120	112	100	92	83	73
1.900	3	2913	419	202	155	125	117	104	96	86	76
2.050	1	1255	184	77	60	48	45	43	40	36	34
2.050	2	2817	366	162	126	105	99	91	85	77	69
2.050	3	2963	380	179	135	111	105	96	90	83	75
2.201	1	1248	204	77	61	49	44	39	40	35	32
2.201	2	2799	414	162	128	103	94	84	79	71	66
2.201	3	2987	453	184	139	110	101	90	84	78	70
2.350	1	1260	200	78	61	50	45	44	42	37	34
2.350	2	2819	393	164	126	102	96	91	86	78	71
2.350	3	3032	424	182	136	109	103	97	92	83	76
2.499	1	1238	203	87	71	61	55	53	49	46	41
2.499	2	2815	406	182	150	128	122	111	103	94	85
2.499	3	3033	430	203	161	138	131	119	110	100	90

Geophones			0	200	300	450	600	900	1200	1500	1800
Chainage	Stress	Load	D1	D2	D3	D4	D5	D6	D7	D8	D9
2.649	1	1245	188	75	62	51	48	45	43	39	36
2.649	2	2819	377	156	128	106	100	93	87	81	74
2.649	3	3034	391	172	138	113	106	99	94	86	79
2.801	1	1238	197	70	58	50	48	45	45	39	36
2.801	2	2809	382	142	116	106	100	95	90	82	74
2.801	3	3004	408	164	125	113	108	103	97	88	80
2.950	1	1261	175	77	73	73	72	66	61	55	47
2.950	2	2831	353	169	158	159	157	143	130	115	102
2.950	3	3058	384	191	172	173	169	155	141	124	110
3.100	1	1260	158	85	78	74	72	70	64	58	53
3.100	2	2846	330	184	168	162	158	148	137	123	110
3.100	3	3067	348	202	181	173	170	159	147	132	119
3.101	1	1255	162	85	79	75	72	70	64	57	52
3.101	2	2840	330	186	169	161	158	148	137	123	110
3.101	3	3054	356	205	183	173	170	159	147	133	119
3.102	1	1262	172	87	79	75	73	69	65	58	53
3.102	2	2839	343	187	169	161	158	148	136	122	109
3.102	3	3023	383	201	180	173	169	158	146	132	119
3.249	1	1251	168	73	65	64	62	59	58	47	42
3.249	2	2834	342	158	141	137	135	127	112	103	89
3.249	3	3020	359	178	151	148	145	137	124	111	99
3.400	1	1243	176	90	78	76	70	69	59	53	47
3.400	2	2791	370	200	175	169	163	147	132	115	101
3.400	3	3063	403	225	190	184	178	160	143	125	109
3.401	1	1237	190	88	78	75	71	65	59	52	46
3.401	2	2790	392	198	175	170	164	147	132	115	100
3.401	3	2987	415	216	188	182	176	158	142	125	110
3.402	1	1246	198	90	80	75	71	67	61	52	46
3.402	2	2802	400	197	173	170	165	147	132	115	100
3.402	3	2949	431	210	187	182	175	158	142	125	110
3.529	1	1270	133	77	66	60	58	53	48	42	37
3.529	2	2857	285	168	148	132	128	117	106	93	82
3.529	3	2997	307	176	156	141	136	124	113	99	88

Table 5 : Back-calculated layer moduli for Runway pavement along 3m L from centreline

Chainage	Layer thickness		Backcalculated layer modulus			
	H1	H2	E1	E2	E3	E4
0.000	100	400	1262	9748	689	
0.051	100	400	1551	5531	561	
0.101	100	400	1535	5029	617	
0.151	100	400	1332	5587	567	
0.201	100	400	2820	4006	522	
0.251	100	400	2881	3207	541	
0.300	100	400	2262	3246	592	
0.350	100	400	1122	5421	747	
0.401	100	400	5362	5233	675	
0.451	100	400	1272	7437	567	
0.500	100	400	1710	6761	617	
0.550	100	400	2364	4126	589	
0.600	100	400	1209	5587	623	
0.650	100	400	1276	5967	538	
0.701	100	400	1291	6761	662	
0.751	100	400	1872	5393	581	
0.801	100	400	1133	8263	617	
0.850	100	400	1089	5345	538	
0.900	100	400	1068	6693	510	
0.951	100	400	1659	5723	422	
1.000	100	400	1566	3520	419	
1.050	100	400	1451	4822	483	
1.099	100	400	2245	3400	567	
1.151	100	400	1414	4165	544	
1.200	100	400	1028	6453	567	
1.251	100	400	2477	3278	430	
1.301	100	400	1999	4755	553	
1.350	100	400	1680	4457	528	
1.400	100	400	1423	3265	533	
1.450	100	400	3018	11257	612	
1.500	100	400	1231	7437	679	
1.551	100	400	2064	5476	611	
1.600	100	400	2270	7106	689	
1.650	100	400	1354	7289	679	
1.700	100	400	1017	7512	567	
1.751	100	400	1970	5547	648	
1.800	100	400	1017	10099	623	
1.851	100	400	1096	5079	520	
1.901	100	400	1269	5587	567	
1.951	100	400	1225	6300	608	
2.001	100	400	1007	11977	611	
2.051	100	400	1206	8040	706	
2.100	100	400	1005	13345	642	
2.151	100	400	1444	8056	633	
2.200	100	400	1017	7855	639	
2.251	100	400	4002	7383	713	

Chainage	H1	H2	E1	E2	E3	E4
2.301	100	400	1361	16429	770	
2.350	100	400	2033	10736	678	
2.401	100	400	1341	18445	503	
2.451	100	400	1556	15909	484	
2.501	100	400	1331	46201	421	
2.550	100	400	1512	13315	497	
2.600	100	400	1941	9274	623	
2.650	100	400	1408	11502	623	
2.700	100	400	1237	18072	700	
2.750	100	400	1535	1290	53333	1125
2.801	100	400	1480	1808	8164	607
2.863	100	400	1295	1886	14970	333
2.901	100	400	2233	2242	8835	297
2.950	100	400	1242	3227	3745	225
3.001	100	400	1479	1975	20221	358
3.050	100	400	1102	9765	9765	333
3.100	100	400	974	4336	2918	123
3.150	100	400	822	6349	5771	348
3.202	100	400	1167	6046	5235	330
3.250	100	400	1950	1959	14198	420
3.300	100	400	1428	3694	7195	415
3.351	100	400	1236	6017	6619	350
3.401	100	400	1280	4301	6201	323
3.451	100	400	2313	2249	8105	285
3.501	100	400	1496	1752	24109	439
3.542	100	400	1645	4825	9202	483

Table 6: Back-calculated layer moduli for Runway pavement along 6m L from centreline

Chainage	H1	H2	H3	H4	E1	E2	E3	E4
0	500	150			1997	14680	714	
0.075	500	150			1862	14012	703	
0.15	500	150			1715	7650	528	
0.225	500	150			1960	8036	491	
0.3	500	150			1693	11766	574	
0.374	500	150			1911	8267	753	
0.45	500	150			1779	14722	526	
0.524	500	150			1986	8701	716	
0.601	500	150			2276	8450	721	
0.675	500	150			1960	7370	607	
0.749	500	150			1881	9669	552	
0.825	500	150			1737	22043	510	
0.901	500	150			1881	6999	596	
0.974	500	150			2152	5250	357	
1.05	500	150			2503	3736	419	
1.125	500	150			1946	27193	485	
1.2	500	150			1887	19524	472	
1.275	500	150			2207	7008	421	
1.35	500	150			2048	20222	546	
1.424	500	150			2312	11937	577	
1.5	500	150			2312	10055	678	
1.575	500	150			1839	11766	581	
1.651	500	150			1972	57316	630	
1.725	500	150			2247	11029	721	
1.799	500	150			2032	8176	559	
1.875	500	150			2178	20715	577	
1.95	500	150			1847	7162	623	
2.025	500	150			2184	7914	668	
2.101	500	150			2074	17884	735	
2.174	500	150			2184	7664	590	
2.25	390	300			2074	7682	721	
2.325	390	300			2665	10548	612	
2.4	390	300			2023	17221	541	
2.474	390	300			1848	20015	678	
2.55	390	300			2135	13361	607	
2.624	390	300			2282	7333	655	
2.7	390	300			2497	10201	753	
2.772	150	400	250		2255	2090	9593	651
2.85	150	400	250		5306	1046	3383	277
2.923	150	400	250		2989	2075	4359	289
3.001	150	400	250		2170	2187	9934	260
3.074	150	400	250		2645	3468	17467	347
3.15	150	400	250		2541	16113	14579	321
3.224	150	400	250		1973	5071	5758	263
3.3	150	400	250		2107	7934	10116	378
3.374	150	400	250		1728	2363	9180	422
3.45	150	400	250		2533	8620	9748	350
3.524	150	400	250		4781	3656	27117	326

Table 7: Back-calculated layer moduli for Runway pavement along 9m L from centreline

Chainage	H1	H2	H3	H4	E1	E2	E3	E4
0	500	150			1316	25221	651	
0.1	500	150			2069	3796	611	
0.2	500	150			1363	4566	528	
0.299	500	150			1350	16184	703	
0.399	500	150			1279	11272	685	
0.5	500	150			1350	13467	668	
0.6	500	150			1385	21444	695	
0.699	500	150			1385	11004	638	
0.799	500	150			1600	10004	667	
0.901	500	150			1227	6999	596	
0.999	500	150			1272	3665	448	
1.1	500	150			1244	31353	534	
1.2	500	150			1417	13467	575	
1.3	500	150			1524	17773	616	
1.4	500	150			1333	53106	595	
1.5	500	150			1815	13020	793	
1.6	500	150			1350	18821	735	
1.7	500	150			1470	12400	824	
1.8	500	150			1787	5402	492	
1.9	500	150			1276	8185	623	
2	500	150			1485	12961	833	
2.1	500	150			1215	23013	816	
2.2	500	150			1215	20562	694	
2.2	390	300			1151	7856	633	
2.3	390	300			1080	26076	541	
2.4	390	300			1303	13132	546	
2.5	390	300			1007	12585	523	
2.6	390	300			1203	19539	680	
2.7	390	300			1601	32327	854	
2.7	150	400	250		1471	2539	16946	913
2.8	150	400	250		1161	2054	10522	700
2.9	150	400	250		2331	1681	7493	456
3	150	400	250		1351	5348	8344	364
3.1	150	400	250		1247	7538	12379	399
3.2	150	400	250		1109	3021	11010	446
3.3	150	400	250		1106	7000	7700	466
3.4	150	400	250		1228	6898	10201	399
3.5	150	400	250		1365	4862	8363	335
3.542	150	400	250		925	5182	6271	483

Table 8 : Back-calculated layer moduli for Runway pavement along 20m L from centreline

Chainage	H1	H2	H3	H4	E1	E2	E3	E4
0	500	150			2666	10307	536	
0.1	500	150			2024	10564	552	
0.25	500	150			1973	10125	497	
0.4	500	150			2250	5186	567	
0.55	500	150			2170	22516	678	
0.701	500	150			1959	139745	452	
0.849	500	150			2268	15445	446	
1	500	150			2381	7033	369	
1.15	500	150			2170	6848	560	
1.3	500	150			2387	18608	685	
1.449	500	150			2326	7892	633	
1.6	500	150			2136	7174	639	
1.75	500	150			2387	16561	555	
1.9	500	150			2291	11029	721	
2.05	500	150			2585	16504	793	
2.201	390	300			1758	13648	753	
2.35	390	300			1919	24006	653	
2.499	390	300			2107	17846	526	
2.649	390	300			2168	26769	610	
2.801	150	400	250		1296	9181	12343	415
2.95	150	400	250		1850	10130	8047	344
3.1	150	400	250		2703	7712	12570	323
3.101	150	400	250		2634	7017	13029	324
3.102	150	400	250		1964	8913	9810	323
3.249	150	400	250		1851	10718	11789	319
3.4	150	400	250		2379	4503	10943	356
3.401	150	400	250		1917	5701	7856	352
3.402	150	400	250		1569	7605	7124	299
3.529	150	400	250		3469	4974	16925	413

Table 9 :HWD deflection data for at 3m LHS from centreline before the work

Geophone distances (mm):			0	200	300	450	600	900	1200	1500	1800
Chainage	Drop	Stress kpa	D1 Mic.	D2 Mic.	D3 Mic.	D4 Mic.	D5 Mic.	D6 Mic.	D7 Mic.	D8 Mic.	D9 Mic.
0	3	3866	728	341	283	252	227	195	172	152	134
0.05	3	3887	678	456	391	332	288	236	201	173	146
0.1	3	3828	733	467	393	331	288	232	192	166	143
0.15	3	3808	891	613	535	483	427	341	276	225	180
0.2	3	3847	868	596	529	481	430	341	274	223	182
0.25	3	3702	1117	727	614	537	472	392	321	256	206
0.3	3	3812	1145	605	467	369	328	277	235	201	168
0.35	3	3798	819	519	459	400	363	299	250	210	171
0.4	3	3827	745	429	369	320	286	239	204	175	150
0.45	3	3834	969	600	486	403	345	277	233	196	164
0.5	3	3836	774	452	387	331	299	244	206	176	148
0.55	3	3799	878	471	402	345	299	238	208	177	149
0.6	3	3806	823	466	394	344	306	248	205	174	146
0.65	3	3786	806	439	381	350	312	253	223	193	161
0.7	3	3770	661	349	312	280	255	210	183	162	126
0.75	3	3791	786	476	409	367	323	259	213	179	152
0.8	3	3830	569	338	299	266	240	194	161	137	116
0.85	3	3819	644	414	369	333	296	229	183	150	127
0.9	3	3816	631	396	356	315	284	228	189	160	135
0.95	3	3802	649	420	377	342	310	254	211	179	151
1	3	3831	783	512	443	381	333	264	217	186	158
1.05	3	3816	806	527	457	413	361	284	228	191	159
1.1	3	3822	813	483	418	368	316	256	214	180	160
1.15	3	3803	911	517	443	389	345	275	231	192	161
1.2	3	3806	899	572	512	471	417	330	265	217	177
1.25	3	3810	887	569	498	429	379	299	237	198	161
1.3	3	3812	892	513	426	368	326	257	208	173	144
1.35	3	3824	815	492	426	368	326	265	215	182	151
1.4	3	3820	738	415	340	283	244	197	166	143	120
1.45	3	3877	748	434	370	322	289	238	200	171	146
1.5	3	3834	645	360	310	268	241	193	164	140	123
1.55	3	3789	853	488	425	367	330	267	221	188	157
1.6	3	3777	783	381	311	268	237	198	171	151	130
1.65	3	3792	687	395	343	300	273	225	200	171	152
1.7	3	3772	687	415	356	312	279	224	181	154	131
1.75	3	3771	790	447	377	319	283	225	191	163	137
1.8	3	3778	586	360	321	291	263	214	178	154	131
1.85	3	3729	676	408	355	320	280	224	184	159	134
1.9	3	3753	641	381	330	285	255	218	189	166	143
1.95	3	3721	713	373	314	280	256	212	181	160	135
2	3	3696	713	410	341	287	253	207	175	154	130
2.05	3	3728	741	379	308	258	226	186	162	144	126
2.1	3	3749	597	309	263	237	215	182	160	141	121
2.15	3	3769	827	430	368	322	284	233	196	169	146

2.2	3	3784	673	332	280	248	226	192	165	143	126	
2.25	3	3766	766	390	322	261	222	177	152	132	115	
2.3	3	3781	472	217	213	196	187	170	153	137	120	
2.35	3	3730	607	330	287	267	249	220	194	171	147	
2.4	3	3692	593	297	254	232	222	197	176	155	138	
2.45	3	3713	510	228	194	186	178	162	149	133	121	
2.5	3	3715	584	308	264	247	224	205	186	156	146	
2.55	3	3670	582	305	251	238	222	185	168	149	130	
2.6	3	3704	598	299	254	240	229	205	184	164	144	
2.65	3	3763	538	285	245	227	214	188	169	150	132	
2.7	3	3710	553	253	223	196	176	149	130	117	99	
2.75	3	3780	633	336	287	322	295	245	213	183	156	
2.8	3	3768	502	204	198	193	184	166	146	129	114	
2.85	3	3719	396	218	218	204	200	185	165	148	131	
2.9	3	3742	543	348	352	286	276	246	214	190	166	
2.95	3	3707	447	231	226	225	222	210	196	183	139	
3	3	3732	505	286	262	238	188	155	144	128	114	
3.05	3	3712	532	232	226	214	212	192	172	153	137	
3.05	3	3788	539	244	233	219	215	196	177	159	138	
3.1	3	3892	416	214	215	206	201	186	169	154	130	
3.15	3	3886	417	263	289	258	250	222	194	169	146	
3.2	3	3864	459	232	228	219	213	195	174	155	136	
3.25	3	3849	488	258	234	232	223	195	167	145	123	
3.3	3	3854	500	280	262	222	215	192	168	148	128	
3.35	3	3878	459	230	207	199	195	178	158	139	121	
3.4	3	3834	469	316	298	257	248	223	196	174	154	
3.45	3	3850	418	234	219	213	208	193	173	156	139	
3.5	3	3818	684	232	195	185	179	162	146	131	113	

Table 10 : Back-calculated layer moduli for Runway pavement along 3m L from centreline before the works.

Chainage	Layer Thickness				Layer Moduli			
(m)	H1	H2	H3	H4	E1	E2	E3	E4
0	500	150			1878	4452	539	
0.05	500	150			2761	781	409	
0.1	500	150			2300	938	415	
0.15	500	150			2208	371	286	
0.2	500	150			2437	424	253	
0.25	500	150			1522	571	245	
0.3	500	150			1159	1515	374	
0.35	500	150			2245	879	321	
0.4	500	150			2184	1667	410	
0.45	500	150			1595	895	352	
0.5	500	150			2084	1719	398	
0.55	500	150			1654	1900	405	
0.6	500	150			1882	1604	397	
0.65	500	150			2026	1405	384	
0.7	500	150			2422	1900	472	
0.75	500	150			2093	1520	366	
0.8	500	150			2953	2710	488	
0.85	500	150			2894	668	426	
0.9	500	150			2927	1073	420	
0.95	500	150			2937	1553	364	
1	500	150			2280	691	364	
1.05	500	150			2294	561	342	
1.1	500	150			1993	1432	373	
1.15	500	150			1723	1264	356	
1.2	500	150			2104	546	287	
1.25	500	150			1977	573	328	
1.3	500	150			1722	1079	389	
1.35	500	150			2005	1480	365	
1.4	500	150			2018	1173	516	
1.45	500	150			2163	1962	414	
1.5	500	150			2396	2594	498	
1.55	500	150			1928	807	381	
1.6	500	150			1740	2044	531	
1.65	500	150			2473	1337	431	
1.7	500	150			2344	1749	426	
1.75	500	150			1878	1910	422	
1.8	500	150			3146	1190	446	
1.85	500	150			2453	1456	417	
1.9	500	150			2705	1144	446	
1.95	500	150			2061	2092	473	
2	500	150			2056	1765	456	
2.05	500	150			1880	1630	536	
2.1	500	150			2461	5689	513	
2.15	500	150			1738	2380	420	

Chainage	Layer Thickness (mm)				Moduli (MPa)			
	H1	H2	H3	H4	E1	E2	E3	E4
2.2	500	150			2258	1457	555	
2.25	390	300			1670	2128	531	
2.3	390	300			2635	29731	418	
2.35	390	300			2208	10570	351	
2.4	390	300			2024	16110	376	
2.45	390	300			2140	42672	408	
2.5	390	300			2168	14330	365	
2.55	390	300			2147	9920	413	
2.6	390	300			2004	19975	348	
2.65	390	300			2397	15187	400	
2.7	390	300			2093	9947	554	
2.75	150	400	250		1654	5289	2771	304
2.8	150	400	250		1489	10034	6299	427
2.85	150	400	250		2753	9827	9063	346
2.9	150	400	250		3312	4047	1984	314
2.95	150	400	250		31296	2917	1488	365
3	150	400	250		2753	3557	2174	500
3.05	150	400	250		1558	7812	8317	348
3.05	150	400	250		1468	9060	7989	342
3.1	150	400	250		2465	11205	8759	361
3.15	150	400	250		3444	15423	317	364
3.2	150	400	250		2126	10021	7259	350
3.25	150	400	250		2153	7238	3948	394
3.3	150	400	250		2544	4827	4340	409
3.35	150	400	250		2110	7849	8488	408
3.4	150	400	250		3939	5239	2487	343
3.45	150	400	250		2559	11131	7033	345
3.5	150	400	250		2956	6705	6848	468

APPENDIX B

Table 1 Measured Deflection data on stand 37

Chainage	Drop	Stress kPa	D1 Mic.	D2 Mic.	D3 Mic.	D4 Mic.	D5 Mic.	D6 Mic.	D7 Mic.	D8 Mic.	D9 Mic.
1.100	1	1401	96	89	85	75	77	67	59	55	13
1.100	2	2454	158	151	146	135	131	119	104	94	94
1.100	3	4116	257	247	240	222	215	192	173	151	151
2.100	1	1420	99	96	96	86	82	74	67	58	58
2.100	2	2459	169	162	162	145	139	125	112	101	101
2.100	3	4145	273	263	261	235	227	204	182	161	161
3.100	1	1415	92	82	82	83	70	72	59	55	55
3.100	2	2467	150	145	141	137	131	118	105	91	91
3.100	3	4165	257	236	229	222	216	191	171	147	147
3.210	1	1418	115	119	108	94	87	76	66	58	58
3.210	2	2478	196	203	185	157	149	129	113	99	99
3.210	3	4169	310	322	296	248	237	205	180	156	156
3.220	1	1405	117	119	80	93	85	75	67	57	57
3.220	2	2471	198	208	142	156	151	129	113	98	98
3.220	3	4145	326	345	241	260	244	211	186	161	161
4.100	1	1416	132	123	121	115	108	96	83	71	71
4.100	2	2474	231	214	208	199	190	166	143	124	124
4.100	3	4173	378	355	344	327	311	274	238	206	206
5.100	1	1432	83	77	74	74	76	67	59	54	54
5.100	2	2489	144	133	129	130	122	111	104	89	89
5.100	3	4211	236	217	212	208	206	184	169	151	151
6.100	1	1426	88	82	81	77	73	66	59	52	52
6.100	2	2481	152	143	140	130	127	115	99	92	92
6.100	3	4225	251	235	231	220	211	188	170	150	150
6.220	1	1410	141	150	66	112	105	96	79	67	67
6.220	2	2467	240	253	113	190	178	156	133	111	111
6.220	3	4185	399	420	181	310	296	254	219	186	186
6.230	1	1419	110	114	107	87	82	76	62	56	56
6.230	2	2486	191	198	187	154	142	130	112	97	97
6.230	3	4205	315	330	311	253	242	211	185	158	158
7.100	1	1409	86	78	79	69	70	59	52	46	46
7.100	2	2455	140	135	135	118	120	102	92	80	80
7.100	3	4190	235	224	223	198	193	171	153	133	133
8.100	1	1410	85	77	76	72	68	62	56	49	49
8.100	2	2461	145	135	132	121	121	106	98	88	88
8.100	3	4203	241	223	218	206	200	180	164	148	148
9.100	1	1419	96	92	90	81	78	69	64	54	54
9.100	2	2456	164	157	156	140	134	120	107	96	96
9.100	3	4196	272	260	258	232	221	201	178	160	160

9.100	1	1419	96	92	90	81	78	69	64	54	47
9.100	2	2456	164	157	156	140	134	120	107	96	81
9.100	3	4196	272	260	258	232	221	201	178	160	135
10.100	1	1421	90	81	80	77	75	66	60	52	44
10.100	2	2482	151	136	140	135	132	112	109	92	80
10.100	3	4226	250	234	228	221	214	194	173	153	133
11.100	1	1392	140	126	122	123	113	99	86	73	65
11.100	2	2445	238	224	217	210	201	173	152	130	111
11.100	3	4179	390	367	354	345	329	284	249	213	187
12.100	1	1432	88	83	80	74	72	67	58	53	46
12.100	2	2481	150	142	138	130	125	113	104	91	81
12.100	3	4228	251	236	232	216	209	189	172	152	134
13.100	1	1423	95	89	88	79	77	67	61	54	46
13.100	2	2487	157	154	153	134	127	118	103	95	81
13.100	3	4238	261	254	250	227	220	193	169	153	132
13.220	1	1420	177	195	102	131	123	101	86	69	56
13.220	2	2473	284	312	182	212	198	163	140	113	93
13.220	3	4210	439	478	296	332	310	259	223	185	155
13.230	1	1418	133	142	131	102	98	81	73	59	49
13.230	2	2485	224	238	218	174	161	139	118	105	87
13.230	3	4222	360	384	354	283	265	223	196	164	139
14.100	1	1411	86	79	79	75	70	62	58	49	44
14.100	2	2464	147	135	135	127	119	109	99	86	76
14.100	3	4231	243	229	224	211	204	184	166	146	126
15.100	1	1404	95	98	91	78	79	67	58	51	46
15.100	2	2462	161	158	155	136	131	114	103	90	76
15.100	3	4205	266	257	255	222	216	187	170	145	128
16.100	1	1416	95	89	89	78	87	75	64	55	53
16.100	2	2482	162	155	149	147	139	126	115	102	88
16.100	3	4245	270	252	247	242	229	207	187	167	142
17.100	1	1400	87	81	81	74	74	63	57	51	45
17.100	2	2449	150	140	138	129	125	111	101	88	77
17.100	3	4215	248	235	231	212	207	184	165	147	127

Table 2 Measured deflection data on stand 38

Chainage	Drop	Stress kPa	D1 Mic.	D2 Mic.	D3 Mic.	D4 Mic.	D5 Mic.	D6 Mic.	D7 Mic.	D8 Mic.	D9 Mic.
1.100	1	1381	92	85	84	78	74	64	58	52	43
1.100	2	2424	154	151	149	134	128	110	102	85	74
1.100	3	3602	230	218	214	191	183	161	147	123	109
2.100	1	1420	84	74	76	72	69	64	58	52	46
2.100	2	2486	144	134	131	124	120	109	101	91	80
2.100	3	4248	242	224	218	209	204	185	169	151	137
2.210	1	1420	131	136	122	98	95	79	68	58	45
2.210	2	2488	221	235	209	170	160	133	115	97	82
2.210	3	4257	359	386	345	279	262	221	191	161	136
2.220	1	1394	133	137	96	98	92	86	67	56	47
2.220	2	2672	229	243	177	174	165	140	120	103	83
2.220	3	3874	319	335	247	243	229	196	170	144	122
3.100	1	1429	93	88	86	81	79	70	63	56	48
3.100	2	2492	160	150	147	139	135	121	108	93	81
3.100	3	4334	270	255	249	233	226	202	182	161	136
4.100	1	1423	84	77	77	74	73	66	59	53	48
4.100	2	2485	144	136	134	126	122	110	100	90	81
4.100	3	4334	242	231	226	211	204	186	169	152	136
5.100	1	1423	86	80	77	77	72	70	62	56	48
5.100	2	2471	146	136	132	132	125	116	106	95	83
5.100	3	4324	250	234	228	223	215	195	181	161	143
6.100	1	1397	94	82	79	79	75	61	61	52	45
6.100	2	2453	157	147	144	137	129	115	106	92	79
6.100	3	4203	266	252	247	229	222	197	177	154	132
6.220	1	1393	152	168	89	114	105	90	72	61	50
6.220	2	2437	266	290	157	197	184	151	129	108	90
6.220	3	4221	445	484	266	331	310	256	220	184	155
6.230	1	1407	160	173	127	117	112	86	76	58	45
6.230	2	2466	268	288	220	198	185	150	130	107	88
6.230	3	4241	436	469	366	321	301	249	213	177	152
7.100	1	1399	87	79	79	74	75	66	61	53	44
7.100	2	2401	146	134	131	124	122	108	97	85	75
7.100	3	4052	240	223	217	207	199	178	159	140	123
8.100	1	1386	81	76	73	72	69	62	56	49	43
8.100	2	2419	141	129	126	121	117	105	95	84	74
8.100	3	3788	215	198	193	184	179	161	146	129	113
9.100	1	1385	90	82	82	76	71	63	57	52	45
9.100	2	2599	165	157	152	140	135	120	110	97	83
9.100	3	4022	244	234	229	210	202	181	162	144	127
10.100	1	1395	85	77	76	73	68	65	58	51	46
10.100	2	2316	136	127	124	117	111	100	91	80	72
10.100	3	3811	223	205	200	188	181	163	146	130	113
11.100	1	1438	101	92	87	83	79	68	58	51	44
11.100	2	2565	168	167	150	143	135	120	102	88	73112
11.100	3	4020	257	237	230	212	204	179	158	135	47

Chainage	Drop	Stress kPa	D1 Mic.	D2 Mic.	D3 Mic.	D4 Mic.	D5 Mic.	D6 Mic.	D7 Mic.	D8 Mic.	D9 Mic.
12.100	1	1450	87	77	75	74	70	64	59	53	47
12.100	2	2505	144	134	131	126	120	110	101	91	83
12.100	3	4174	241	221	215	206	199	180	163	148	134
12.220	1	1435	137	142	115	102	94	82	69	57	48
12.220	2	2475	219	232	192	169	156	135	116	93	87
12.220	3	4145	349	372	308	272	255	214	189	154	136
12.230	1	1420	134	143	131	102	98	80	72	58	45
12.230	2	2476	225	241	218	173	159	134	119	98	80
12.230	3	4135	358	384	349	276	259	218	188	157	132
13.100	1	1428	90	83	84	75	72	65	60	55	51
13.100	2	2474	151	139	138	126	125	112	106	95	78
13.100	3	4146	249	230	224	214	207	186	167	148	128
14.100	1	1391	90	86	85	76	68	64	56	47	43
14.100	2	2435	153	147	147	126	117	108	96	81	71
14.100	3	4085	248	236	237	206	195	176	155	132	116
15.100	1	1415	86	77	76	70	67	61	54	39	35
15.100	2	2470	133	134	133	118	107	100	91	79	73
15.100	3	4110	232	217	213	193	188	165	150	129	112
16.100	1	1444	88	79	78	71	72	66	59	53	44
16.100	2	2491	147	139	135	127	122	112	103	92	81
16.100	3	4149	241	225	220	209	200	183	167	150	133
17.100	1	1422	85	78	76	72	69	62	57	50	49
17.100	2	2488	147	140	135	128	122	108	93	84	90
17.100	3	4159	243	227	223	209	205	182	165	147	122

Table 3 Measured deflection data on stand 39

Chainage	Drop	Stress kPa	D1 Mic.	D2 Mic.	D3 Mic.	D4 Mic.	D5 Mic.	D6 Mic.	D7 Mic.	D8 Mic.	D9 Mic.
1.100	1	1390	97	89	87	80	79	70	63	56	43
1.100	2	2413	149	148	145	135	128	115	107	95	86
1.100	3	4109	262	245	239	225	220	197	177	160	135
2.100	1	1414	86	79	77	74	71	63	56	49	43
2.100	2	2503	150	139	135	129	125	112	100	89	77
2.100	3	4193	246	227	221	210	204	182	163	143	124
2.220	1	1397	146	157	77	108	104	84	73	62	51
2.220	2	2453	232	253	148	177	164	141	120	103	88
2.220	3	4063	368	398	236	281	263	222	191	163	140
2.230	1	1408	126	130	118	95	90	75	65	54	46
2.230	2	2456	209	224	202	165	153	131	113	93	81
2.230	3	4257	349	367	333	268	253	214	187	157	132
3.100	1	1418	76	65	67	67	65	58	52	50	43
3.100	2	2471	132	119	118	116	108	100	90	80	69
3.100	3	4301	223	209	203	194	181	174	150	135	122
4.100	1	1395	92	90	86	80	73	68	61	52	46
4.100	2	2450	156	151	145	135	127	115	103	87	78
4.100	3	4238	263	250	244	224	216	193	173	152	131
5.100	1	1423	77	74	73	71	69	61	55	51	46
5.100	2	2471	140	129	126	123	117	107	98	88	79
5.100	3	4280	235	220	215	206	200	181	165	148	133
5.210	1	1420	138	143	114	102	93	83	70	60	49
5.210	2	2467	230	245	202	176	161	141	119	102	85
5.210	3	4252	379	406	341	291	274	232	199	166	140
5.220	1	1407	144	156	93	107	102	84	70	57	48
5.220	2	2447	236	257	170	176	165	135	116	100	84
5.220	3	4243	381	415	287	286	271	225	194	163	138
6.100	1	1417	89	84	87	76	72	68	58	53	39
6.100	2	2464	151	147	145	129	122	110	98	88	78
6.100	3	4271	254	246	244	214	207	185	164	146	122
7.100	1	1401	145	145	145	120	113	97	84	70	57
7.100	2	2439	249	245	244	200	192	164	142	119	99
7.100	3	4220	416	413	411	340	327	280	244	205	172
8.100	1	1415	83	75	78	68	65	67	64	54	48
8.100	2	2472	147	138	137	128	122	112	101	90	80
8.100	3	4291	248	237	232	215	207	188	171	150	132
9.100	1	1434	84	82	77	71	69	66	58	52	49
9.100	2	2500	143	135	130	124	120	109	98	88	76
9.100	3	4325	241	224	219	208	200	182	165	148	129
10.100	1	1425	88	77	78	74	71	65	58	52	45
10.100	2	2466	138	131	131	124	119	107	97	87	76
10.100	3	4299	239	225	220	208	201	181	165	147	129
11.100	1	1395	89	81	79	79	76	70	68	64	61
11.100	2	2437	149	136	133	132	129	120	116	108	104
11.100	3	4241	253	234	228	221	216	202	193	185	181
12.100	1	1406	80	76	75	72	71	61	56	49	45

Chainage	Drop	Stress kPa	D1 Mic.	D2 Mic.	D3 Mic.	D4 Mic.	D5 Mic.	D6 Mic.	D7 Mic.	D8 Mic.	D9 Mic.
12.100	2	2463	141	131	128	121	118	104	94	84	74
12.100	3	4263	238	223	218	204	198	175	159	141	124
13.100	1	1415	85	78	78	72	71	64	57	50	44
13.100	2	2468	143	136	131	126	119	109	98	88	78
13.100	3	4290	247	231	227	215	204	185	166	147	128
13.210	1	1406	139	148	119	105	100	81	69	58	48
13.210	2	2456	229	251	205	175	165	137	119	99	84
13.210	3	4268	371	401	341	287	272	226	196	165	139
13.220	1	1414	161	174	100	119	109	90	75	68	56
13.220	2	2464	259	285	180	192	182	150	135	108	89
13.220	3	4267	416	454	310	313	291	249	210	180	158
14.100	1	1398	89	82	80	78	72	66	59	53	47
14.100	2	2414	149	140	135	129	123	110	100	89	78
14.100	3	4128	247	229	225	212	205	184	166	148	130
15.100	1	1411	89	77	79	78	71	66	62	54	47
15.100	2	2449	148	141	136	127	120	112	101	89	78
15.100	3	3989	236	219	216	201	195	179	160	146	128
16.100	1	1408	87	81	80	74	72	65	58	52	44
16.100	2	2427	145	137	134	125	121	108	97	85	74
16.100	3	3871	230	214	209	195	189	168	151	132	115
17.100	1	1367	79	72	71	68	66	59	52	46	39
17.100	2	2391	132	121	118	113	109	100	88	78	68
17.100	3	3686	203	184	179	172	165	148	133	117	100

Table 4 1 Measured deflection data on stand 40

Chainage	Drop	Stress kPa	D1 Mic.	D2 Mic.	D3 Mic.	D4 Mic.	D5 Mic.	D6 Mic.	D7 Mic.	D8 Mic.	D9 Mic.
1.100	1	1418	110	107	108	94	91	79	70	61	52
1.100	2	2484	187	196	183	160	155	137	122	108	92
1.100	3	4257	310	310	303	266	260	227	203	176	149
2.100	1	1390	75	75	73	66	64	57	52	46	41
2.100	2	2401	130	125	123	112	108	97	89	78	69
2.100	3	4113	217	206	201	186	179	162	147	130	116
3.100	1	1393	87	84	83	76	73	67	61	52	44
3.100	2	2375	148	143	140	129	123	111	98	89	80
3.100	3	3721	230	214	214	194	188	170	151	135	117
3.220	1	1390	187	200	73	142	132	113	96	79	68
3.220	2	2419	297	326	121	231	212	188	163	133	115
3.220	3	3905	469	508	179	363	347	287	248	209	170
3.230	1	1395	152	158	71	118	108	95	83	69	58
3.230	2	2656	267	285	149	210	197	171	148	125	105
3.230	3	3834	358	379	220	282	265	230	202	170	143
4.100	1	1379	85	79	76	74	73	66	60	52	46
4.100	2	2286	137	128	124	121	118	106	95	87	78
4.100	3	3710	218	204	198	192	185	169	153	138	125
5.100	1	1417	101	97	96	85	84	72	64	55	48
5.100	2	2750	190	183	180	161	156	137	123	105	88
5.100	3	3827	254	246	242	217	210	186	166	142	122
6.100	1	1423	90	83	81	78	77	71	59	53	41
6.100	2	2482	157	146	143	137	133	117	106	94	81
6.100	3	4302	266	247	240	229	223	200	179	157	134
6.220	1	1405	122	125	89	95	89	81	65	58	48
6.220	2	2487	207	212	157	160	153	132	117	101	84
6.220	3	4280	343	357	264	269	256	219	193	165	140
6.230	1	1371	123	125	100	94	87	75	66	56	47
6.230	2	2449	210	221	181	165	157	131	115	97	84
6.230	3	4210	348	367	302	270	256	217	191	162	137
7.100	1	1413	84	77	75	70	73	60	56	48	41
7.100	2	2490	146	133	130	123	118	105	95	83	73
7.100	3	4283	238	224	216	205	198	176	159	139	121
8.100	1	1413	122	114	112	100	97	91	78	67	54
8.100	2	2454	200	191	189	173	167	147	131	113	96
8.100	3	4232	323	310	306	279	268	240	211	182	153
9.100	1	1417	88	82	82	74	72	60	58	49	43
9.100	2	2486	151	145	142	129	125	107	99	86	74
9.100	3	4276	251	237	235	212	203	187	163	144	123
10.100	1	1415	92	85	87	77	74	68	60	51	45
10.100	2	2470	159	151	150	134	131	116	103	90	76
10.100	3	4278	263	256	250	226	218	195	174	152	132
11.100	1	1406	195	178	173	176	168	145	122	99	78
11.100	2	2469	321	295	284	279	266	232	199	163	131
11.100	3	4228	507	475	458	444	423	366	315	261	211
12.100	1	1429	98	91	91	86	87	72	66	57	48

Chainage	Drop	Stress kPa	D1 Mic.	D2 Mic.	D3 Mic.	D4 Mic.	D5 Mic.	D6 Mic.	D7 Mic.	D8 Mic.	D9 Mic.
12.100	2	2496	172	160	158	149	143	128	113	98	84
12.100	3	4295	290	269	262	248	243	213	191	166	141
13.100	1	1412	99	91	88	89	85	79	68	60	54
13.100	2	2463	170	156	152	151	147	132	120	103	89
13.100	3	4292	284	262	254	254	247	220	200	172	147
13.210	1	1407	121	124	92	95	90	79	69	60	52
13.210	2	2479	208	212	164	164	153	137	119	104	90
13.210	3	4281	340	357	282	272	262	224	198	170	145
13.220	1	1403	122	124	92	94	89	77	67	56	47
13.220	2	2473	207	212	162	159	151	130	114	97	83
13.220	3	4304	344	356	277	267	253	217	192	162	141
14.100	1	1415	87	81	79	79	77	70	62	53	47
14.100	2	2477	150	139	134	134	134	118	105	92	80
14.100	3	4308	252	230	223	221	213	197	177	155	134
15.100	1	1414	91	86	84	82	80	69	62	54	46
15.100	2	2468	157	150	145	141	134	120	108	93	83
15.100	3	4311	266	246	239	234	227	202	181	158	135
16.100	1	1409	93	87	85	83	80	70	64	56	48
16.100	2	2460	167	155	150	145	140	125	112	98	83
16.100	3	4275	282	260	252	245	238	210	189	166	143
17.100	1	1417	86	76	75	75	70	65	57	50	48
17.100	2	2473	151	136	134	129	126	111	100	89	77
17.100	3	4287	253	237	229	219	208	190	170	147	134

Table 5 Measured deflection data on stand 41

Geophone distances (mm):			0	200	300	450	600	900	1200	1500	1800
Chainage	Drop	Stress	D1	D2	D3	D4	D5	D6	D7	D8	D9
			Mic.	Mic.	Mic.	Mic.	Mic.	Mic.	Mic.	Mic.	Mic.
1.1	3	4296	239	232	229	207	200	180	163	143	123
2.1	1	1427	79	72	72	70	67	63	54	49	45
2.1	2	2478	142	131	127	124	120	107	99	87	72
2.1	3	4296	238	220	213	210	201	183	163	146	132
2.21	1	1409	113	116	109	86	82	73	60	54	46
2.21	2	2474	198	210	188	156	147	125	109	93	79
2.21	3	4273	333	351	315	260	245	209	182	157	134
2.22	1	1416	100	100	72	78	73	67	58	50	45
2.22	2	2477	173	177	133	137	128	114	100	87	76
2.22	3	4313	292	304	234	233	221	191	169	146	125
3.1	1	1407	91	86	72	74	73	64	58	56	46
3.1	2	2453	152	142	134	132	127	115	106	92	83
3.1	3	4279	259	239	234	223	216	195	176	156	136
4.1	1	1421	101	95	91	89	87	82	72	61	51
4.1	2	2466	173	162	155	151	147	133	118	102	88
4.1	3	4288	293	274	267	257	248	223	199	172	146
5.1	1	1409	130	121	119	111	108	93	84	70	61
5.1	2	2465	223	206	202	188	178	156	137	121	107
5.1	3	4259	374	352	343	315	301	265	234	207	183
6.1	1	1412	84	81	77	74	69	62	57	51	45
6.1	2	2468	147	136	132	126	124	112	100	87	73
6.1	3	4308	248	236	226	218	210	189	169	151	132
6.22	1	1402	141	151	96	105	99	84	71	59	32
6.22	2	2463	238	255	169	177	167	139	119	100	111
6.22	3	4275	392	422	285	296	279	231	199	167	127
6.23	1	1411	130	140	101	99	94	79	69	58	48
6.23	2	2473	222	233	179	169	159	135	117	98	84
6.23	3	4277	365	387	305	279	264	223	195	164	139
7.1	1	1413	84	79	75	75	73	62	58	49	42
7.1	2	2465	144	133	127	127	120	106	94	83	71
7.1	3	4302	243	225	218	209	204	180	160	140	118
9.1	1	1387	88	83	82	74	74	65	59	52	40
9.1	2	2441	151	141	139	130	124	113	100	88	78
9.1	3	4279	255	238	233	219	211	190	170	149	131
10.1	1	1419	94	87	85	80	75	70	61	54	45
10.1	2	2467	157	145	141	136	129	115	102	90	78
10.1	3	4306	268	253	242	228	221	198	176	155	133
11.1	1	1396	90	84	82	80	76	69	63	55	45
11.1	2	2449	154	143	138	133	128	119	107	93	80
11.1	3	4273	259	241	233	225	218	195	176	156	139
12.1	1	1387	110	102	100	95	90	83	75	68	63
12.1	2	2452	186	177	170	164	159	142	131	117	109
12.1	3	4273	316	294	288	271	259	239	218	204	187
13.1	1	1418	89	81	81	77	72	67	58	49	43

13.1	2	2477	156	147	144	134	128	115	103	90	77
13.1	3	4330	266	251	246	228	220	196	177	155	133
13.22	1	1409	137	147	86	105	98	84	72	59	51
13.22	2	2465	231	248	146	179	169	141	122	105	87
13.22	3	4302	381	409	244	297	282	238	207	177	149
13.23	1	1411	128	134	121	100	91	77	71	57	47
13.23	2	2465	220	231	207	169	160	135	117	100	84
13.23	3	4303	363	385	349	285	269	228	198	169	141
14.1	1	1405	83	77	76	73	72	64	55	50	42
14.1	2	2456	143	134	132	124	118	110	97	86	73
14.1	3	4324	246	230	226	214	208	186	165	147	125
15.1	1	1419	84	76	76	73	69	67	60	53	49
15.1	2	2475	147	132	130	127	123	111	102	92	85
15.1	3	4329	248	230	224	216	210	189	172	156	143
16.1	1	1383	80	73	71	68	69	60	53	47	43
16.1	2	2444	136	124	125	118	113	104	93	84	75
16.1	3	4295	228	214	210	201	195	176	161	143	128
17	1	1412	91	83	81	80	76	68	61	54	48
17	2	2460	150	140	137	131	128	115	104	91	81
17	3	4315	256	240	234	226	216	196	176	157	135
18.1	1	1415	89	83	81	78	75	69	61	55	46
18.1	2	2465	155	144	143	135	130	117	104	92	79
18.1	3	4309	264	248	242	230	222	198	178	156	136

Table 6 Measured deflection data on stand 42

Chainage	Drop	Stress kPa	D1 Mic.	D2 Mic.	D3 Mic.	D4 Mic.	D5 Mic.	D6 Mic.	D7 Mic.	D8 Mic.	D9 Mic.
1.100	1	1366	104	100	99	88	86	75	68	59	49
1.100	2	2377	175	172	169	154	140	126	116	100	85
1.100	3	4098	290	283	280	249	237	210	188	163	137
2.100	1	1410	89	81	78	84	79	69	62	53	45
2.100	2	2501	160	144	141	141	134	120	109	94	82
2.100	3	4232	254	236	230	226	219	196	176	153	134
2.210	1	1400	95	93	87	77	73	69	59	53	47
2.210	2	2452	169	170	158	137	129	119	104	92	76
2.210	3	4281	295	300	283	241	228	203	178	156	131
2.220	1	1407	95	91	84	77	72	63	61	49	42
2.220	2	2461	165	168	142	134	131	112	97	88	77
2.220	3	4125	276	279	232	223	212	187	165	144	126
3.100	1	1405	100	88	87	87	78	76	69	59	54
3.100	2	2445	167	157	152	147	153	127	114	101	83
3.100	3	4276	283	264	258	247	241	217	194	167	143
4.100	1	1403	119	106	104	107	101	94	81	73	61
4.100	2	2454	198	181	176	179	170	155	136	120	102
4.100	3	4281	326	303	293	290	279	252	224	195	161
5.100	1	1424	115	102	101	101	99	85	76	64	53
5.100	2	2487	191	175	170	168	164	143	127	109	91
5.100	3	4313	315	290	281	276	268	237	210	180	152
6.100	1	1433	94	87	84	81	82	69	64	58	53
6.100	2	2489	157	145	141	136	124	120	107	95	83
6.100	3	4278	261	244	238	229	225	197	180	158	140
6.220	1	1395	133	137	76	102	95	83	72	63	54
6.220	2	2446	225	237	139	176	163	140	125	108	88
6.220	3	4292	384	409	250	300	284	242	212	178	152
6.230	1	1424	114	117	110	92	84	73	62	53	43
6.230	2	2482	199	208	195	160	147	128	110	91	76
6.230	3	4275	333	349	328	265	251	214	186	158	135
7.100	1	1421	88	81	78	75	73	62	58	50	44
7.100	2	2468	147	137	133	128	122	109	97	85	74
7.100	3	4253	249	230	225	215	205	183	163	143	124
8.100	1	1394	78	76	75	69	65	62	55	47	40
8.100	2	2455	137	130	129	118	114	105	95	82	72
8.100	3	4253	232	220	217	199	193	175	158	140	123
9.100	1	1426	89	75	81	76	71	66	62	54	49
9.100	2	2475	154	141	139	133	127	115	103	92	80
9.100	3	4285	259	242	235	224	215	193	175	153	132
10.100	1	1432	101	95	91	85	84	74	66	56	44
10.100	2	2476	166	160	154	143	136	125	111	97	83
10.100	3	4271	276	263	258	239	232	205	184	158	134
11.100	1	1429	94	87	85	80	79	69	60	53	45
11.100	2	2480	161	150	146	137	134	120	106	94	81
11.100	3	4291	271	254	248	236	228	204	181	161	138
11.220	1	1398	146	154	118	104	99	85	72	67	48

Chainage	Drop	Stress kPa	D1 Mic.	D2 Mic.	D3 Mic.	D4 Mic.	D5 Mic.	D6 Mic.	D7 Mic.	D8 Mic.	D9 Mic.
11.220	2	2456	244	262	207	185	169	147	128	107	92
11.220	3	4227	405	440	344	312	294	247	214	181	150
11.230	1	1422	142	150	122	105	104	88	74	62	53
11.230	2	2472	239	255	210	183	173	147	125	106	89
11.230	3	4257	389	423	348	303	288	241	210	176	143
12.100	1	1417	100	95	91	82	84	81	68	62	49
12.100	2	2472	168	160	153	150	140	125	114	96	88
12.100	3	4272	278	260	253	242	234	212	190	167	141
13.100	1	1400	80	70	68	68	67	60	55	48	41
13.100	2	2461	139	126	120	118	115	103	92	81	71
13.100	3	4256	233	215	209	200	195	174	157	138	120
14.100	1	1399	82	78	75	69	66	63	54	49	44
14.100	2	2452	143	129	127	123	116	106	94	82	71
14.100	3	4235	237	221	215	205	198	179	159	141	122
15.100	1	1405	92	84	83	80	76	69	62	55	49
15.100	2	2448	155	145	142	134	129	116	107	93	82
15.100	3	4226	263	245	240	227	219	197	178	157	138
16.100	1	1418	99	85	86	80	81	72	65	57	49
16.100	2	2468	161	148	145	140	135	122	110	95	83
16.100	3	4272	271	252	245	236	227	205	184	161	139

Table 7 Measured deflection data on stand 43

Chainage	Drop	Stress kPa	D1 Mic.	D2 Mic.	D3 Mic.	D4 Mic.	D5 Mic.	D6 Mic.	D7 Mic.	D8 Mic.	D9 Mic.
1.100	1	1404	99	113	113	112	101	87	77	70	56
1.100	2	2434	195	181	178	169	164	146	129	114	95
1.100	3	4186	308	298	291	276	266	239	209	178	148
2.100	1	1422	107	97	96	91	94	77	70	60	49
2.100	2	2462	187	173	168	160	152	135	118	100	85
2.100	3	4262	304	285	275	262	251	222	194	165	142
2.210	1	1406	114	119	103	91	86	74	65	56	47
2.210	2	2447	200	205	178	158	146	129	113	96	82
2.210	3	4233	342	362	312	270	252	219	192	161	138
2.220	1	1420	121	121	105	97	89	77	69	58	48
2.220	2	2458	204	207	180	162	153	137	117	99	90
2.220	3	4261	347	358	311	282	259	224	198	167	140
3.100	1	1410	96	85	90	79	84	73	70	56	49
3.100	2	2457	159	148	154	138	133	123	113	98	87
3.100	3	4249	262	248	251	231	220	203	185	162	140
4.100	1	1409	95	86	84	83	81	72	65	58	48
4.100	2	2456	158	147	143	140	136	123	110	97	83
4.100	3	4257	265	243	238	232	220	202	178	161	138
5.100	1	1412	112	102	103	101	98	89	81	68	61
5.100	2	2462	188	172	166	168	160	149	132	115	104
5.100	3	4253	306	281	272	274	263	238	214	186	160
6.220	1	1405	138	148	89	108	101	87	76	65	54
6.220	2	2463	236	253	157	185	174	149	130	110	94
6.220	3	4263	397	426	276	310	292	251	216	184	156
6.223	1	1393	115	105	102	98	86	83	75	54	45
6.223	2	2429	192	185	180	167	154	139	123	95	75
6.223	3	4225	320	302	294	269	262	226	195	170	145
6.230	1	1395	117	120	104	96	89	78	70	61	50
6.230	2	2459	207	209	186	169	159	137	121	105	90
6.230	3	4244	351	365	324	281	269	231	204	176	148
7.100	1	1408	92	85	82	80	76	71	64	56	50
7.100	2	2458	155	143	140	135	132	119	109	94	82
7.100	3	4272	260	239	233	229	225	203	183	160	138
8.100	1	1386	138	126	120	116	110	94	82	68	61
8.100	2	2438	232	211	203	194	183	159	140	118	99
8.100	3	4211	379	346	331	314	298	259	228	192	161
9.100	1	1415	99	91	90	88	89	78	68	63	55
9.100	2	2460	171	155	152	149	143	130	117	99	85
9.100	3	4263	280	256	249	247	234	214	193	162	139
10.100	1	1404	103	93	93	92	88	82	70	62	51
10.100	2	2479	178	163	158	156	150	135	118	102	85
10.100	3	4291	287	266	259	253	243	219	193	167	138
11.100	1	1369	109	98	99	98	93	84	75	64	54
11.100	2	2438	185	169	166	164	157	140	124	107	89
11.100	3	4246	303	278	267	265	254	226	202	173	147
12.100	1	1381	104	96	93	87	85	77	70	58	46

Chainage	Drop	Stress kPa	D1 Mic.	D2 Mic.	D3 Mic.	D4 Mic.	D5 Mic.	D6 Mic.	D7 Mic.	D8 Mic.	D9 Mic.
12.100	2	2452	181	169	162	158	151	137	120	103	90
12.100	3	4296	301	282	273	258	251	227	200	172	144
12.220	1	1386	109	113	81	88	84	73	65	57	50
12.220	2	2448	193	201	140	157	148	129	115	100	84
12.220	3	4259	341	357	239	272	259	225	198	172	148
12.230	1	1409	101	104	91	83	79	69	62	54	46
12.230	2	2464	183	187	163	146	140	125	110	93	82
12.230	3	4305	318	329	287	251	239	214	187	160	138
13.100	1	1415	87	78	76	76	74	66	60	53	43
13.100	2	2465	147	131	129	128	120	112	100	88	77
13.100	3	4305	247	227	222	215	204	189	171	148	130
14.100	1	1392	101	90	88	90	83	79	68	65	52
14.100	2	2446	168	155	149	150	143	130	116	104	87
14.100	3	4246	275	253	247	244	237	214	192	166	142
15.100	1	1406	100	93	89	89	85	76	69	59	50
15.100	2	2446	172	157	153	150	144	130	116	102	87
15.100	3	4257	288	264	256	252	242	218	196	171	147
16.100	1	1395	108	97	95	97	90	85	76	64	58
16.100	2	2444	179	166	160	161	159	139	126	108	88
16.100	3	4250	294	271	262	257	248	226	201	173	149

APPENDIX – C

Table 1 : Back-calculated layer moduli of Stand 37

Chainage	Layer Thickness(mm)				Moduli(Mpa)			
	H1	H2	H3	H4	E1	E2	E3	E4
1.100	425	350	600		28134	468	558	385
2.100	425	350	600		24417	678	541	350
3.100	425	350	600		30044	406	471	423
4.100	425	350	600		17924	240	354	314
5.100	425	350	600		39514	607	640	360
6.100	425	350	600		31489	462	555	402
7.100	425	350	600		27279	742	593	446
8.100	425	350	600		31890	731	667	382
9.100	425	350	600		23762	551	657	369
10.100	425	350	600		34750	450	431	404
11.100	425	350	600		17615	257	309	302
12.100	425	350	600		30159	712	624	369
13.100	425	350	600		25384	568	616	390
14.100	425	350	600		32853	532	505	418
15.100	425	350	600		22234	676	569	406
16.100	425	350	600		31861	405	458	369
17.100	425	350	600		29651	585	541	410

Table 2 : Back-calculated layer moduli of Stand 38

Chainage	**Layer Thickness(mm)**				**Moduli(Mpa)**			
	H1	**H2**	**H3**	**H4**	**E1**	**E2**	**E3**	**E4**
1.100	425	350	600		21832	719	574	406
2.100	425	350	600		34946	659	841	351
3.100	425	350	600		29696	494	457	394
4.100	425	350	600		34080	866	567	377
5.100	425	350	600		36850	689	624	342
6.100	425	350	600		28133	342	504	415
7.100	425	350	600		30331	445	654	408
8.100	425	350	600		32733	675	556	410
9.100	425	350	600		28698	485	579	400
10.100	425	350	600		28947	769	517	419
11.100	425	350	600		23294	370	593	464
12.100	425	350	600		31506	590	1276	341
13.100	425	350	600		30937	478	583	399
14.100	425	350	600		22388	526	775	433
15.100	425	350	600		27577	641	593	464
16.100	425	350	600		32378	750	743	354
17.100	425	350	600		30902	694	419	419

Table 3: Back-calculated layer moduli of Stand 39

Chainage	Layer Thickness(mm)				Moduli(Mpa)			
	H1	H2	H3	H4	E1	E2	E3	E4
1.100	425	350	600		28390	601	541	357
2.100	425	350	600		29809	563	620	411
3.100	425	350	600		34716	865	817	407
4.100	425	350	600		25121	658	642	381
5.100	425	350	600		35643	847	678	368
6.100	425	350	600		23674	776	659	409
7.100	425	350	600		11833	406	239	346
8.100	425	350	600		30448	613	729	378
9.100	425	350	600		32996	692	792	382
10.100	425	350	600		33240	680	682	390
11.100	425	350	600		36905	3385	1294	216
12.100	425	350	600		31384	651	602	427
13.100	425	350	600		30762	532	725	399
14.100	425	350	600		30503	620	516	395
15.100	425	350	600		30714	622	789	361
16.100	425	350	600		29156	519	587	419
17.100	425	350	600		31854	674	520	465

Table 4 : Back-calculated layer moduli of Stand 40

Chainage	Layer Thickness(mm)				Moduli(Mpa)			
	H1	H2	H3	H4	E1	E2	E3	E4
1.100	425	350	600		20284	538	317	375
2.100	425	350	600		32704	754	861	410
3.100	425	350	600		27898	507	573	396
4.100	425	350	600		34173	683	790	332
5.100	425	350	600		34173	627	410	332
6.100	425	350	600		30260	489	452	403
7.100	425	350	600		31384	633	530	447
8.100	425	350	600		21840	356	285	377
9.100	425	350	600		27601	541	646	422
10.100	425	350	600		25756	510	676	389
11.100	425	350	600		13296	106	188	312
12.100	425	350	600		27192	370	334	416
13.100	425	350	600		30698	441	363	364
14.100	425	350	600		34896	736	424	385
15.100	425	350	600		31475	463	369	416
16.100	425	350	600		28655	432	409	384
17.100	425	350	600		30553	602	541	402

Table 5 : Back-calculated layer moduli of Stand 41

Chainage	Layer Thickness(mm)				Moduli(Mpa)			
	H1	H2	H3	H4	E1	E2	E3	E4
1.100	425	350	600		29517	710	693	407
2.100	425	350	600		35241	633	757	380
3.100	425	350	600		31364	547	582	378
4.100	425	350	600		28460	375	281	401
5.100	425	350	600		16855	453	463	287
6.100	425	350	600		32746	534	572	399
7.100	425	350	600		32614	464	418	484
9.100	425	350	600		30368	540	464	423
10.100	425	350	600		27307	564	521	399
11.100	425	350	600		31854	549	486	387
12.100	425	350	600		23913	999	831	243
13.100	425	350	600		26620	705	522	392
14.100	425	350	600		32784	439	552	436
15.100	425	350	600		34008	767	847	340
16.100	425	350	600		37958	733	596	400
17.000	425	350	600		33639	464	498	395
18.100	425	350	600		30035	442	567	392

Table 6 : Back-calculated layer moduli of Stand 42

Chainage	**Layer Thickness(mm)**				**Moduli(Mpa)**			
	H1	**H2**	**H3**	**H4**	**E1**	**E2**	**E3**	**E4**
1.100	425	350	600		20480	563	430	373
2.100	425	350	600		33870	498	379	406
3.100	425	350	600		30336	294	384	396
4.100	425	350	600		24597	457	283	334
5.100	425	350	600		25799	361	235	402
6.100	425	350	600		32687	515	440	385
7.100	425	350	600		30344	525	439	453
8.100	425	350	600		32258	775	562	424
9.100	425	350	600		29840	498	578	397
10.100	425	350	600		26492	377	474	409
11.100	425	350	600		28732	428	559	383
12.100	425	350	600		29880	469	364	385
13.100	425	350	600		34747	546	523	451
14.100	425	350	600		34722	458	463	455
15.100	425	350	600		29542	627	427	388
16.100	425	350	600		30826	427	415	394

Table 7 : Back-calculated layer moduli of Stand 43

Chainage	Layer Thickness(mm)				Moduli(Mpa)			
	H1	H2	H3	H4	E1	E2	E3	E4
1.100	425	350	600		24793	250	293	389
2.100	425	350	600		23428	290	400	411
3.100	425	350	600		31256	559	473	364
4.100	425	350	600		31091	511	475	383
5.100	425	350	600		29919	382	274	348
6.223	425	350	600		18866	475	364	387
7.100	425	350	600		36036	427	356	398
8.100	425	350	600		16046	353	275	364
9.100	425	350	600		29615	400	361	397
10.100	425	350	600		29225	322	256	443
11.100	425	350	600		25845	403	297	389
12.100	425	350	600		24853	468	328	386
13.100	425	350	600		34440	557	558	401
14.100	425	350	600		32996	312	374	388
15.100	425	350	600		29506	420	351	374
16.100	425	350	600		28428	463	301	372

APPENDIX D

Table1 : Pavement survey data for case study (Jetpur- Somnath Road)

Pavement Condition Survey Data (per Km)									
Start	End	X-Axis	Total Cracking	Rutting Depth	Pot Holes (Sqm/Km	Patching (Sqm/km	Edge Break	Ravelling (% of	Edge Drop
43	44	43 -44	5.3	5.5	0.0	0.0	0.0	0.0	25.0
44	45	44 -45	26.1	17.3	0.0	0.0	0.0	0.0	16.5
45	46	45 -46	13.0	10.0	0.0	0.0	0.0	0.0	34.8
46	47	46 -47	0.0	6.4	0.0	0.0	2.2	0.0	32.5
47	48	47 -48	15.4	6.3	0.0	0.0	0.0	0.0	19.5
48	49	48 -49	6.0	3.2	0.0	2.7	0.0	0.0	27.2
49	50	49 -50	16.8	5.0	0.0	0.0	0.0	0.0	20.0
50	51	50 -51	16.2	7.2	0.0	0.0	0.0	0.0	22.4
51	52	51 -52	15.6	13.7	0.0	0.1	0.0	0.0	34.2
52	53	52 -53	12.9	6.4	0.0	0.0	0.0	0.0	24.7
53	54	53 -54	6.3	5.1	0.0	0.0	0.0	0.0	23.5
54	55	54 -55	39.3	22.5	0.0	0.0	0.0	0.0	10.0
55	56	55 -56	15.5	12.3	0.1	0.0	0.0	0.0	18.0
56	57	56 -57	5.5	5.8	0.0	0.1	0.0	0.0	10.0
57	58	57 -58	8.8	8.5	0.0	0.2	0.0	0.0	12.5
58	59	58 -59	11.1	7.5	0.0	0.0	0.0	0.0	53.2
59	60	59 -60	10.5	6.6	0.0	0.0	0.0	0.0	38.8
60	61	60 -61	12.0	5.0	0.0	0.0	0.0	0.0	19.5
61	62	61 -62	4.8	5.6	0.0	0.0	0.0	0.0	33.7
62	63	62 -63	13.4	5.4	0.0	0.2	0.0	0.0	16.0
63	64	63 -64	0.0	5.6	0.0	0.0	0.0	0.0	11.5
64	65	64 -65	0.0	6.0	0.0	0.0	0.0	0.0	15.5
65	66	65 -66	0.0	5.0	0.0	0.0	0.0	0.0	19.5
66	67	66 -67	0.0	5.0	0.0	0.0	0.0	0.0	18.3
79	80	79 -80	0.0	5.8	0.0	0.0	0.0	0.0	18.5
80	81	80 -81	0.0	6.3	0.0	0.0	0.0	0.0	10.0
81	82	81 -82	3.8	7.8	0.0	0.0	0.0	0.0	12.0
82	83	82 -83	7.3	6.3	0.0	0.0	0.0	0.0	15.0
83	84	83 -84	5.5	7.6	0.0	0.1	0.0	0.0	19.5
84	85	84 -85	6.5	7.5	0.0	0.0	0.0	35.0	18.3
85	86	85 -86	19.3	6.3	0.0	0.0	0.0	14.5	10.5
86	87	86 -87	6.0	6.2	0.0	0.0	0.0	23.5	19.5
87	88	87 -88	5.0	6.4	0.0	0.0	0.0	10.5	20.0
88	89	88 -89	5.0	6.1	0.0	0.1	0.0	10.5	19.5
89	90	89 -90	0.3	4.8	0.0	0.0	0.0	42.5	19.5
90	91	90 -91	0.0	8.0	0.0	0.0	0.0	30.5	19.5
91	92	91 -92	14.8	7.4	0.0	0.0	0.0	13.5	23.0
92	93	92 -93	0.0	6.0	0.0	0.0	0.0	20.0	19.5
93	94	93 -94	0.0	5.3	0.0	0.0	0.0	20.0	19.5
94	95	94 -95	3.0	5.3	0.0	0.0	0.0	0.0	19.5
95	96	95 -96	35.0	8.5	0.0	0.0	0.0	0.0	19.5
96	97	96 -97	12.0	6.2	0.0	0.1	0.0	5.5	20.0
97	98	97 -98	0.0	5.0	0.0	0.0	0.0	1.5	19.5
98	99	98 -99	0.0	5.3	0.0	0.1	0.0	0.0	20.0
99	100	99 -100	0.0	5.0	0.0	0.0	0.0	20.0	20.0
100	101	100 -101	10.0	7.2	0.0	0.0	0.0	15.0	19.5
101	102	101 -102	24.8	6.0	0.0	0.0	0.0	0.0	19.5
102	103	102 -103	25.0	8.0	0.0	0.0	0.0	0.0	19.5
103	104	103 -104	12.0	6.3	0.0	0.0	0.0	1.1	20.0
104	105	104 -105	20.0	7.3	0.0	0.1	0.0	0.0	20.0
105	106	105 -106	15.3	7.8	0.0	0.3	0.0	20.0	20.0
106	107	106 -107	15.3	11.0	0.1	0.1	0.0	0.0	20.0
107	108	107 -108	14.5	6.7	0.0	0.1	0.0	0.0	20.0
108	109	108 -109	21.5	7.0	0.2	0.1	0.0	20.0	20.0
109	110	109 -110	14.8	7.0	0.0	0.1	0.0	20.0	20.0
110	111	110 -111	12.0	7.0	0.0	0.0	0.0	0.0	20.0
111	112	111 -112	14.5	8.4	0.0	0.0	0.0	20.0	20.0
112	113	112 -113	24.3	6.3	0.0	0.0	0.0	0.0	20.0
113	114	113 -114	47.0	8.8	0.5	0.2	0.0	7.5	20.0
114	115	114 -115	22.3	8.3	0.0	0.1	0.0	20.0	20.0
115	116	115 -116	36.5	6.3	0.0	0.0	0.0	0.0	20.0
116	117	116 -117	12.0	7.0	0.0	0.1	0.0	20.0	20.0
117	118	117 -118	15.8	6.0	0.0	0.0	0.0	0.0	20.0
118	119	118 -119	33.8	7.2	0.0	0.5	0.0	20.0	20.0
119	120	119 -120	28.0	7.0	0.0	0.0	0.0	0.0	20.0
120	121	120 -121	39.8	7.0	0.1	0.1	0.0	20.0	20.0
121	122	121 -122	27.5	7.0	0.1	0.1	0.0	0.0	20.0
122	123	122 -123	25.0	6.0	0.0	0.1	0.0	0.0	20.0
123	124	123 -124	25.0	6.5	0.0	0.0	0.0	0.0	20.0
124	125	124 -125	25.0	9.4	0.2	0.4	0.0	20.0	20.0
125	126	125 -126	30.0	6.5	0.0	0.0	0.0	0.0	20.0
126	127	126 -127	25.0	6.5	0.0	0.0	0.0	0.0	21.5

Table 2. Pavement condition values.

Chainage (km)		X-Axis	PCI value	Pavement Condition
From	To			
43	44	43-44	83.14	GOOD
44	45	44-45	64.64	FAIR
45	46	45-46	70.07	FAIR
46	47	46-47	77.23	GOOD
48	49	48-49	78.65	GOOD
49	50	49-50	78.37	GOOD
50	51	50-51	78.50	GOOD
51	52	51-52	76.02	GOOD
52	53	52-53	65.74	FAIR
53	54	53-54	77.61	GOOD
54	55	54-55	83.46	GOOD
55	56	55-56	55.24	FAIR
56	57	56-57	74.61	FAIR
57	58	57-58	89.71	GOOD
58	59	58-59	84.03	GOOD
59	60	59-60	64.60	FAIR
60	61	60-61	72.37	FAIR
61	62	61-62	81.77	GOOD
62	63	62-63	79.24	GOOD
63	64	63-64	81.93	GOOD
64	65	64-65	92.72	GOOD
65	66	65-66	90.51	GOOD
66	67	66-67	89.43	GOOD
79	80	79-80	98.00	GOOD
80	81	80-81	98.00	GOOD
81	82	81-82	95.17	GOOD
82	83	82-83	91.72	GOOD
83	84	83-84	94.12	GOOD
84	85	84-85	92.36	GOOD
85	86	85-86	67.88	FAIR
86	87	86-87	86.91	GOOD
87	88	87-88	83.41	GOOD
88	89	88-89	89.40	GOOD
89	90	89-90	92.55	GOOD
90	91	90-91	78.79	GOOD
91	92	91-92	72.52	FAIR
92	93	92-93	90.38	GOOD
93	94	93-94	88.41	GOOD
94	95	94-95	87.02	GOOD
95	96	95-96	76.02	GOOD
96	97	96-97	88.22	GOOD
97	98	97-98	95.02	GOOD
98	99	98-99	97.89	GOOD
99	100	99-100	98.18	GOOD
100	101	100-101	82.80	GOOD
101	102	101-102	73.96	FAIR
102	103	102-103	81.86	GOOD
103	104	103-104	88.63	GOOD
104	105	104-105	84.36	GOOD
105	106	105-106	86.90	GOOD
106	107	106-107	76.86	GOOD
107	108	107-108	79.50	GOOD
108	109	108-109	65.40	FAIR
109	110	109-110	69.72	FAIR
110	111	110-111	80.89	GOOD
111	112	111-112	68.95	FAIR
112	113	112-113	73.55	FAIR
113	114	113-114	53.78	POOR
114	115	114-115	64.09	FAIR
115	116	115-116	65.72	FAIR
116	117	116-117	71.47	FAIR
117	118	117-118	79.14	GOOD
118	119	118-119	57.43	FAIR
119	120	119-120	70.68	FAIR
120	121	120-121	53.76	POOR
121	122	121-122	70.99	FAIR
122	123	122-123	73.25	FAIR
123	124	123-124	72.92	FAIR
124	125	124-125	61.54	FAIR
125	126	125-126	69.73	FAIR
126	127	126-127	72.22	FAIR

Table 3 Measured FWD Deflection data (Case Study II)

Chainage	Sequence	Press	Force	D1	D2	D3	D4	D5	D6	D7	D8	D9	Surf Temp
[m]		[kPa]	[kN]	0	300	450	600	900	1200	1500	1800	2100	[°C]
0	1	566	40	506	367	270	203	112	68	50	39	34	36.8
0	2	566	40	493	360	267	203	115	72	53	41	37	36.8
0	3	566	40	483	357	267	203	115	72	53	41	35	36.8
60	1	566	40	340	264	184	138	67	43	37	35	34	37.1
60	2	566	40	335	269	183	137	64	45	36	34	32	37.1
60	3	566	40	337	268	181	140	66	46	32	31	30	37.1
120	1	566	40	332	263	195	124	78	58	38	34	30	36.7
120	2	566	40	338	269	196	129	77	56	36	34	30	36.7
120	3	566	40	333	262	194	127	74	55	37	35	33	36.7
180	1	566	40	484	358	244	186	127	69	47	45	36	37.3
180	2	566	40	487	356	246	188	132	61	47	46	35	37.3
180	3	566	40	483	361	247	189	135	64	41	40	32	37.3
240	1	566	40	467	333	230	182	128	63	42	37	34	37
240	2	566	40	463	334	224	183	129	65	44	38	34	37
240	3	566	40	461	330	221	180	129	65	45	37	33	37
300	1	566	40	498	321	288	190	146	64	41	34	32	36.8
300	2	566	40	499	328	284	191	151	61	47	36	34	36.8
300	3	566	40	492	323	283	191	154	62	48	35	33	36.8
360	1	566	40	500	326	225	157	80	51	40	33	28	36.9
360	2	566	40	489	320	222	156	81	52	42	35	31	36.9
360	3	566	40	488	318	221	156	80	52	41	34	30	36.9
420	1	566	40	387	261	199	109	62	40	39	35	25	36.1
420	2	566	40	384	258	193	103	66	48	44	38	22	36.1
420	3	566	40	382	260	196	107	69	42	41	34	23	36.1
480	1	566	40	367	269	174	115	78	54	42	38	27	36.2
480	2	566	40	368	264	174	119	71	52	44	37	25	36.2
480	3	566	40	364	263	173	117	74	51	43	35	29	36.2
540	1	566	40	371	251	183	131	62	45	43	37	28	36.4
540	2	566	40	373	256	177	130	65	44	42	34	25	36.4
540	3	566	40	374	252	180	127	63	49	47	31	22	36.4
600	1	566	40	490	359	241	182	129	60	43	41	36	36.7
600	2	566	40	487	360	249	181	133	63	46	45	39	36.7
600	3	566	40	486	362	244	179	134	63	47	45	38	36.7
660	1	566	40	475	322	282	185	137	68	49	46	34	36.1
660	2	566	40	476	326	276	187	131	65	48	42	36	36.1
660	3	566	40	477	327	279	187	132	66	44	42	35	36.1
720	1	566	40	493	358	233	181	144	61	46	43	31	36.5
720	2	566	40	491	352	231	189	147	68	42	40	35	36.5
720	3	566	40	495	355	230	188	149	69	41	39	34	36.5
780	1	566	40	432	345	285	161	129	66	49	46	30	36.9
780	2	566	40	435	349	281	161	133	61	47	45	36	36.9
780	3	566	40	433	342	283	162	135	63	44	40	32	36.9
840	1	566	40	357	287	196	161	64	48	45	36	35	36.1
840	2	566	40	356	290	200	163	62	46	43	39	37	36.1
840	3	566	40	353	283	201	166	65	47	44	31	30	36.1
900	1	566	40	390	246	165	132	78	55	48	36	24	35
900	2	566	40	391	243	168	135	75	52	44	30	29	35
900	3	566	40	394	240	163	136	77	54	46	30	30	35
960	1	566	40	347	225	188	146	64	46	44	39	24	35
960	2	566	40	342	222	187	140	61	48	45	35	22	35
960	3	566	40	341	221	190	144	62	49	43	36	28	35
1020	1	566	40	374	256	180	139	70	53	48	33	23	36.3
1020	2	566	40	375	255	184	133	72	56	47	36	22	36.3
1020	3	566	40	379	251	187	134	71	58	42	36	25	36.3
1080	1	566	40	469	386	255	183	110	63	43	41	36	34.9
1080	2	566	40	465	386	254	186	115	69	45	42	34	34.9
1080	3	566	40	461	388	258	185	114	65	48	46	39	34.9
1140	1	566	40	487	379	244	179	112	68	46	45	38	36
1140	2	566	40	488	377	242	174	114	65	43	41	31	36
1140	3	566	40	481	376	242	177	117	67	44	43	33	36
1200	1	566	40	444	367	247	161	103	65	49	42	35	35.9
1200	2	566	40	445	368	248	167	107	62	48	46	36	35.9
1200	3	566	40	446	363	245	165	111	62	43	41	38	35.9

1260	1	566	40	328	202	196	106	68	46	41	36	27	34.6
1260	2	566	40	324	207	199	109	63	49	42	36	24	34.6
1260	3	566	40	326	203	194	104	67	44	40	37	21	34.6
1320	1	566	40	373	294	198	130	74	57	39	33	27	34.8
1320	2	566	40	371	297	192	132	73	58	38	37	25	34.8
1320	3	566	40	370	290	196	133	72	52	37	35	26	34.8
1380	1	566	40	428	335	248	195	133	63	45	41	33	35.9
1380	2	566	40	429	339	248	197	136	66	47	41	37	35.9
1380	3	566	40	423	336	243	195	137	67	49	42	38	35.9
1440	1	566	40	447	391	278	198	103	61	49	47	37	35.8
1440	2	566	40	446	395	271	199	107	63	45	42	34	35.8
1440	3	566	40	448	394	272	201	109	64	46	44	39	35.8
1500	1	566	40	497	366	286	196	123	60	43	41	32	35
1500	2	566	40	494	361	287	193	128	61	46	42	36	35
1500	3	566	40	491	365	282	193	127	62	45	44	30	35
1560	1	566	40	465	309	286	174	114	65	48	46	39	33.3
1560	2	566	40	461	307	286	175	118	66	49	47	33	33.3
1560	3	566	40	467	302	287	173	117	68	46	45	36	33.3
1620	1	566	40	408	386	251	194	143	67	48	44	35	35.1
1620	2	566	40	412	380	252	196	147	60	47	42	32	35.1
1620	3	566	40	414	389	251	194	149	63	48	45	34	35.1
1680	1	566	40	330	259	184	128	64	49	47	36	21	34.6
1680	2	566	40	326	256	182	131	69	47	42	31	28	34.6
1680	3	566	40	321	255	181	124	70	48	46	30	26	34.6
1740	1	566	40	372	217	195	121	77	55	49	38	21	33.7
1740	2	566	40	374	214	198	126	78	53	43	31	25	33.7
1740	3	566	40	375	215	202	123	75	59	46	32	28	33.7
1800	1	566	40	388	246	184	141	63	47	46	32	29	34.4
1800	2	566	40	385	240	181	134	65	43	41	35	25	34.4
1800	3	566	40	389	241	187	139	69	48	44	32	24	34.4
1860	1	566	40	386	213	170	117	61	47	43	33	26	34.7
1860	2	566	40	383	215	177	116	66	47	45	34	30	34.7
1860	3	566	40	382	215	174	119	69	46	44	36	24	34.7
1920	1	566	40	360	254	182	125	78	53	37	35	23	34.6
1920	2	566	40	361	250	181	123	74	55	39	36	29	34.6
1920	3	566	40	367	255	181	122	77	56	35	33	24	34.6
1980	1	566	40	459	398	216	184	137	65	49	45	36	34.5
1980	2	566	40	457	399	216	188	140	63	47	42	35	34.5
1980	3	566	40	458	395	210	187	144	60	44	42	39	34.5
2040	1	566	40	482	339	220	184	108	67	41	38	34	34.4
2040	2	566	40	483	331	219	184	111	65	40	39	32	34.4
2040	3	566	40	486	334	224	182	107	62	48	42	39	34.4
2100	1	566	40	435	309	211	192	148	64	44	39	32	34.2
2100	2	566	40	431	302	210	198	144	64	46	40	31	34.2
2100	3	566	40	439	303	212	194	149	64	46	41	34	34.2
2160	1	566	40	461	321	256	162	103	65	47	46	32	37.1
2160	2	566	40	464	320	259	160	102	63	47	43	33	37.1
2160	3	566	40	465	326	261	158	99	61	45	44	30	37.1
2220	1	566	40	438	334	223	175	125	61	44	42	30	37.7
2220	2	566	40	439	330	220	175	125	62	45	43	31	37.7
2220	3	566	40	435	329	219	172	127	63	47	45	39	37.7
2280	1	566	40	354	267	179	105	68	46	45	37	30	37.5
2280	2	566	40	353	271	177	104	67	47	45	38	30	37.5
2280	3	566	40	357	269	175	104	61	48	44	37	29	37.5
2340	1	566	40	328	263	183	133	73	54	44	35	20	37.2
2340	2	566	40	326	264	186	131	71	59	49	33	24	37.2
2340	3	566	40	324	262	188	136	76	57	48	32	22	37.2
2400	1	566	40	497	382	217	145	105	65	40	37	38	38.1
2400	2	566	40	498	383	215	146	106	61	42	40	38	38.1
2400	3	566	40	491	381	218	144	109	61	43	41	35	38.1
2460	1	566	40	483	391	237	199	118	63	49	44	39	37.6
2460	2	566	40	486	397	235	192	113	65	47	45	32	37.6
2460	3	566	40	484	394	233	194	116	67	46	42	34	37.6

2520	1	566	40	368	269	206	156	88	54	41	34	29	36.6
2520	2	566	40	362	266	204	155	89	55	42	34	30	36.6
2520	3	566	40	360	263	203	154	88	55	42	34	30	36.6
2580	1	566	40	476	354	270	182	128	64	47	42	33	37.6
2580	2	566	40	481	357	274	185	124	67	46	43	38	37.6
2580	3	566	40	479	358	276	183	126	61	49	45	33	37.6
2640	1	566	40	412	302	235	178	102	67	49	40	35	37.3
2640	2	566	40	407	299	233	177	106	67	50	40	35	37.3
2640	3	566	40	403	297	231	177	105	67	50	39	34	37.3
2700	1	566	40	417	320	253	196	118	75	53	44	36	37.2
2700	2	566	40	413	318	251	194	118	75	54	44	37	37.2
2700	3	566	40	395	316	251	195	119	77	56	46	39	37.2
2760	1	566	40	364	271	215	168	101	66	47	36	31	37.1
2760	2	566	40	360	269	214	168	102	67	48	38	32	37.1
2760	3	566	40	361	266	211	166	101	66	48	37	31	37.1
2820	1	566	40	476	368	221	195	133	64	49	46	34	36.8
2820	2	566	40	474	366	220	195	135	62	42	41	35	36.8
2820	3	566	40	473	363	218	193	134	67	43	40	36	36.8
2880	1	566	40	423	349	258	185	115	59	43	42	39	37
2880	2	566	40	427	343	257	183	116	61	44	41	38	37
2880	3	566	40	429	342	256	182	117	63	45	44	34	37
2940	1	566	40	328	272	183	115	62	49	43	37	27	37.1
2940	2	566	40	325	273	183	119	61	49	43	38	24	37.1
2940	3	566	40	326	275	186	114	64	50	43	33	26	37.1
3000	1	566	40	461	320	291	196	124	66	44	37	33	37.3
3000	2	566	40	462	321	291	196	127	68	45	39	33	37.3
3000	3	566	40	468	318	290	196	125	68	44	37	32	37.3
3060	1	566	40	386	254	166	121	78	57	46	36	21	37.2
3060	2	566	40	389	251	160	113	75	58	41	34	20	37.2
3060	3	566	40	387	249	160	119	76	58	46	38	22	37.2
3120	1	566	40	385	236	165	116	66	48	40	33	28	37.5
3120	2	566	40	374	232	163	115	66	48	39	33	27	37.5
3120	3	566	40	371	231	162	114	66	48	40	33	26	37.5
3180	1	566	40	347	223	162	119	72	50	39	32	25	36.3
3180	2	566	40	338	218	158	116	71	49	38	31	25	36.3
3180	3	566	40	317	216	158	116	72	50	38	32	27	36.3
3240	1	566	40	431	387	244	182	105	63	46	42	37	36.8
3240	2	566	40	434	381	249	184	107	67	47	41	34	36.8
3240	3	566	40	438	385	246	181	106	66	49	45	32	36.8
3330	1	566	40	355	242	175	125	63	47	44	36	31	37.2
3330	2	566	40	351	247	173	121	63	46	45	37	31	37.2
3330	3	566	40	354	249	172	127	62	49	44	36	30	37.2
3390	1	566	40	361	232	198	116	75	52	41	33	21	36.3
3390	2	566	40	363	236	193	115	79	55	43	34	22	36.3
3390	3	566	40	368	230	197	117	77	56	46	35	24	36.3
3450	1	566	40	448	332	246	167	133	63	48	42	39	37.1
3450	2	566	40	442	338	242	163	141	60	42	41	37	37.1
3450	3	566	40	445	336	243	164	143	62	45	44	33	37.1
3510	1	566	40	478	327	259	181	129	68	46	44	35	37.2
3510	2	566	40	476	322	258	184	132	63	48	47	37	37.2
3510	3	566	40	474	325	261	183	135	65	40	39	31	37.2
3570	1	566	40	464	394	267	176	113	64	44	42	36	36.2
3570	2	566	40	463	399	265	176	119	66	45	41	36	36.2
3570	3	566	40	461	396	265	176	115	67	46	44	40	36.2
3630	1	566	40	353	247	199	147	74	55	46	38	21	36.7
3630	2	566	40	358	249	195	159	79	54	45	39	23	36.7
3630	3	566	40	354	247	191	168	78	56	46	35	24	36.7
3690	1	566	40	488	262	182	121	66	49	41	34	31	37.2
3690	2	566	40	476	270	180	121	67	50	41	34	29	37.2
3690	3	566	40	473	268	180	120	67	50	41	34	30	37.2
3750	1	566	40	472	329	245	182	133	59	45	40	34	36.9
3750	2	566	40	474	328	244	180	137	60	44	42	38	36.9
3750	3	566	40	477	322	241	180	138	64	46	43	35	36.9
3810	1	566	40	386	260	192	140	81	54	43	35	33	37.6
3810	2	566	40	383	257	190	140	82	54	42	35	30	37.6
3810	3	566	40	380	255	188	138	81	53	41	34	29	37.6
3870	1	566	40	497	302	210	152	88	61	46	37	30	36.7
3870	2	566	40	490	298	209	152	89	61	46	36	29	36.7
3870	3	566	40	463	297	208	152	88	61	47	39	34	36.7
3930	1	566	40	324	276	161	108	62	44	42	38	35	37
3930	2	566	40	321	269	167	110	65	44	43	32	30	37
3930	3	566	40	329	272	164	111	66	42	41	34	33	
3990	1	566	40	535	363	273	209	124	79	55	42	34	
3990	2	566	40	533	360	271	208	124	79	56	42	34	

4050	1	566	40	538	320	266	220	131	71	58	42	34	36.9
4050	2	566	40	535	314	268	220	130	71	60	47	39	36.9
4050	3	566	40	532	318	268	220	134	70	56	49	35	36.9
4110	1	566	40	324	238	186	150	69	46	43	35	27	36.6
4110	2	566	40	327	235	187	152	65	47	41	36	28	36.6
4110	3	566	40	321	232	188	151	64	48	47	36	24	36.6
4170	1	566	40	422	367	277	172	105	64	48	44	40	36.8
4170	2	566	40	427	361	276	176	109	66	45	43	34	36.8
4170	3	566	40	425	365	274	176	109	66	49	47	39	36.8
4230	1	566	40	341	210	198	111	66	40	38	37	33	36.7
4230	2	566	40	343	212	196	111	68	41	40	39	34	36.7
4230	3	566	40	348	209	195	109	68	40	38	34	33	36.7
4290	1	566	40	384	257	173	108	70	53	46	32	27	36.4
4290	2	566	40	389	261	176	110	74	50	49	33	29	36.4
4290	3	566	40	387	259	177	106	71	51	45	32	26	36.4
4350	1	566	40	485	358	235	174	115	69	45	42	34	36.6
4350	2	566	40	489	361	234	179	116	69	48	43	36	36.6
4350	3	566	40	484	356	233	177	116	69	49	43	35	36.6
4410	1	566	40	496	396	240	157	105	63	49	48	30	38
4410	2	566	40	492	399	242	158	101	66	47	45	32	38
4410	3	566	40	498	394	238	161	107	65	44	42	31	38
4470	1	566	40	468	317	264	165	113	69	47	44	36	36.7
4470	2	566	40	464	320	265	168	117	68	48	45	35	36.7
4470	3	566	40	462	314	265	169	119	67	49	46	37	36.7
4530	1	566	40	374	209	171	147	63	43	42	31	25	36.2
4530	2	566	40	370	205	176	142	65	48	45	37	24	36.2
4530	3	566	40	372	204	175	140	66	41	40	39	23	36.2
4590	1	566	40	330	215	193	129	79	53	37	34	25	36.4
4590	2	566	40	325	213	197	127	77	55	39	36	22	36.4
4590	3	566	40	327	217	198	128	73	56	33	31	24	36.4
4650	1	566	40	497	323	275	183	136	68	48	44	39	36.1
4650	2	566	40	498	317	276	183	139	61	46	40	35	36.1
4650	3	566	40	492	319	271	181	142	63	49	47	33	36.1
4710	1	566	40	454	373	295	192	125	64	48	47	35	36.3
4710	2	566	40	455	375	293	194	131	69	45	44	32	36.3
4710	3	566	40	456	371	292	196	129	68	48	46	31	36.3
4770	1	566	40	473	359	247	164	101	65	48	44	38	36.2
4770	2	566	40	476	351	251	168	107	64	42	41	35	36.2
4770	3	566	40	472	356	250	160	105	61	40	39	30	36.2
4830	1	566	40	348	222	172	108	62	45	44	32	21	36.6
4830	2	566	40	340	221	174	107	68	47	46	37	23	36.6
4830	3	566	40	345	215	175	103	63	48	46	33	22	36.6
4890	1	566	40	355	282	180	120	67	42	41	37	28	36.9
4890	2	566	40	353	289	179	119	60	44	42	39	26	36.9
4890	3	566	40	356	288	178	116	64	43	40	35	25	36.9
4950	1	566	40	359	293	176	112	75	51	39	31	28	37
4950	2	566	40	357	294	175	113	78	53	38	33	26	37
4950	3	566	40	355	290	175	110	74	56	37	36	22	37
5010	1	566	40	354	286	179	140	61	49	42	31	20	36.2
5010	2	566	40	352	282	175	139	65	48	47	35	23	36.2
5010	3	566	40	351	289	172	137	64	48	47	34	23	36.2
5070	1	566	40	319	260	197	131	78	54	38	32	27	38
5070	2	566	40	314	256	193	129	71	52	37	31	21	38
5070	3	566	40	315	254	191	128	73	57	35	34	22	38
5130	1	566	40	425	311	254	180	124	64	46	44	32	37.6
5130	2	566	40	421	310	253	180	125	63	48	47	34	37.6
5130	3	566	40	429	308	252	181	126	62	49	45	33	37.6
5190	1	566	40	484	391	212	192	110	65	47	41	32	36.9
5190	2	566	40	487	393	210	198	112	67	46	42	32	36.9
5190	3	566	40	486	394	214	196	116	66	48	44	31	36.9
5250	1	566	40	324	237	163	104	69	49	44	39	26	37.4
5250	2	566	40	322	235	167	104	69	48	46	37	23	37.4
5250	3	566	40	328	233	164	102	68	45	43	38	22	37.4
5310	1	566	40	357	261	194	108	75	55	35	32	23	37.5
5310	2	566	40	352	262	196	103	70	56	36	30	26	37.5
5310	3	566	40	355	257	197	102	73	53	37	33	25	37.5
5370	1	566	40	464	335	202	169	115	67	48	47	38	37.3
5370	2	566	40	466	337	206	163	114	68	49	46	36	37.3
5370	3	566	40	465	330	209	167	118	64	43	41	34	37.3
5430	1	566	40	455	314	289	169	117	67	48	47	38	37
5430	2	566	40	452	319	290	173	115	62	43	41	35	37
5430	3	566	40	453	316	287	173	116	63	44	42	31	37
5490	1	566	40	466	367	293	181	115	65	48	45	33	37.6

5490	2	566	40	463	371	292	180	116	62	49	41	36	37.6
5490	3	566	40	465	369	292	179	117	61	47	42	34	37.6
5550	1	566	40	347	249	172	104	68	49	47	35	24	37.2
5550	2	566	40	342	246	171	110	65	48	43	38	27	37.2
5550	3	566	40	346	248	174	107	67	46	43	37	26	37.2
5610	1	566	40	323	241	190	134	77	56	39	36	25	37.1
5610	2	566	40	328	244	194	139	75	59	38	37	21	37.1
5610	3	566	40	327	247	197	136	79	54	39	34	24	37.1
5670	2	566	40	316	283	171	111	68	49	46	36	34	38
5730	2	566	40	454	354	256	188	108	64	49	45	30	37.7
5790	1	566	40	451	312	231	173	107	65	44	42	32	36.4
5850	1	566	40	465	384	253	193	137	67	47	45	34	36.4
5910	3	566	40	437	385	264	174	165	62	48	43	36	36.9
5970	1	566	40	471	360	248	190	101	66	48	47	33	36.7
6030	3	566	40	363	290	174	119	67	49	47	36	24	37.5
6090	1	566	40	379	264	164	113	70	59	39	36	22	38.1
6150	1	566	40	487	330	234	184	112	68	40	39	32	37.1
6210	2	566	40	458	344	237	177	135	68	43	46	35	36.4
6270	3	566	40	439	387	298	193	109	68	47	43	32	36.8
6330	1	566	40	567	381	280	202	111	71	54	44	36	37.8

Table 4 Back-calculated layer moduli values

Chainage	Layer Modulus			Temp.	Corrected layer moduli		
	Surface	Base	Subgrade	correctio	Surface	Base	Subgrade
0	1489.2	101.6	100	1.08	1614.469	101.6	100
0	1429	100	100	1.08	1549.205	100	100
0	1389.2	101.6	99.8	1.08	1506.057	101.6	99.8
60	1454.8	290	100	1.10	1598.95	290	100
60	1482.8	249	100	1.10	1629.725	249	100
60	1444.1	202.1	100	1.10	1587.19	202.1	100
120	1475.3	220.8	100	1.08	1592.133	220.8	100
120	1489.2	231.4	100	1.08	1607.133	231.4	100
120	1477.4	258.4	100	1.08	1594.399	258.4	100
180	1453.8	104.3	100	1.11	1612.594	104.3	100
180	1365.6	100.4	99.9	1.11	1514.761	100.4	99.9
180	1343	101.2	100	1.11	1489.692	101.2	100
240	1476.3	112.1	100	1.09	1615.168	112.1	100
240	1406.5	118.4	100	1.09	1538.802	118.4	100
240	1498.9	101.2	100	1.09	1639.893	101.2	100
300	1392.5	101.6	99.9	1.08	1509.634	101.6	99.9
300	1388.2	101.6	100	1.08	1504.973	101.6	100
300	1361.3	107	100	1.08	1475.81	107	100
360	1318.3	109.8	100	1.09	1435.728	109.8	100
360	1307.5	126.6	100	1.09	1423.966	126.6	100
360	1259.1	117.6	100	1.09	1371.255	117.6	100
420	1454.8	238	100	1.05	1527.955	238	100
420	1495.7	247.4	100	1.05	1570.911	247.4	100
420	1487.1	219.6	100	1.05	1561.879	219.6	100
480	1489.2	262.7	100	1.06	1571.147	262.7	100
480	1457	258.7	99.9	1.06	1537.175	258.7	99.9
480	1454.8	253.7	100	1.06	1534.854	253.7	100
540	1487.1	271.3	100	1.06	1583.17	271.3	100
540	1481.7	216.5	100	1.06	1577.421	216.5	100
540	1451.6	223.9	100	1.06	1545.376	223.9	100
600	1479.6	104.7	100	1.08	1596.773	104.7	100
600	1477.4	101.6	100	1.08	1594.399	101.6	100
600	1458.1	103.9	100	1.08	1573.571	103.9	100
660	1478.5	109	99.9	1.05	1552.846	109	99.9
660	1495.7	105.9	100	1.05	1570.911	105.9	100
660	1468.8	101.2	100	1.05	1542.659	101.2	100
720	1373.1	102.7	99.9	1.07	1468.441	102.7	99.9
720	1473.1	102	99.8	1.07	1575.384	102	99.8
720	1484.9	102	100	1.07	1588.004	102	100
780	1455.9	114.9	100	1.09	1585.585	114.9	100
780	1459.1	114.1	100	1.09	1589.07	114.1	100
780	1318.3	108.6	100	1.09	1435.728	108.6	100
840	1463.4	225.9	100	1.05	1536.987	225.9	100
840	1500	228.3	100	1.05	1575.428	228.3	100
840	1462.4	193.5	100	1.05	1535.937	193.5	100
900	1407.5	215.3	100	1.00	1407.5	215.3	100
900	1392.5	222.4	100	1.00	1392.5	222.4	100
900	1448.4	215.3	100	1.00	1448.4	215.3	100
960	1465.6	243.9	100	1.00	1465.6	243.9	100
960	1489.2	247.8	100	1.00	1489.2	247.8	100
960	1454.8	281.4	100	1.00	1454.8	281.4	100
1020	1459.1	207.5	100	1.06	1546.354	207.5	100
1020	1474.2	201.3	100	1.06	1562.357	201.3	100
1020	1492.5	200.1	100	1.06	1581.751	200.1	100
1080	1404.3	100	100	1.00	1398.111	100	100
1080	1418.3	100.4	99.8	1.00	1412.049	100.4	99.8
1080	1468.8	106.3	100	1.00	1462.326	106.3	100
1140	1444.1	101.6	99.8	1.05	1509.911	101.6	99.8
1140	1423.7	104.3	100	1.05	1488.581	104.3	100
1140	1460.2	100.8	100	1.05	1526.744	100.8	100
1200	1444.1	127.8	100	1.04	1503.147	127.8	100
1200	1457	105.9	100	1.04	1516.574	105.9	100
1200	1408.6	113.7	99.9	1.04	1466.195	113.7	99.9
1260	1498.9	413.2	100	0.98	1472.709	413.2	100
1260	1464.5	360	100	0.98	1438.91	360	100
1260	1479.6	337.3	100	0.98	1453.747	337.3	100

1320	1449.5	180.5	100	0.99	1436.761	180.5	100
1320	1482.8	180.9	100	0.99	1469.768	180.9	100
1320	1461.3	188	100	0.99	1448.457	188	100
1380	1439.8	104.7	99.9	1.04	1498.671	104.7	99.9
1380	1498.9	116.8	100	1.04	1560.187	116.8	100
1380	1491.4	127	99.9	1.04	1552.381	127	99.9
1440	1433.3	102.3	99.9	1.04	1485.233	102.3	99.9
1440	1377.4	102.7	99.9	1.04	1427.308	102.7	99.9
1440	1482.8	100.4	100	1.04	1536.527	100.4	100
1500	1258.1	100	100	1.00	1258.1	100	100
1500	1357	100.4	100	1.00	1357	100.4	100
1500	1398.9	102.3	100	1.00	1398.9	102.3	100
1560	1400	115.2	100	0.93	1299.864	115.2	100
1560	1426.9	113.3	100	0.93	1324.84	113.3	100
1560	1465.6	120.7	100	0.93	1360.772	120.7	100
1620	1492.5	108.2	99.9	1.00	1499.117	108.2	99.9
1620	1492.5	100.4	100	1.00	1499.117	100.4	100
1620	1494.6	113.3	100	1.00	1501.227	113.3	100
1680	1404.3	207.5	100	0.98	1379.762	207.5	100
1680	1497.8	275.2	100	0.98	1471.629	275.2	100
1680	1474.2	260.3	100	0.98	1448.441	260.3	100
1740	1467.7	248.2	100	0.94	1386.504	248.2	100
1740	1490.3	220.8	100	0.94	1407.854	220.8	100
1740	1491.4	256.4	100	0.94	1408.893	256.4	100
1800	1447.3	213	100	0.97	1409.589	213	100
1800	1482.8	223.9	100	0.97	1444.164	223.9	100
1800	1498.9	198.1	100	0.97	1459.844	198.1	100
1860	1482.8	320.9	100	0.99	1463.31	320.9	100
1860	1458.1	336.2	100	0.99	1438.935	336.2	100
1860	1478.5	259.5	100	0.99	1459.067	259.5	100
1920	1474.2	218.5	100	0.98	1448.441	218.5	100
1920	1481.7	259.1	100	0.98	1455.81	259.1	100
1920	1409.7	201.3	100	0.98	1385.068	201.3	100
1980	1483.9	107	99.9	0.98	1451.585	107	99.9
1980	1492.5	100.4	99.9	0.98	1459.997	100.4	99.9
1980	1487.1	102.3	100	0.98	1454.715	102.3	100
2040	1452.7	111.3	99.9	0.97	1414.848	111.3	99.9
2040	1380.6	101.6	100	0.97	1344.627	101.6	100
2040	1289.2	125	100	0.97	1255.608	125	100
2100	1492.5	120.3	100	0.97	1440.95	120.3	100
2100	1486	116.4	100	0.97	1434.675	116.4	100
2100	1330.1	127.4	100	0.97	1284.159	127.4	100
2160	1497.8	132.8	100	1.10	1646.211	132.8	100
2160	1480.6	120.3	99.9	1.10	1627.307	120.3	99.9
2160	1368.8	118	100	1.10	1504.429	118	100
2220	1426.9	126.2	100	1.13	1612.271	126.2	100
2220	1474.2	118.8	100	1.13	1665.715	118.8	100
2220	1491.4	127.4	100	1.13	1685.15	127.4	100
2280	1474.2	333.8	100	1.12	1650.369	333.8	100
2280	1444.1	418.3	100	1.12	1616.672	418.3	100
2280	1457	433.5	100	1.12	1631.113	433.5	100
2340	1492.5	197.8	100	1.10	1647.929	197.8	100
2340	1359.1	251.3	100	1.10	1500.637	251.3	100
2340	1467.7	211	100	1.10	1620.546	211	100
2400	1425.8	114.1	100	1.15	1641.311	114.1	100
2400	1316.1	118.4	100	1.15	1515.03	118.4	100
2400	1439.8	115.6	100	1.15	1657.427	115.6	100
2460	1453.8	102.3	100	1.12	1635.073	102.3	100
2460	1497.8	103.9	100	1.12	1684.56	103.9	100
2460	1419.4	103.9	100	1.12	1596.384	103.9	100
2520	1458.1	161.4	100	1.11	1617.364	161.4	100
2520	1478.5	159.4	100	1.11	1639.992	159.4	100
2520	1491.4	204	100	1.11	1654.301	204	100
2580	1429	100	99.9	1.07	1535.172	100	99.9
2580	1343	102.3	99.9	1.07	1442.782	102.3	99.9
2580	1449.5	103.1	99.9	1.07	1557.195	103.1	99.9

2640	1404.3	136.8	100	1.12	1579.401	136.8	100
2640	1453.8	137.5	100	1.12	1635.073	137.5	100
2640	1483.9	156.3	100	1.12	1668.926	156.3	100
2700	1437.6	119.9	99.9	1.11	1594.625	119.9	99.9
2700	1488.2	137.5	99.9	1.11	1650.752	137.5	99.9
2700	1500	154.3	99.9	1.11	1663.841	154.3	99.9
2760	1493.5	159.8	100	1.10	1649.033	159.8	100
2760	1457	170.4	100	1.10	1608.732	170.4	100
2760	1460.2	174.3	99.9	1.10	1612.265	174.3	99.9
2820	1469.9	101.6	99.9	1.10	1615.547	101.6	99.9
2820	1416.1	110.9	100	1.10	1556.416	110.9	100
2820	1472	113.7	99.9	1.10	1617.855	113.7	99.9
2880	1476.3	110.6	100	1.08	1600.484	110.6	100
2880	1441.9	112.1	100	1.08	1563.19	112.1	100
2880	1474.2	118	99.9	1.08	1598.207	118	99.9
2940	1488.2	339.7	100	1.09	1628.187	339.7	100
2940	1481.7	283	100	1.09	1621.075	283	100
2940	1488.2	290.4	100	1.09	1628.187	290.4	100
3000	1407.5	101.6	100	1.10	1546.964	101.6	100
3000	1477.4	100.8	100	1.10	1623.79	100.8	100
3000	1430.1	107.4	99.9	1.10	1571.803	107.4	99.9
3060	1441.9	152	100	1.11	1599.395	152	100
3060	1453.8	393.3	100	1.11	1612.594	393.3	100
3060	1465.6	497.7	100	1.11	1625.683	497.7	100
3120	1412.9	318.2	100	1.10	1560.04	318.2	100
3120	1484.9	304.5	100	1.10	1639.538	304.5	100
3120	1462.4	268.9	100	1.10	1614.695	268.9	100
3180	1428	254.4	100	1.12	1598.648	254.4	100
3180	1459.1	343.6	100	1.12	1633.464	343.6	100
3180	1464.5	401.9	100	1.12	1639.51	401.9	100
3240	1443	109.4	100	1.06	1529.291	109.4	100
3240	1465.6	101.1	100	1.06	1553.243	101.1	100
3240	1424.7	119.6	100	1.06	1509.897	119.6	100
3330	1478.5	340.1	100	1.08	1602.869	340.1	100
3330	1463.4	358.8	100	1.08	1586.498	358.8	100
3330	1468.8	318.6	100	1.08	1592.353	318.6	100
3390	1403.2	220.8	100	1.10	1549.329	220.8	100
3390	1426.9	202.2	100	1.10	1575.498	202.2	100
3390	1400	231	100	1.10	1545.796	231	100
3450	1460.2	110.2	100	1.06	1547.52	110.2	100
3450	1460.2	110.6	99.9	1.06	1547.52	110.6	99.9
3450	1495.7	114.5	100	1.06	1585.143	114.5	100
3510	1435.5	105.5	100	1.10	1577.738	105.5	100
3510	1469.9	107.7	99.9	1.10	1615.547	107.7	99.9
3510	1459.1	103.5	99.9	1.10	1603.676	103.5	99.9
3570	1429	100	100	1.10	1577.816	100	100
3570	1401.1	100.8	100	1.10	1547.011	100.8	100
3570	1453.8	103.9	99.9	1.10	1605.199	103.9	99.9
3630	1495.7	187.6	100	1.06	1578.005	187.6	100
3630	1390.3	177	100	1.06	1466.805	177	100
3630	1467.7	187.2	100	1.06	1548.464	187.2	100
3690	1186	201.7	100	1.08	1279.922	201.7	100
3690	1355.7	188.8	100	1.08	1463.061	188.8	100
3690	1446.2	208.8	100	1.08	1560.728	208.8	100
3750	1381.7	103.5	99.9	1.10	1525.59	103.5	99.9
3750	1434.4	114.9	100	1.10	1583.779	114.9	100
3750	1467.7	121.9	100	1.10	1620.546	121.9	100
3810	1489.2	206.4	100	1.09	1621.851	206.4	100
3810	1491.4	202.8	100	1.09	1624.247	202.8	100
3810	1450.5	229.8	100	1.09	1579.704	229.8	100

3870	1491.4	132.8	100	1.12	1677.362	132.8	100
3870	1389.2	132.8	100	1.12	1562.418	132.8	100
3870	1420.4	124.2	99.9	1.12	1597.509	124.2	99.9
3930	1458.1	481.2	100	1.08	1573.571	481.2	100
3930	1493.5	376.4	100	1.08	1611.774	376.4	100
3930	1462.4	353.4	100	1.08	1578.211	353.4	100
3990	1451.6	100.8	100	1.09	1588.144	100.8	100
3990	1436.6	100.8	99.9	1.09	1571.733	100.8	99.9
3990	1423.7	100.8	100	1.09	1557.62	100.8	100
4050	1338.7	101.6	99.6	1.09	1457.945	101.6	99.6
4050	1453.8	102.7	99.8	1.09	1583.298	102.7	99.8
4050	1453.8	103.9	99.8	1.09	1583.298	103.9	99.8
4110	1491.4	482.8	100	1.07	1602.208	482.8	100
4110	1469.9	269.7	100	1.07	1579.111	269.7	100
4110	1487.1	269.3	100	1.07	1597.589	269.3	100
4170	1441.9	112.1	100	1.08	1563.19	112.1	100
4170	1486	114.9	99.9	1.08	1611	114.9	99.9
4170	1465.6	125	100	1.08	1588.884	125	100
4230	1496.8	434.3	100	1.08	1615.335	434.3	100
4230	1487.1	486.7	100	1.08	1604.867	486.7	100
4230	1498.9	487.5	100	1.08	1617.602	487.5	100
4290	1492.5	263.8	100	1.06	1588.919	263.8	100
4290	1435.5	268.5	100	1.06	1528.236	268.5	100
4290	1487.1	260.7	100	1.06	1583.17	260.7	100
4350	1476.3	113.7	100	1.07	1585.986	113.7	100
4350	1438.7	118.8	100	1.07	1545.593	118.8	100
4350	1469.9	104.7	100	1.07	1579.111	104.7	100
4410	1453.8	102.7	100	1.15	1665.746	102.7	100
4410	1474.2	107.4	100	1.15	1689.12	107.4	100
4410	1378.5	105.9	100	1.15	1579.468	105.9	100
4470	1491.4	121.5	100	1.08	1609.508	121.5	100
4470	1496.8	126.9	100	1.08	1615.335	126.9	100
4470	1447.3	118	99	1.08	1561.915	118	99
4530	1496.8	252.1	100	1.06	1579.165	252.1	100
4530	1476.3	283.4	100	1.06	1557.537	283.4	100
4530	1486	218.5	100	1.06	1567.771	218.5	100
4590	1463.4	216.1	100	1.06	1557.939	216.1	100
4590	1474.2	229.8	100	1.06	1569.436	229.8	100
4590	1481.7	202.1	100	1.06	1577.421	202.1	100
4650	1462.4	117.2	99.9	1.05	1535.937	117.2	99.9
4650	1462.4	105.9	99.9	1.05	1535.937	105.9	99.9
4650	1424.7	105.1	100	1.05	1496.341	105.1	100
4710	1498.9	109.1	99.9	1.06	1588.534	109.1	99.9
4710	1436.6	104.7	99.8	1.06	1522.508	104.7	99.8
4710	1426.9	103.1	100	1.06	1512.228	103.1	100
4770	1444.1	121.1	100	1.06	1523.565	121.1	100
4770	1446.2	102.3	100	1.06	1525.781	102.3	100
4770	1486	107	100	1.06	1567.771	107	100
4830	1460.2	300.2	100	1.07	1568.69	300.2	100
4830	1478.5	302.9	100	1.07	1588.35	302.9	100
4830	1463.4	341.6	100	1.07	1572.128	341.6	100
4890	1490.3	262.7	100	1.09	1623.049	262.7	100
4890	1489.2	281	100	1.09	1621.851	281	100
4890	1469.9	274	100	1.09	1600.832	274	100
4950	1493.5	228.6	100	1.09	1633.985	228.6	100
4950	1441.9	224.7	100	1.09	1577.532	224.7	100
4950	1466.7	207.9	100	1.09	1604.665	207.9	100
5010	1437.6	198.5	100	1.06	1516.708	198.5	100
5010	1437.6	198.5	100	1.06	1516.708	198.5	100
5010	1469.9	216.5	100	1.06	1550.785	216.5	100

5070	1476.3	211.8	100	1.15	1691.527	211.8	100
5070	1475.3	227.9	100	1.15	1690.381	227.9	100
5070	1452.7	220.4	100	1.15	1664.486	220.4	100
5130	1465.6	115.2	100	1.12	1648.345	115.2	100
5130	1465.6	115.2	100	1.12	1648.345	115.2	100
5130	1483.9	119.63	100	1.12	1668.926	119.63	100
5190	1483.9	102.7	100	1.09	1616.079	102.7	100
5190	1368.8	102	99	1.09	1490.726	102	99
5190	1496.8	100	100	1.09	1630.128	100	100
5250	1430.1	380	100	1.11	1593.628	380	100
5250	1480.6	336.2	100	1.11	1649.903	336.2	100
5250	1463.4	375.3	100	1.11	1630.736	375.3	100
5310	1494.6	188.4	100	1.12	1673.207	188.4	100
5310	1474.2	248.2	100	1.12	1650.369	248.2	100
5310	1480.6	258	100	1.12	1657.534	258	100
5370	1424.7	141.1	99.9	1.11	1580.316	141.1	99.9
5370	1430.1	139.1	100	1.11	1586.306	139.1	100
5370	1487.1	120.7	100	1.11	1649.532	120.7	100
5430	1450.5	119.6	99.9	1.09	1586.941	119.6	99.9
5430	1447.3	111.3	100	1.09	1583.44	111.3	100
5430	1487.1	118	99.9	1.09	1626.983	118	99.9
5490	1459.1	103.9	100	1.12	1641.034	103.9	100
5490	1484.9	100	99.8	1.12	1670.051	100	99.8
5490	1495.7	103.1	99.9	1.12	1682.198	103.1	99.9
5550	1466.7	304.9	100	1.10	1619.442	304.9	100
5550	1471	335.8	100	1.10	1624.19	335.8	100
5550	1484.9	299	100	1.10	1639.538	299	100
5610	1492.5	263.4	100	1.10	1640.386	263.4	100
5610	1484.9	190.3	100	1.10	1632.033	190.3	100
5610	1467.7	213.8	100	1.10	1613.129	213.8	100
5670	1486	412	100	1.15	1702.641	412	100
5730	1458.1	104.7	99.8	1.13	1647.524	104.7	99.8
5790	1474.2	114.5	99.9	1.06	1569.436	114.5	99.9
5850	1495.7	100.4	100	1.06	1592.325	100.4	100
5910	1496.8	112.9	99.9	1.09	1630.128	112.9	99.9
5970	1457	110.6	99.9	1.08	1572.383	110.6	99.9
6030	1489.2	232.2	100	1.12	1667.161	232.2	100
6090	1473.1	232.6	100	1.15	1695.761	232.6	100
6150	1436.6	112.1	100	1.10	1578.947	112.1	100
6210	1441.9	105.5	99.8	1.06	1535.05	105.5	99.8
6270	1459.1	101.6	99.8	1.08	1581.837	101.6	99.8
6330	1159.1	105.1	100	1.14	1315.774	105.1	100

Table 5 Measured Deflections for a section of pavement

Chainage	Stress	Load	D1	D2	D3	D4	D5	D6	D7	D8	D9
0	566	40.01	483	357	267	203	115	72	53	41	35
60	566	40.01	337	268	181	140	66	46	32	31	30
120	566	40.01	333	262	194	127	74	55	37	35	33
180	566	40.01	483	361	247	189	135	64	41	40	32
240	566	40.01	461	330	221	180	129	65	45	37	33
300	566	40.01	492	323	283	191	154	62	48	35	33
360	566	40.01	488	318	221	156	80	52	41	34	30
420	566	40.01	382	260	196	107	69	42	41	34	23
480	566	40.01	364	263	173	117	74	51	43	35	29
540	566	40.01	374	252	180	127	63	49	37	31	22
600	566	40.01	486	362	244	179	134	63	47	45	38
660	566	40.01	477	327	279	187	132	66	44	42	35
720	566	40.01	495	355	230	188	149	69	41	39	34
780	566	40.01	433	342	283	162	135	63	44	40	32
840	566	40.01	353	283	201	166	65	47	44	31	30
900	566	40.01	394	240	163	136	77	54	46	30	30
960	566	40.01	341	221	190	144	62	49	43	36	28
1020	566	40.01	379	251	187	134	71	58	42	36	25
1080	566	40.01	461	388	258	185	114	65	48	46	39
1140	566	40.01	481	376	242	177	117	67	44	43	33
1200	566	40.01	446	363	245	165	111	62	43	41	38
1260	566	40.01	326	660	550	440	200	44	40	37	21
1320	566	40.01	370	290	196	133	72	52	37	35	26
1380	566	40.01	423	336	243	195	137	67	49	42	38
1440	566	40.01	491	365	282	193	127	62	45	44	30
1500	566	40.01	467	302	287	173	117	68	46	45	36
1560	566	40.01	414	389	251	194	149	63	48	45	34
1620	566	40.01	321	255	181	124	70	48	46	30	26
1680	566	40.01	375	215	202	123	75	59	46	32	28
1740	566	40.01	389	241	187	139	69	48	44	32	24

Table 6 Back-calculated values from ELMOD-6 software

Section	Chainage	Drop	H1	H2	H3	H4	E1	E2	E3
1	0	3	150	550	0	0	2882	102	52
1	60	3	150	550	0	0	4322	135	68
1	120	3	150	550	0	0	4434	135	77
1	180	3	150	550	0	0	2454	110	54
1	240	3	150	550	0	0	1880	160	53
1	300	3	150	550	0	0	1813	159	47
1	360	3	150	550	0	0	1755	129	58
1	420	3	150	550	0	0	2428	158	67
1	480	3	150	550	0	0	2652	162	81
1	540	3	150	550	0	0	2569	154	81
1	600	3	150	550	0	0	2313	116	55
1	660	3	150	550	0	0	2428	129	51
1	720	3	150	550	0	0	1848	143	50
1	780	3	150	550	0	0	3740	100	55
1	840	3	150	550	0	0	5018	98	78
1	900	3	150	550	0	0	1517	227	77
1	960	3	150	550	0	0	2537	229	70
1	1020	3	150	550	0	0	2184	180	79
1	1080	3	150	550	0	0	3462	85	56
1	1140	3	150	550	0	0	2661	96	58
1	1200	3	150	550	0	0	3437	89	61
1	1260	3	150	550	0	0	6863	24	106
1	1320	3	150	550	0	0	3608	115	81
1	1380	3	150	550	0	0	3787	105	64
1	1440	3	150	550	0	0	2808	94	54
1	1500	3	150	550	0	0	2041	151	51
1	1560	3	150	550	0	0	5095	85	51
1	1620	3	150	550	0	0	4412	143	80
1	1680	3	150	550	0	0	1582	264	69
1	1740	3	150	550	0	0	1913	195	72
					Average		3015	136	65
				15th Percencentile			1835.95	92.49567	51.2781

Table 7 Back-calculated values from KGPBACK software

Chainage	Sequence	H1	H2	Layer Modulus		
				E1	E2	E3
0	3	150	500	1389.2	101.6	99.8
60	3	150	500	1444.1	202.1	100
120	3	150	500	1477.4	258.4	100
180	3	150	500	1343	101.2	100
240	3	150	500	1498.9	101.2	100
300	3	150	500	1361.3	107	100
360	3	150	500	1259.1	117.6	100
420	3	150	500	1487.1	219.6	100
480	3	150	500	1454.8	253.7	100
540	3	150	500	1451.6	223.9	100
600	3	150	500	1458.1	103.9	100
660	3	150	500	1468.8	101.2	100
720	3	150	500	1484.9	102	100
780	3	150	500	1318.3	108.6	100
840	3	150	500	1462.4	193.5	100
900	3	150	500	1448.4	215.3	100
960	3	150	500	1454.8	281.4	100
1020	3	150	500	1492.5	200.1	100
1080	3	150	500	1468.8	106.3	100
1140	3	150	500	1460.2	100.8	100
1200	3	150	500	1408.6	113.7	99.9
1260	3	150	500	1479.6	337.3	100
1320	3	150	500	1461.3	188	100
1380	3	150	500	1491.4	127	99.9
1440	3	150	500	1482.8	100.4	100
1500	3	150	500	1398.9	102.3	100
1560	3	150	500	1465.6	120.7	100
1620	3	150	500	1494.6	113.3	100
1680	3	150	500	1474.2	260.3	100
1740	3	150	500	1491.4	256.4	100
		Average		1444	164	100
		15^{th} Percencentile		1379.435	101.2	100

Ouriginal by Turnitin

Document Information

Analyzed document	Komaldeep Thesis.docx (D142886298)
Submitted	8/13/2022 9:32:00 PM
Submitted by	Kumari Monu
Submitter email	kumari.monu@thapar.edu
Similarity	11.4%
Analysis address	kumari.monu.thapar@analysis.urkund.com

Sources included in the report

SA **Thapar Institute Of Engineering And Technology / Thesis Report.pdf** 13
Document Thesis Report.pdf (D77350908)
Submitted by: manpreetsingh2@thapar.edu
Receiver: manpreetsingh2.thapar@analysis.urkund.com

SA **Saurashtra University / REPORT_FINAL.docx** 15
Document REPORT_FINAL.docx (D37164869)
Submitted by: jrank91@gmail.com
Receiver: jrank91.saura@analysis.urkund.com

SA **RK University / RUK_Synopsis_Ujjval-_FWD.docx** 3
Document RUK_Synopsis_Ujjval-_FWD.docx (D26839909)
Submitted by: jignesh.vishapara@rku.ac.in
Receiver: jignesh.vishapara.rku@analysis.urkund.com

SA **Rajiv Gandhi Proudyogiki Vishwavidyalaya / M.Tech Thesis-01.03.2021.docx** 9
Document M.Tech Thesis-01.03.2021.docx (D101217397)
Submitted by: mayankg598@gmail.com
Receiver: mayankg598.rgpv@analysis.urkund.com

SA **RK University / RKU_Ujjval_Solanki_Journal paper- STM- A Study on FWD Deflection Bowl Parameters For Structural Evaluation of Flexible Pavement.pdf** 2
Document RKU_Ujjval_Solanki_Journal paper- STM- A Study on FWD Deflection Bowl Parameters For Structural Evaluation of Flexible Pavement.pdf (D30240360)
Submitted by: jignesh.vishapara@rku.ac.in
Receiver: jignesh.vishapara.rku@analysis.urkund.com

SA **RK University / RKU_Ujjval_Solanki_Pavement Evaluation-FWD a Novel Approach.pdf** 3
Document RKU_Ujjval_Solanki_Pavement Evaluation-FWD a Novel Approach.pdf (D30240362)
Submitted by: jignesh.vishapara@rku.ac.in
Receiver: jignesh.vishapara.rku@analysis.urkund.com

SA **Universidade de Lisboa / Trabalho.pdf** 1
Document Trabalho.pdf (D30827641)
Submitted by: cristina.n.ventura@tecnico.ulisboa.pt
Receiver: manuelcorrea.ul@analysis.urkund.com

Ouriginal by Turnitin

SA	**Danmarks Tekniske Universitet / Highway Pavements - June 2012.pdf** Document Highway Pavements - June 2012.pdf (D6100030) Submitted by: s061656.arcdtu@submitters.urkund.com Receiver: arcanic_urkund.dtu@analys.urkund.se	1
SA	**Lingaya's University / Mohd Alam M.Tech Thesis.pdf** Document Mohd Alam M.Tech Thesis.pdf (D72994806) Submitted by: siteshlpu@gmail.com Receiver: siteshlpu.ling@analysis.urkund.com	5
SA	**Thapar Institute Of Engineering And Technology / 22-6-22-report 1.pdf** Document 22-6-22-report 1.pdf (D142532933) Submitted by: vivek.gupta1@thapar.edu Receiver: vivek.gupta1.thapar@analysis.urkund.com	1
SA	**RK University / RKU_Ujjval_Solanki_Thesis_13-02-2018.docx** Document RKU_Ujjval_Solanki_Thesis_13-02-2018.docx (D35694442) Submitted by: jignesh.vishapara@rku.ac.in Receiver: jignesh.vishapara.rku@analysis.urkund.com	1